1958

The ultimate strength of prestressed and conventionally reinforced concrete under the combined action of moment and shear, (Progress Report No. 17), Lehigh University, (May 1958) Ph.D.

R. E. Walther

Prestressed Concrete Bridge Members

Progress Report 17

THE ULTIMATE STRENGTH OF PRE-STRESSED AND CONVENTIONALLY REINFORCED CONCRETE UNDER THE COMBINED ACTION OF MOMENT AND SHEAR

by

René E. Walther

LEHIGH UNIVERSITY

Fritz Laboratory Report 223.17

October 1957

ACKNOWLEDGEMENTS

This work has been carried out at

LEHIGH UNIVERSITY
FRITZ ENGINEERING LABORATORY
DEPARTMENT OF CIVIL ENGINEERING

Director
Professor W.J.Eney

as a part of an investigation sponsored by

PENNSYLVANIA STATE HIGHWAY DEPARTMENT
U.S. BUREAU OF PUBLIC ROADS
REINFORCED CONCRETE RESEARCH COUNCIL
CONCRETE PRODUCTS DIVISION, AMERICAN-MARIETTA COMPANY
AMERICAN STEEL AND WIRE DIVISION, U.S. STEEL CORPORATION
JOHN A. ROEBLING'S SONS CORPORATION
LEHIGH UNIVERSITY

The author is especially indebted to

Professor CARL E. EKBERG, JR.
(Chairman of the Concrete Division)
Professor BRUNO THURLIMANN

for their valuable advice

Active assistance in the preparation of this study was given by: Mssrs. Mario J.Danieri, Charles R.Wilson, Jose L.Montemayor, Research Assistants, and Mr. Alex W.Adler. The manuscript was typed by Miss Elizabeth R. Arbogast.

The author wishes to express his sincere thanks and appreciation for all the help and advice he enjoyed in the course of this investigation.

TABLE OF CONTENTS

SYNOPSIS

The prediction of the ultimate strength of prestressed and conventionally reinforced concrete beams under the combined action of moment and shear (abbreviately called shear strength) thus far had to be based on empirical formulas. A theoretical solution was primarily hampered because no failure mechanism pertaining to the region of moment and shear was established.

A rational approach to the problem is sought by stating a hypothesis concerning the failure mechanism for the region of diagonal cracks. The deformations of this region are considered to result from a shear rotation about the neutral axis of the prospective failure cross-section. By observing consecutively the stresses caused by these deformations, the equilibrium conditions and a suitable failure criterion for plain concrete (e.g. Mohr's failure criterion), the condition of failure can be obtained.

The theory is first presented for simply reinforced concrete beams (simply supported or restrained) and later generalized for prestressing, web and compression reinforcement.

Theoretical estimates are compared with test results. Reasonable agreement is obtained.

1. INTRODUCTION

1.1 GENERAL

In the past half-century of concrete research, the question of shear has incessantly occupied a vast interest. A great number of experimental investigations, covering more than a thousand beam tests, have been reported in the literature. In spite of this wide experience, it was not possible to realize a rational approach for the determination of the ultimate strength of reinforced concrete beams under the combined action of moment and shear, abbreviately, but somewhat unprecisely, called "shear strength". The various formulas, suggested in the literature, are all of an empirical nature and bear, therefore the disadvantage that their validity is to some extent restricted to the particular conditions of the tests from which they are derived, especially since most of the test beams can only be considered as reduced models of true structures. It would certainly be preferable to find first a rationally founded theory and use tests later for its verification. In spite of the odds,which have to be expected, such a rational approach is attempted in this investigation.

The scope of this investigation was originally confined to prestressed concrete. The approach made here

permitted, however, the consideration of the problem as a whole, including conventional reinforcement, prestressing, as well as end restraint and the shape of the cross-section. The finding that the ultimate shear strength of prestressed concrete members can be derived from the strength of the similar non-prestressed member is of great practical significance, because the multitude of test results available for conventionally reinforced beams may compensate somewhat for the lack of information concerning the shear strength of prestressed concrete.

1.2 STATEMENT OF THE PROBLEM

The cognition that elastic stresses or strains under working load very often do not represent a satisfactory criterion for the estimation of the safety of a structure, has in the past decade greatly influenced the research on the "problem of shear" in that the interest has more and more been concentrated toward the prediction of the ultimate strength. Especially for a material like prestressed concrete, the determination of the ultimate strength has always been felt to be imperative. While this did not cause any special difficulties for members failing in pure bending, it was not possible, as mentioned before, to find a rational solution for members failing in the region subjected to moment and shear. There exist various empirical formulas for conventionally reinforced beams, but very little information is available for prestressed concrete.

The specific problem of this paper is therefore to determine the ultimate strength of prestressed and conventionally reinforced beams, failing in connection with the development of diagonal cracks in the region subjected to moment and shear (Fig. 1.2/1).

The designation used for such failures is not uniform. Terms like

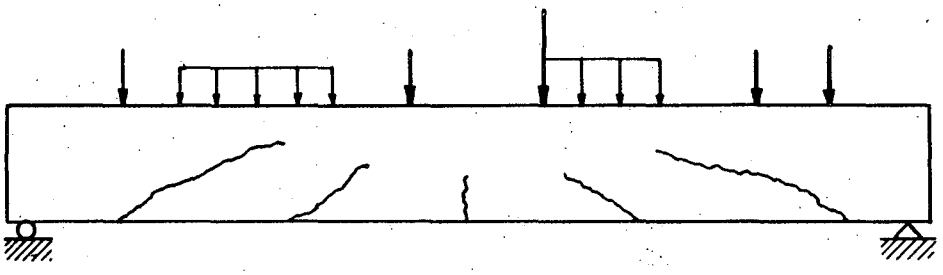

Fig. 1.2/1

Crack Pattern of a Beam Subjected to Moment and Shear

Shear Failure (S)

Diagonal Tension Failure (DT)

Shear Compression Failure (SC)

Bond Failure (B)

can be found in the literature. Even though the term "Shear Failure" is the most unprecise of all, it is the one most often used and serves somewhat as an overall expression for others. Especially in the earlier stage of the research, failures due to slippage of the longitudinal reinforcement, i.e. "Bond Failures," were often erroneously interpreted as shear failures because of their similar appearance to the latter. "Diagonal Tension Failures" are characterized by a sudden development of one or more diagonal cracks immediately followed by failure. If failure occurs by crushing of the concrete compressive zone considerably after the formation of diagonal cracks, it is usually called "Shear Compression Failure." As for the theory stated in this paper, it will not be necessary to distinguish between these different types of failure, because the derivation of the formulas accounts for all the mentioned phemomena, excluding bond.

The ultimate strength of a beam is given by some authors as the shear force V_u acting at the failure cross-section (Fig. 1.2/2) and by others as the corresponding moment, M_{su}.

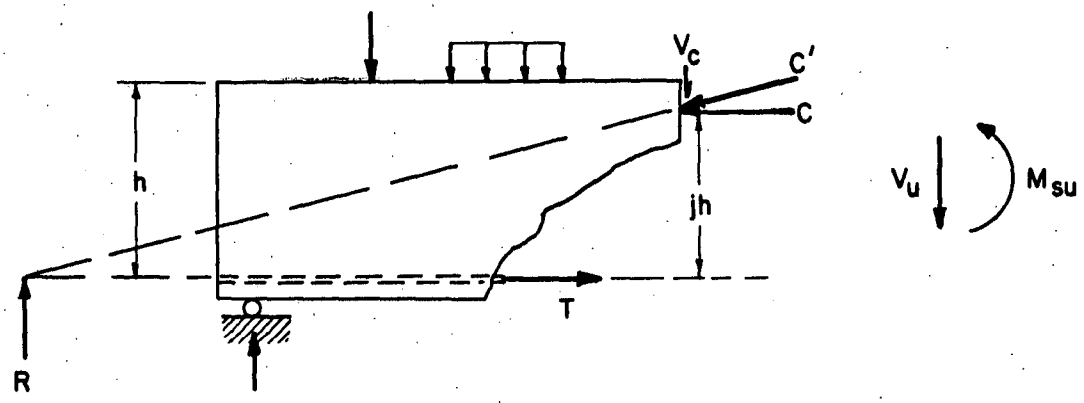

Fig. 1.2/2

Forces at Failure

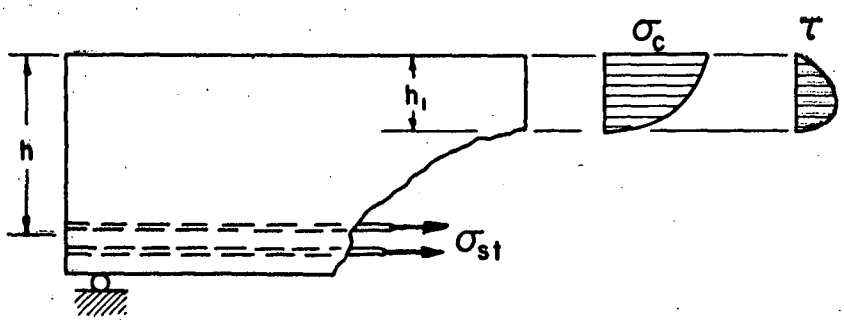

Fig. 1.2/3

Stresses at Failure

As will be shown, both of these quantities taken separately, fail to present a theoretically satisfactory expression for the ultimate strength of a cross-section subjected to moment and shear. The inseparable concatenation of moment and shear requires clearly that the combination of both must be considered. Since it would be rather inconvenient, however, to specify the strength always by two quantities, it has been chosen in this paper, for reasons explained later, to express the strength by the moment capacity of the prospective failure cross-section as a function of the relative magnitude of the shear force, i.e.

$$M_{su} = M_{su}\left(\frac{M}{Vh}\right) \qquad (1/2/1)$$

Instead of carrying on the correct, but somewhat lengthy term, "ultimate moment of a cross-section under the combined action of moment and shear", this quantity M_{su} will henceforth be referred to as "ultimate shear-moment".

In order to determine this moment capacity, it is necessary to obtain information concerning the concrete and steel stresses produced by the moment and shear. The distribution and extension of concrete stresses is of primary importance, since it is always by exhausting the capacity of the concrete compression zone that beams finally

fail. (Failures by rupture of the longitudinal reinforcing occur only for such low percentages of reinforcement as to be outside the range of practicability). The generally accepted simplifying assumptions that

(1) The contribution of the longitudinal reinforcement to the shear transfer is negligible

(2) The shear transfer along the diagonal crack is negligible

together with the knowledge of the stress-strain relationship of steel and concrete, and the statement of equilibrium conditions, are not sufficient to determine the shear strength, as will be explained.

For a beam without web reinforcement, the above assumptions mean that the tension force T (see Fig.1.2/2) acts in the direction of the longitudinal reinforcement and that the lines of action of T , C' (inclined compression force) and R (resultant of the external forces to the left of the considered cross-section) intersect in one point.

To satisfy the equilibrium condition, the horizontal component (C) of the force C' has to be equal to T. The couple C and T constitute the ultimate shear moment

$$C = T = \frac{M_{su}}{jh} \qquad (1.2/2)$$

The vertical component (V_c) of C' in turn has to equal the ultimate shear force V_u

$$V_c = V_u \qquad (1.2/3)$$

Expressed in terms of the stresses (see Fig. 1.2/3) these equations become

$$C = \int_o^{h_1} \sigma_c \, dA_c$$

$$T = \int_{A_{st}} \sigma_{st} dA_{st} \qquad (1.2/4)$$

$$V_c = \int_o^{h_1} \tau \, dA_c$$

A great number of investigators have immortalized their names by assuming various distributions of the concrete normal stresses σ_c, but numerical comparisons show that the deviation of the ultimate moment resulting from various reasonable choices is rather small. What really matters, is the depth of the neutral axis (h_1). If this depth were known, the ultimate shear moment could be determined fairly accurately.

Unfortunately, this quantity h_1, has not, as yet, been derived by rational approaches.

As is sufficiently known, the depth of the neutral axis (h_1) for pure bending, is found with the aid of Navier-Bernoulli's hypothesis that plane cross-sections remain plane after deformation; a hypothesis which is sometimes referred to as deformation condition, strain condition, or compatibility condition, the latter term being used in this paper. This hypothesis does not hold true for regions subjected to moment and shear, especially not after formation of diagonal cracks. Thus it can be said, that the particular difficulty of the problem of shear is caused by the inability to formulate an appropriate compatibility condition.

Before discussing how this difficulty may be overcome, it shall be clarified why cracks in the bending zone usually do not, and why cracks in the shear zone do, devaluate Navier-Bernoulli's hypothesis.

1.3 COMPARISON WITH PURE BENDING

Navier-Bernoulli's hypothesis that plain cross-sections remain plain after deformation was adopted from the very beginning to reinforced concrete design, and it is surprising to note how little concern arose about its adaptability after the formation of cracks.

According to the mathematical theory of elasticity, the hypothesis holds true only for pure bending or bending with axial load, but not if shear is present. Furthermore, it is originally stated in terms of displacements and only on account of continuity is it possible to conclude that the strain distribution over a cross-section must be linear. Since cracks sharply interrupt the continuity, there is no direct reason why this hypothesis should still hold true. In fact, the relative displacement between concrete and steel contradicts such an assumption. Experimental evidence shows (Ref. 1.3/1; Fig. 1.3/1), that not even the steel strains of different layers of reinforcement follow a straight line over a vertical cross-section. Long experience has taught, however, that the assumption of a linear distribution of concrete and steel strains yields, in general, satisfactory results for the prediction of both stresses and strength. The reason can be found by considering first the

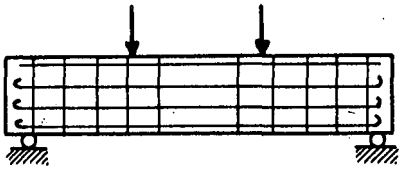

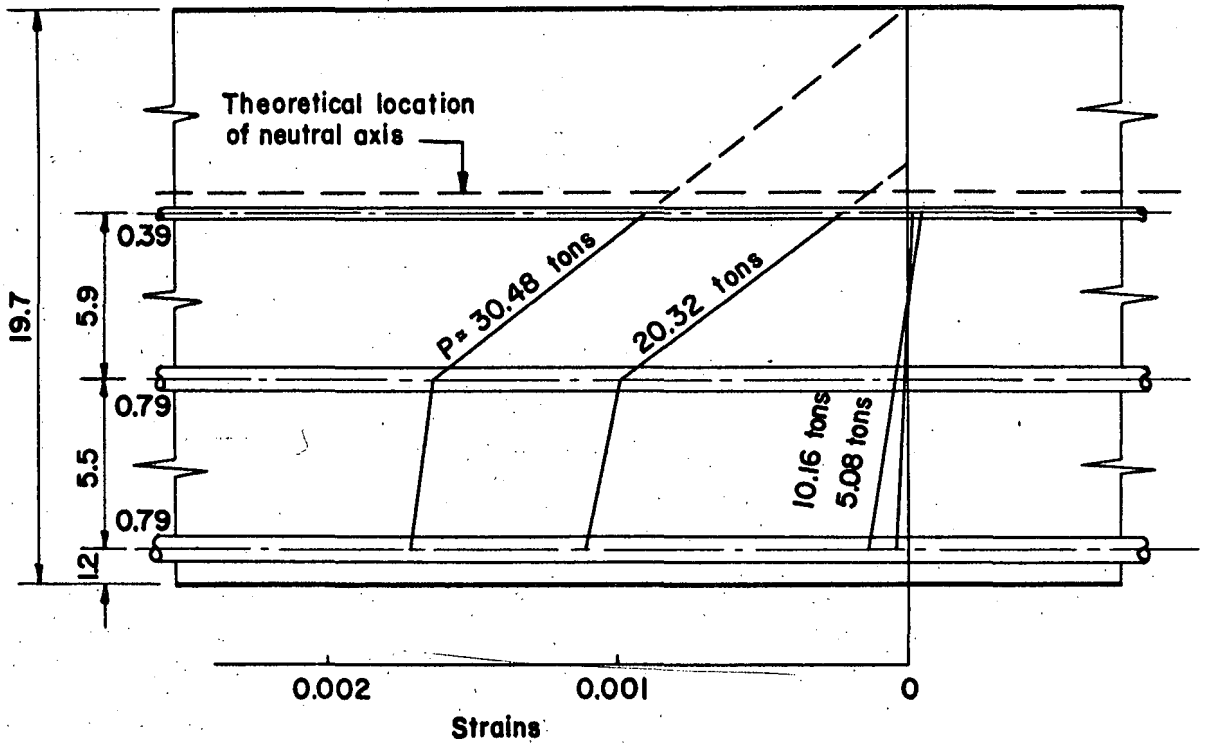

Note: all dimensions in inches

Fig. 1.3/1

Strain Distribution Over a Cross-Section of a Conventionally Reinforced Beam (Tests see Ref. 1.3/1)

actual strain distribution along the whole beam and second, the sensitivity of the ultimate strength to deviations from the straight line assumption.

An example of the distribution of concrete and steel strains for a beam with only vertical cracks in the region of pure bending is shown in Fig. 1.3/2. The relative strain alternations depend mainly on the quality of bond. Since for comparatively good bond the end sections of the portion of pure bending remain plane, one may assume without great error, that the average steel strains, together with the average concrete compressive strains, form a straight line over a vertical cross-section. Such an averaging process is obviously not possible for poor bond (see Fig. 1.3/2). Thus one can conclude that Navier-Bernoulli's hypothesis, in terms of strains, applies only if cracks do not result in a strain concentration.

Considerations of the theory of errors reveal, furthermore, the fact that the ultimate moment is relatively insensitive to deviations from a straight line assumption. A deviation on the part of the steel, as shown in Fig. 1.3/1 will therefore have a rather small effect on the ultimate moment, whereas a strain concentration, which can surpass the surrounding strains by several hundred per cent, can yield results, radically different from those obtained with a straight line assumption.

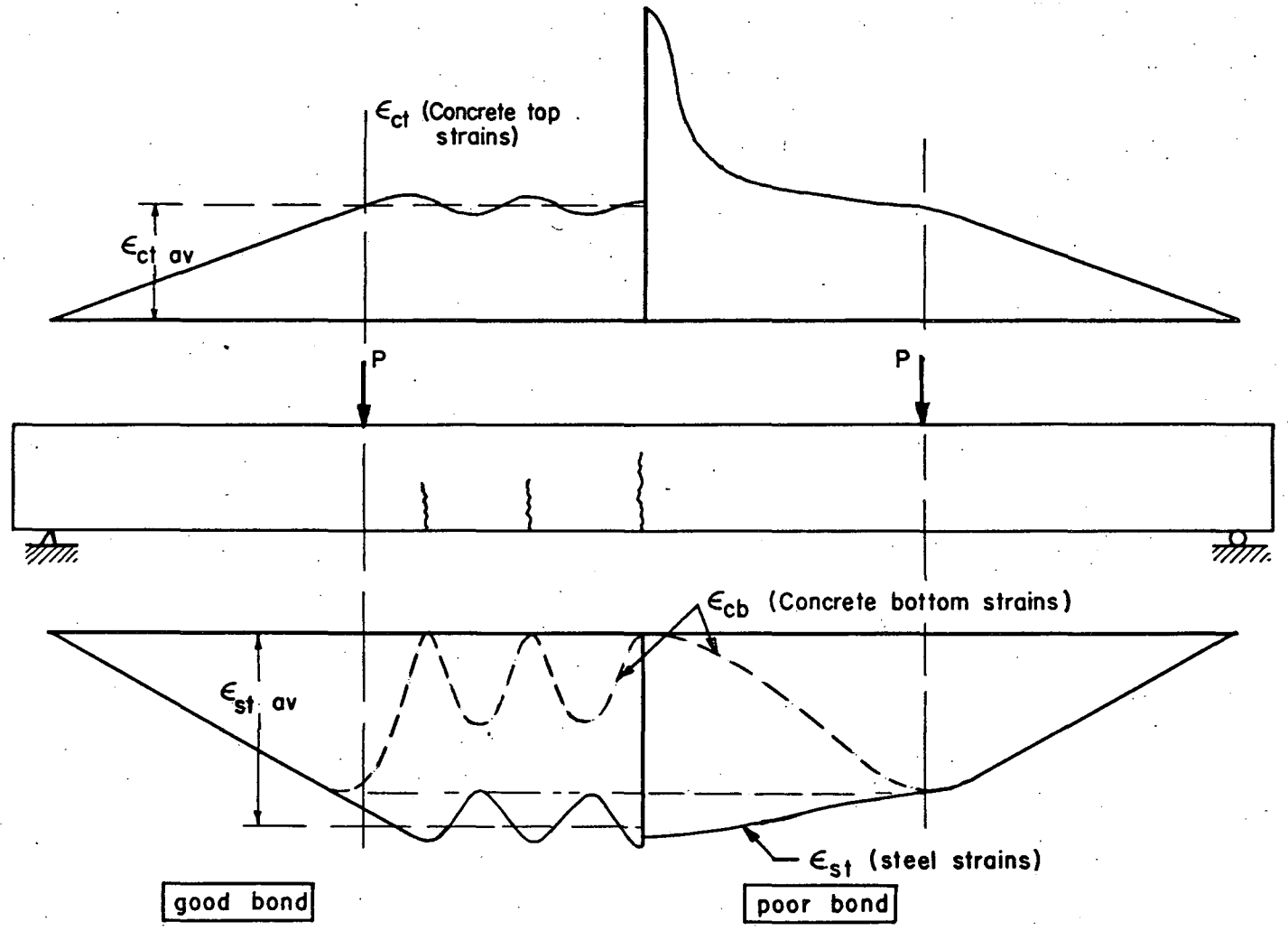

Fig. 1.3 / 2

Strain Distribution of Conventionally Reinforced Beam

Aside from the fact that Navier-Bernoulli's hypothesis is not correct in the region of shear, failures due to diagonal cracks are always associated with a pronounced strain concentration (Fig. 1.3/3). The situation is worsened because the bond stresses not only have to level out the increase of the steel stresses due to cracking, but they have also to build up the tension force in the reinforcement according to the moment gradient. Thus a strain condition of the prospective failure cross-section cannot possibly be stated without considering the surrounding deformations. This is the fundamental difference between vertical and diagonal cracks: the first permit and the latter exclude, in general, a compatibility condition confined to cross-sections only.

It can furthermore be seen that the quality of bond, so far never taken into account quantitatively, is a determining variable of the problem of shear.

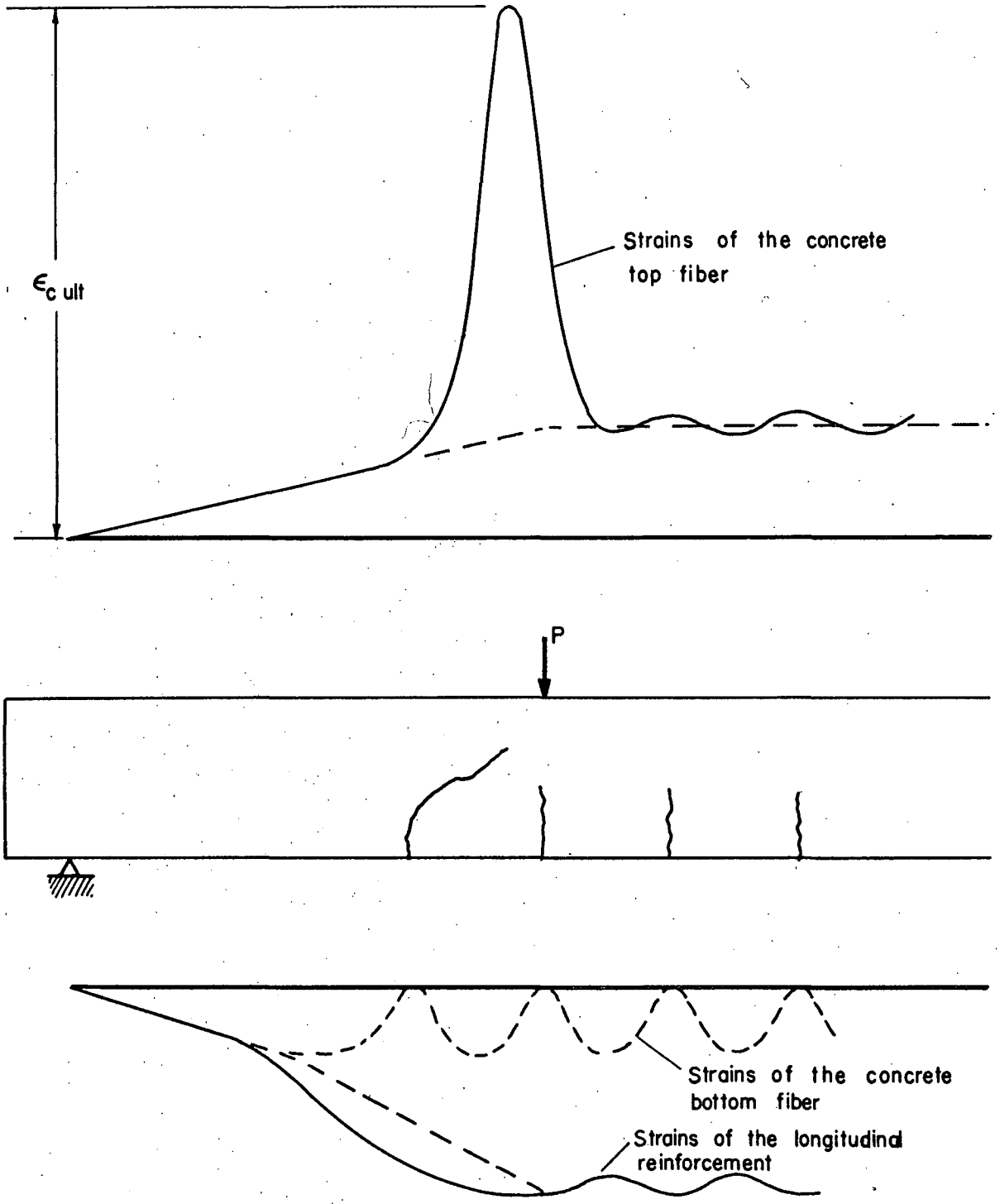

Fig. 1.3/3

Strain Distribution for a Beam With Diagonal Cracks

1.4 POSSIBILITIES OF APPROACH

As implied in the foregoing, there are in principle, two possibilities of attacking the problem, i.e., either to find or to evade a formulation of a compatibility condition. This distinction is chosen to concisely introduce the ideas of some investigators, however, without giving reference to all of them, a task which was already undertaken by the thorough literature research published in Ref. 1.4/1; 1.4/2.

Mörsch (1.4/3), one of the first and most eminent investigators in this field, and Ritter (1.4/4), evaded a compatibility condition by stating the famous "truss-analogy", i.e., by considering the beam as a truss with the longitudinal reinforcement and the concrete top zone as tension and compression chords respectively, the truss bracing being formed by the web reinforcing (tension bars) and by the web concrete acting under 45° in compression. This constitutes clearly a rational approach. The depth of the concrete compression chord remains, however, unknown, thus the truss analogy can only furnish approximate information about the ultimate shear-moment if the failure is due to yielding of the steel. The development of modern reinforcing steels with high distinct yield points or with none at all, has shifted the failure cause from the steel

to the concrete. The truss-analogy must therefore be abandoned for the prediction of the ultimate shear moment. Mörsch's ideas prevail, however, in all specifications, as far as the computation of allowable stresses in the web reinforcement is concerned, by means of the well-known "shear diagram". This was, after all, the ultimate goal of Mörsch's research, i.e., to dimension the web reinforcement such that failure occurs in bending rather than in shear. This school of thought was further developed and refined, notably by Dischinger (1.4/5) and Rausch (1.4/6).

Several investigators, e.g., Richart (1.4/7), Moretto (1.4/8), and Clark (1.4/9), tried to derive the shear strength by formulating the nominal average shearing stress (v_u) at failure as a function of various parameters such as the concrete strength (f'_c), the ratio of longitudinal and web reinforcement (p and r), and the ratio of the shear span* to the effective depth (a/h) of the beam,

$$v_u = \frac{V_u}{bh} = F\ (f'_c;p;r;a/h) \qquad (1.4/1)$$

Since this nominal shearing stress has no actual significance in the configuration of the stresses at failure, it is not surprising that this approach failed to give satisfactory agreement outside the range of the tests set up for the cerivation of the particular formulas.

---

* The shear span is usually understood to be the horizontal distance between the support and the first load

Most of the extensive research performed in the last decade at the University of Illinois belongs in the category of avoiding the formulation of a compatibility condition. The approach suggested in the publication "Strength in Shear of Reinforced Concrete Beams" by Laupa, Siess and Newmark (1.4/2) is characterized by its striking simplicity which marks its special value but also its limitation. Their basic idea was to derive an empirical expression for the quantity

$$\frac{M_{su}}{bh^2 f_c' \ (k + np')}$$

as a function of whatever variable might be of concern. For the interpretation of test results, it proved advantageous to introduce the term k, i.e. the relative depth of the neutral axis as ordinarily determined for transformed areas (straight line theory). The quantity "n" refers to the ratio of the modulus of elasticity of steel to that of concrete and p' is the ratio of the compressive reinforcement. The investigators suggested for beams without web reinforcement

$$\frac{M_{su}}{bh^2 f_c' \ (k + np')} = 0.57 - \frac{4.5 \ f_c'}{10^4} \qquad (1.4/2)$$

This empirical expression was obtained by fitting a straight line through a plot of a great number of test results. Some

limitation lies in the lack of revealing a rational failure mechanism. It was therefore necessary to derive the influence of stirrups again purely empirically, which resulted in a much poorer agreement with test results. For the same reason, no rational modification is possible for prestressed concrete.

Moody, Viest, Elstner, and Hognestad (1.4/10) have chosen to give empirical information about the shear strength essentially in terms of the steel stress at failure.

$$f_s = 0.729 \left[6.9 \times 10^{-4} \, E_{st} \left(-1 + \sqrt{1 + \frac{1450}{p E_s / k_1 k_2 f_c'}} \right) \right] \quad (1.4/3)$$

With this information, the ultimate moment can be calculated by observing the equilibrium conditions alone, which the authors have chosen to formulate very meticulously.

Only one attempt to state an outright rational strain or compatibility condition can be found in the literature. In his dissertation, "Shear Strength Of Simply Supported Prestressed Concrete Beams", Zwoyer (1.4/11) suggested that the average strains of the whole shear span remain in a linear relationship over the depth of the beam. It is hard, however, to conceive what bearing this average strain should have on the stress concentration at the failure cross-section.

As for other methods of attack, one might be inclined to rely on some kind of a lower bound theorem as successfully

used in the plastic analysis of steel structures. It has to be said, however, that due to the development of cracks, the exact dimensions of the load carrying parts of the structure are essentially unknown, thus excluding the application of such methods.

The approach proposed in this paper is an endeavor to obtain a rationally founded compatibility condition. In addition to the variables taken into account in most investigations, the influence of the bond and the influence of the state of stress in the concrete, are considered. This does not make the theory more complicated; on the contrary, they permit a rational numerical explanation of phenomena which so far had to be derived empirically.

2. THE INFLUENCE OF THE STATE OF STRESS ON SHEAR FAILURES

2.1 GENERAL

As mentioned in the introduction, a theoretically satisfactory failure condition can only be expressed by a combination of both moment and shear force. Since the final failure occurs always by destruction of the concrete compressive zone, it will logically depend on the state of stress prevailing in this zone, and not only on the normal stress component as generally presumed. Consequently it will be necessary first to determine the stress configuration produced by the combination of moment and shear and second to compare this configuration with a suitable failure criterion for plain concrete.

The first task will, admittedly, involve some guessing; the influence of its arbitrariness can, however, be estimated.

Concerning the second point, it has to be emphasized that, contrary to some statements in the literature, reliable failure criteria for plain concrete are firmly established. The one stated by Mohr (2.1/1) some 50 years ago, for example, has thoroughly been checked by many tests and many investigators.

2.2 THE STATE OF STRESS OF BEAMS SUBJECTED TO MOMENT AND SHEAR

Prior to the formation of diagonal cracks, the approximate stress distribution can easily be determined, if one retains the assumption that plain cross-section remain plain after deformation of the beam — an assumption which, due to the presence of shear, is theoretically not quite correct, but which seems permissible in view of the far graver idealizations necessary because of the materials employed.

With this assumption the formulas for the stresses over a given cross-section become

$$\sigma_x = \frac{F}{bh} - \frac{Fey}{I} + \frac{M}{I}\, y$$

$$\tau_{xy} = \frac{VQ}{bI} \qquad (2.2/1)$$

where $$Q = \int_{y}^{yc} y \, dA$$

An example of this stress distribution is shown in Fig. 2.2/1 for a rectangular non-prestressed cross-section.

After the formation of diagonal cracks the stress configuration changes abruptly because the internal forces previously carried by the concrete tension zone have to be redistributed (Fig. 2.2/2). This information, however, does

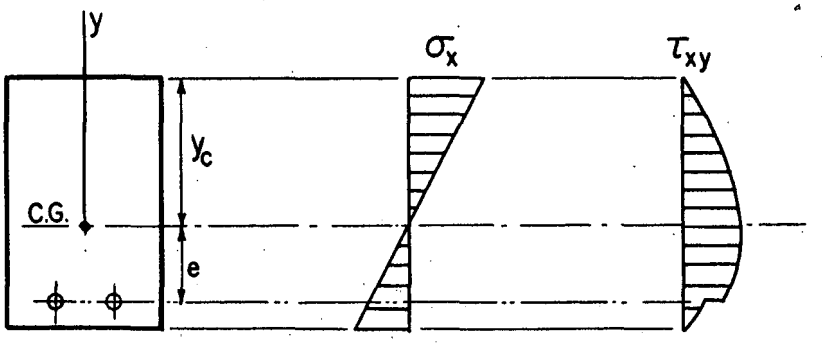

Fig. 2.2/1
Stress Distribution of an Uncracked Rectangular Cross Section

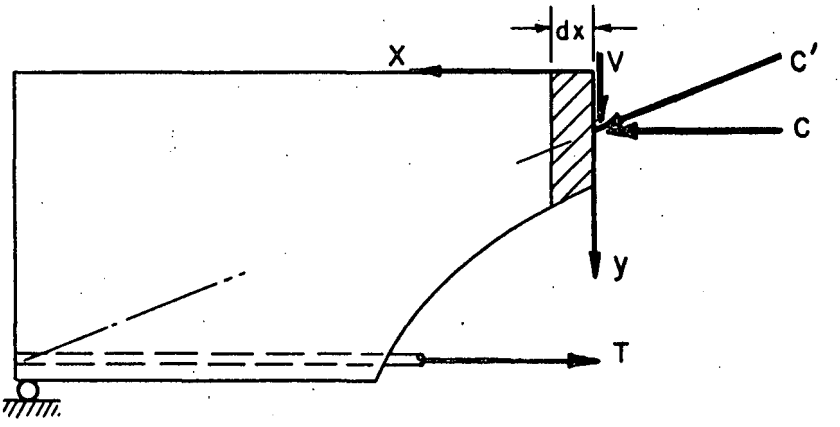

Fig. 2.2/2

Redistribution of Internal Forces After Formation of the Diagonal Crack

not suffice to determine the state of stress prevailing in an element of length dx of the concrete compressive zone (Fig. 2.2/2). This requires the additional, and to some degree arbitrary, assumption that

> the distribution curves of the normal stresses on both sides of dx are second order parabolas with the vertex at the concrete top fiber (Fig. 2.2/3).

This assumption is not so plausible as it might appear at first glance. Firstly, the parabolic shape is not rationally rooted because the vertical sections above the crack must not necessarily remain plane, and secondly, if they do remain plane and if the stress strain relationship of concrete is parabolic, the curve to the left of the element dx could not possibly have its vertex at the same level as the curve to the right. It will therefore be necessary to estimate the influence of the arbitrariness of this assumption. With the notations given in Fig. 2.2/3, the normal stresses become

$$\sigma = \sigma_o \left[1 - \left(\frac{y}{h_1}\right)^2 \right] \qquad (2.2/2)$$

$$\sigma' = \sigma'_o \left[1 - \left(\frac{y}{h_1 + \tan\gamma \cdot dx}\right)^2 \right] \qquad (2.2/3)$$

where the unprimed quantities refer to the right, and the primed to the left side of the element dx. The maximum stresses at y = 0 are denoted by the subscript o.

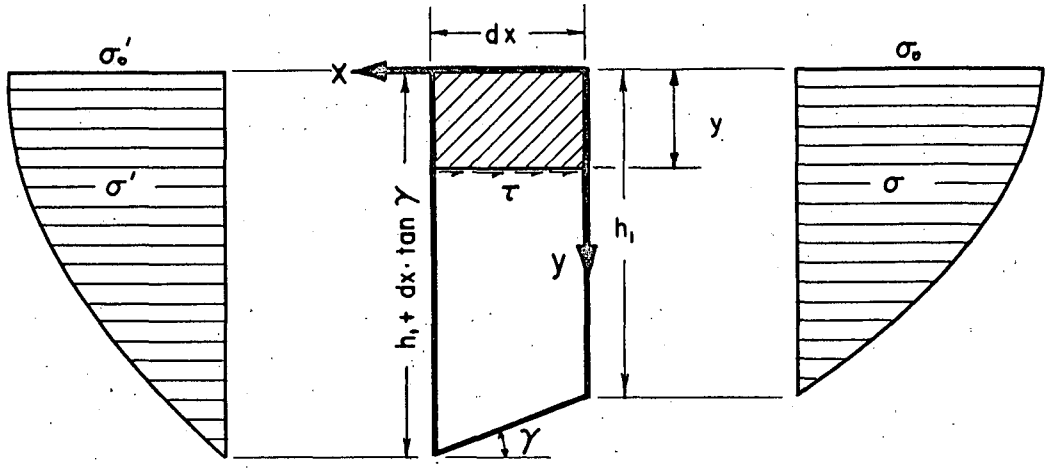

Fig. 2.2/3

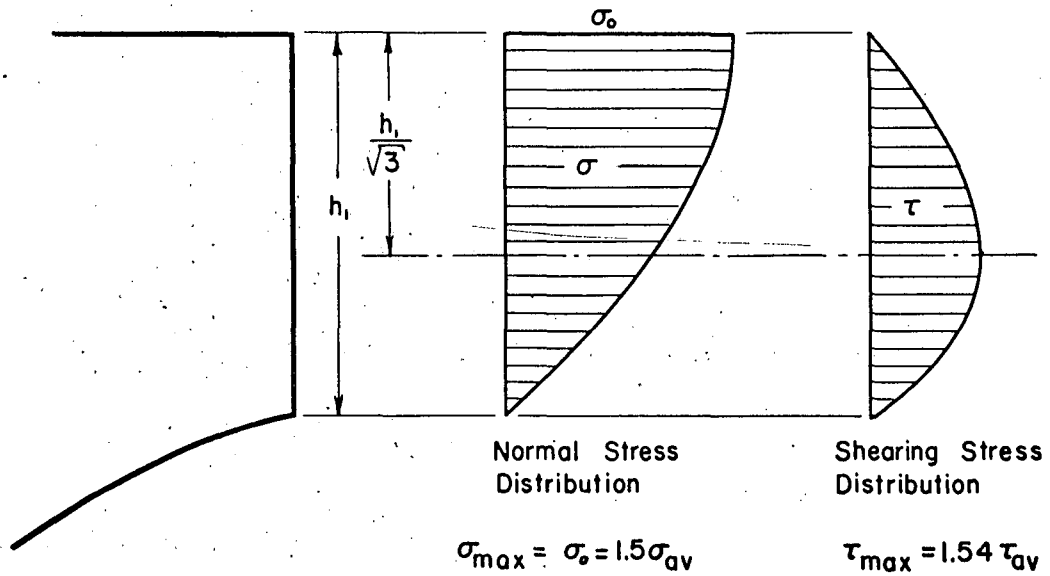

Fig. 2.2/4

Stress Distribution at the Concrete Compressive Zone

For a state of equilibrium, the resultant forces of the two stress blocks have to be equal, thus

$$\sigma_o' = \frac{h_1}{h_1 + \tan\gamma \cdot dx}\ \sigma_o \qquad (2.2/4)$$

This configuration of normal stresses implicitly determines the magnitude and distribution of the shearing stresses which can be found by considering the equilibrium conditions of an element $dx \cdot y$ (shaded in Fig. 2.2/3).

$$\overline{\tau}(y) = \frac{\int_0^y \sigma\, dy - \int_0^y \sigma'\, dy}{dx} \qquad (2.2/5)$$

By substituting 2.2/2, 2.2/3 and 2.2/4 in 2.2/5, one obtains

$$\overline{\tau}(y) = \frac{\sigma_o}{dx} \int_0^y \left[1 - \frac{y^2}{h_1^2} - \frac{h_1}{h_1 + \tan\gamma \cdot dx} + \frac{h_1 y^2}{(h_1 + \tan\gamma \cdot dx)^3} \right] dy$$

$$= \frac{\sigma_o}{dx} \left[y - \frac{y^3}{3h_1^2} - \frac{h_1 y}{h_1 + \tan\gamma \cdot dx} + \frac{h_1 y^3}{3(h_1 + \tan\gamma \cdot dx)^3} \right]$$

$$= \sigma_o \left[\frac{y \cdot \tan\gamma}{h_1 + \tan\gamma\, dx} - \frac{y^3}{3h_1^2} \left(\frac{3h_1^2 \tan\gamma + 3h_1 \tan^2\gamma\, dx + \tan^3\gamma\, dx^2}{(h_1 + \tan\gamma\, dx)^3} \right) \right]$$

Consequently,

$$\tau(y) = \lim_{dx \to 0} \overline{\tau}(y) = \sigma_o \left[\frac{y \cdot \tan\gamma}{h_1} - \frac{y^3 \tan\gamma}{h_1^3} \right]$$

or finally,

$$\tau(y) = \sigma_o \cdot \tan\gamma \left[\frac{y}{h_1} - \frac{y^3}{h_1^3}\right] \qquad (2.2/6)$$

The integral of these shearing stresses over the whole compressive zone must equal the shear force V :

$$V = \int_0^{h_1} b\,\tau\,dy = b\,\sigma_o \tan\gamma \left[\frac{h_1}{2} - \frac{h_1}{4}\right]$$

or

$$\sigma_o = \frac{4V}{\tan\gamma \cdot bh_1} \qquad (2.2/7)$$

and by substituting in 2.2/6

$$\tau(y) = \frac{4V}{bh_1}\left[\frac{y}{h_1} - \frac{y^3}{h_1^3}\right] \qquad (2.2/8)$$

According to the last equation the distribution curve of the shearing stresses is a parabola of the third order (Fig. 2.2/4), with

$$\tau_{max} \sim 1.54\,\tau_{av}$$

at

$$y = \frac{h_1}{\sqrt{3}}$$

The combination of σ and τ as shown in Fig. 2.2/4 determines the state of stress at any point of the prospective failure cross-section if one neglects local vertical normal stresses

produced by concentrated loads. This simplification is maintained also in the vicinity of the loads, a measure which is conservative in the light of failure criteria.

In order to estimate the accuracy of this result, it is compared in Fig. 2.2/5 with two limiting cases, one by assuming a triangular, and one by assuming a rectangular normal-stress block. This comparison permits the conclusion that a failure criterion applied to the parabolic assumption determines the strength of the concrete compressive zone fairly accurately.

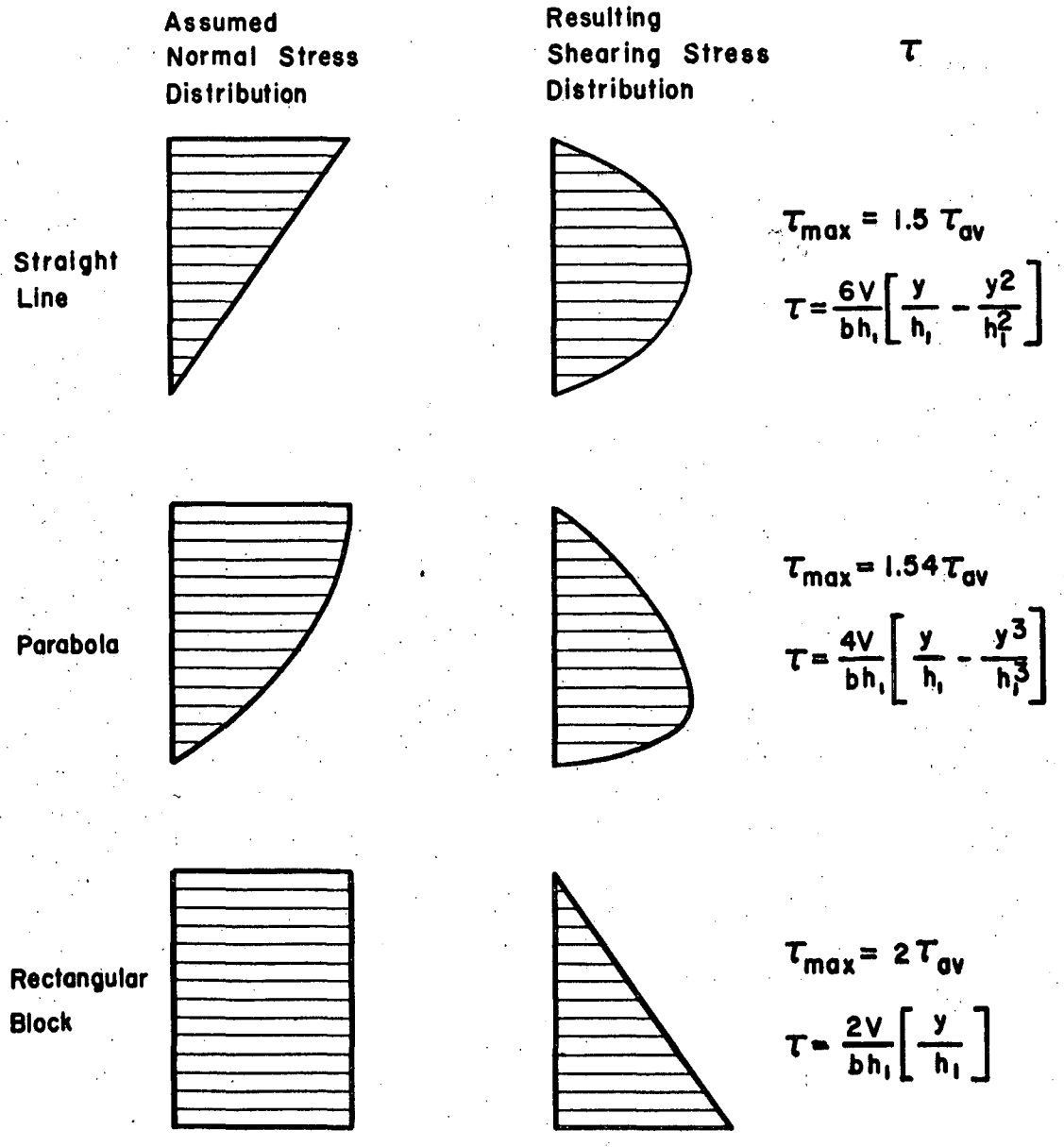

Distribution of Shearing Stresses Resulting From Various Normal Stress Assumptions

Fig. 2.2/5

2.3 MOHR'S FAILURE CRITERION

The failure criterion for plain concrete, introduced by Mohr (2.1/1) does not actually constitute a failure hypothesis, in that no failure cause is presupposed as, for example, in hypotheses of maximum shear or maximum normal stress. It resulted essentially from an apt method of presenting test data, which revealed the fact that the entirety of Mohr's circles representing the states of stress at failure has one common envelope which can be approximated by a parabola of the second order (2.3/1). This experimental root marks the special practicability of Mohr's failure criterion, but also implies its shortcomings. Among the latter counts the fact that it does not reveal any failure mechanism. Consequently, a prediction of the failure plane is, in general, not possible.

Many textbooks give misleading information in this respect by presuming that the angle between the failure plane and the direction of the minor principal stress is equal to one-half of the angle formed in Mohr's presentation by the horizontal axis and the radius of the circle in question, pointing to the contact of circle and envelope. This misinterpretation stems probably from the entirely different concept of Coulomb's failure hypothesis

for soil, which presupposes the failure mechanism by stating that a given plane slides when

$$\tau > \tau_o + k\,\sigma$$

where τ and σ are the stress components of the plane in question, and τ_o and k are material constants. In Mohr's presentation, this would mean that the failure envelope is a straight line, and that the inclination of the failure plane is indeed determines as explained above. Since this concept does not apply to concrete, there is no reason why the rules concerning the inclination of cracks should still be valid. On the contrary, experimental evidence contradicts such rules. In general, cracks form perpendicular to the direction of the minor principal stress. The crack pattern is therefore assumed to follow the stress trajectories.

Mohr's failure criterion is often criticized for another shortcoming: due to experimental difficulties and due to the two-dimensional form of presentation, the influence of the intermediate principal stress σ_3 ($\sigma_1 < \sigma_3 < \sigma_2$) is neglected. This fact is, however, of no concern for this consideration, since the problem dealt with herein involves anyhow, only a plane state of stress.

As known, a plane state of stress can be characterized at any point by the so-called Mohr's stress-circle (Fig. 2.3/1), which can mathematically be expressed as

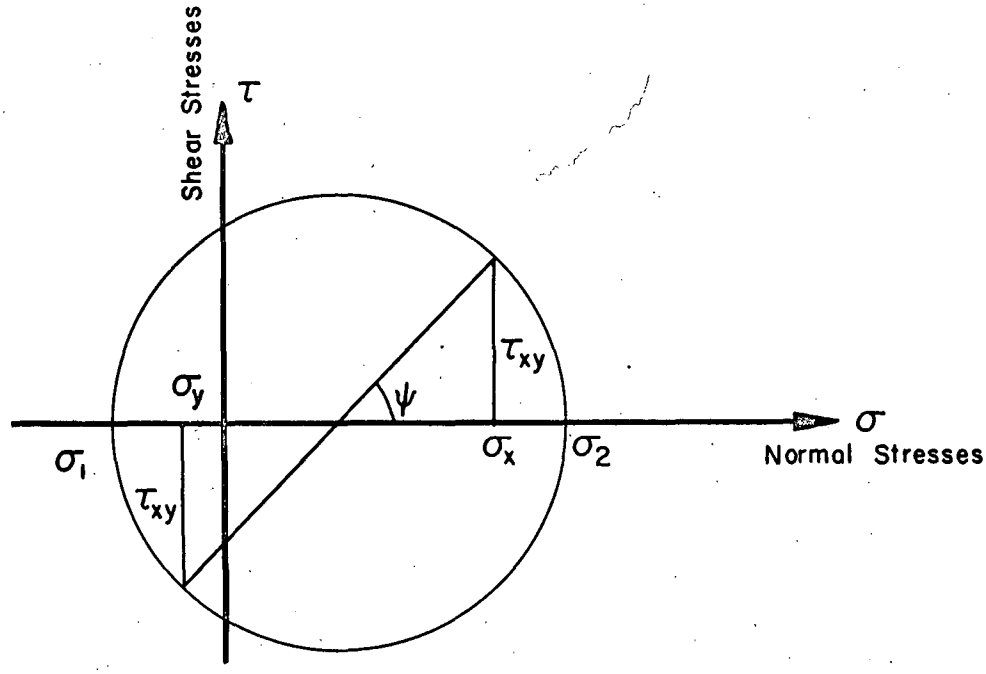

Mohr's Circle

Fig. 2.3/1

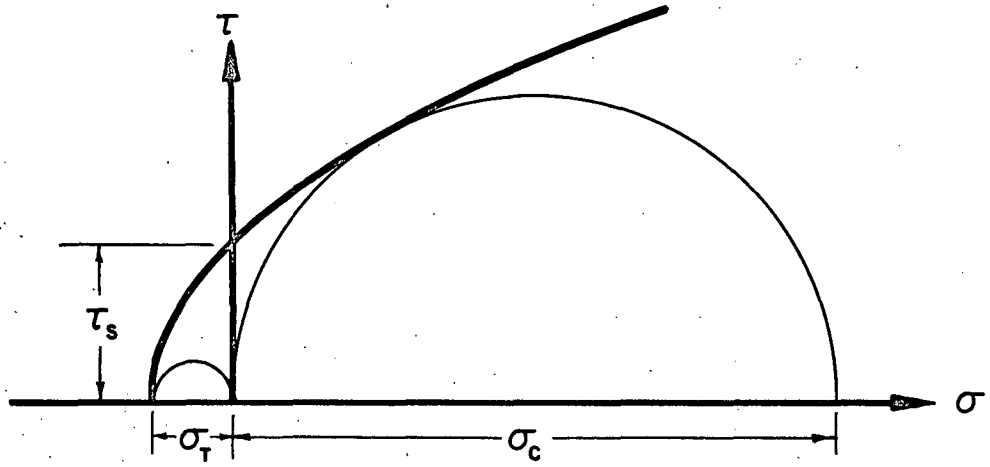

Mohr's Failure Criterion

σ_c = Concrete compressive strength

σ_T = Concrete tensile strength

Fig. 2.3/2

$$\sigma^2 - (\sigma_1 + \sigma_2)\,\sigma + \tau^2 + \sigma_1\sigma_2 = 0 \qquad (2.3/1)$$

where σ_1 and σ_2 are the principal stresses, and σ and τ are the stress variables convention: (σ_1 σ_2; tension (-); compression (+)).

In accordance with a great number of tests, (Ref. 2.2/1), the failure envelope (Fig. 2.3/2) for a given concrete can be written as

$$\left(\frac{\tau}{\tau_s}\right)^2 + \frac{\sigma}{\sigma_T} = 1 \qquad (2.3/2)$$

where σ_T (negative) is the linear tensile strength, and τ_s is the shearing stress at $\sigma = o$. Since τ_s is difficult to obtain experimentally, it is convenient to express the failure parabola in terms of the concrete compressive strength σ_c.

$$\tau^2 = \left[\sigma_c - 2\sigma_T - 2\sqrt{(\sigma_T - \sigma_c)\,\sigma_T}\right](\sigma - \sigma_T) \qquad (2.3/3)$$

or with the abbreviation

$$k = \left|\frac{\sigma_T}{\sigma_c}\right|$$

$$\tau^2 = \sigma_c\left[1 + 2k - 2\sqrt{(k+1)k}\right](\sigma + k\,\sigma_c) \qquad (2.3/4)$$

These equations do not yet constitute a failure criterion for σ and τ, they specify merely the shape of the failure envelope. The failure criterion can be found by observing that a particular stress circle, given by σ_x, σ_y, and τ_{xy}, has to contact the envelope. A general stress circle is given by

$$\sigma^2 + \tau^2 - (\sigma_x + \sigma_y)\,\sigma + \sigma_y\,\sigma_x - \tau_{xy}^2 = 0 \qquad (2.3/5)$$

where σ and τ are the coordinates of any point of the circle, and σ_x, σ_y, and τ_{xy} are the stress components of an element dx dy of a body in the x-y coordinate system (Fig. 2.3/3).

The points of intersection of any circle with the parabola can be found by substituting Eq. 2.3/4 in Eq. 2.3/5. Solved for the o coordinate of the points of intersection (σ_I and σ_{II}), this yields

$$\sigma_{I,II} = \frac{-A\sigma_c + \sigma_x + \sigma_y \pm \sqrt{(A\sigma_c - \sigma_y - \sigma_x)^2 - 4\,(Ak\sigma_c^2 + \sigma_x\sigma_y - \tau_{xy}^2)}}{2} \qquad (2.3/6)$$

where

$$A = 1 + 2k - 2\sqrt{(k+1)\,k}$$

If now the circle shall be tangential to the parabola, then $\sigma_{I,II}$ has to be single-valued, i.e., the square root in Eq. 2.3/6 has to vanish. Consequently,

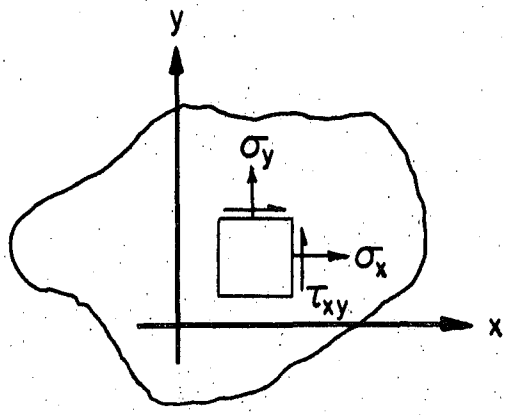

Fig. 2.3/3

Body and Stress Coördinates

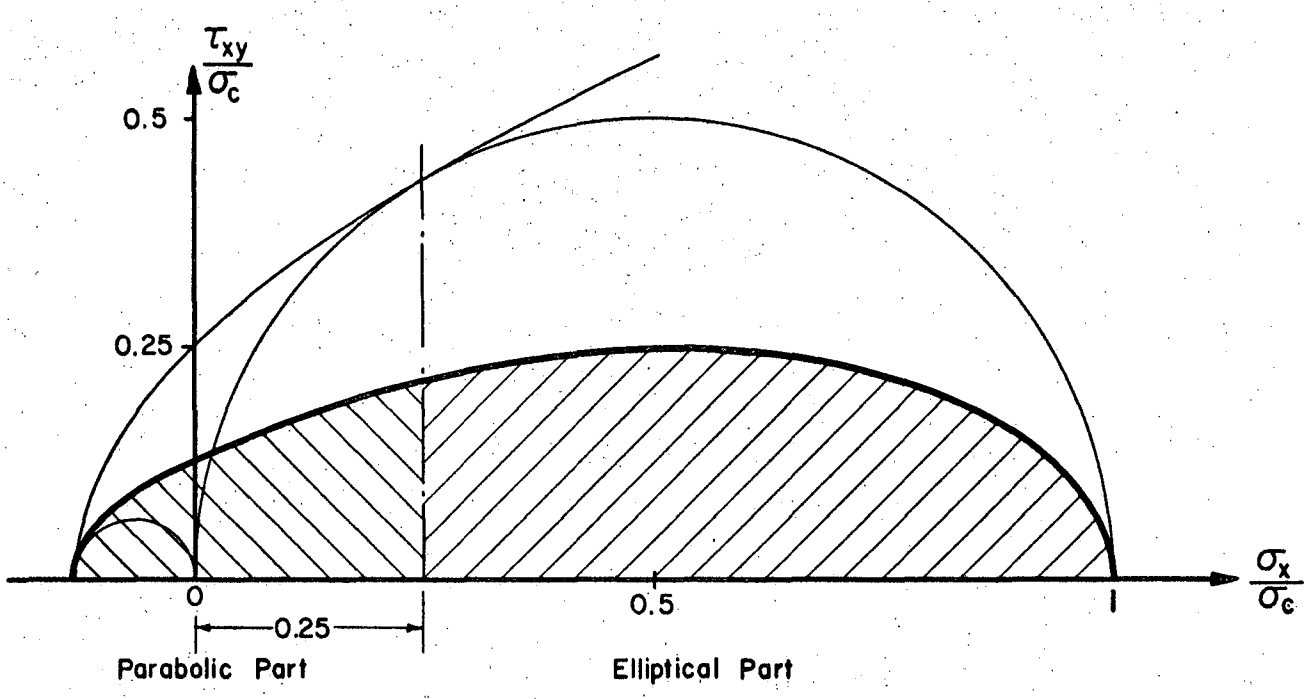

Fig. 2.3/4

Mohr's Failure Criterion

Adapted for plane state of stress with $\sigma_y = 0$ ($\sigma_c = 8\sigma_T$). Any stress combination σ_x, τ_{xy}, $\sigma_y = 0$ outside the shaded area will cause failure.

$$(\sigma_x - \sigma_y)^2 - 2A\sigma_c(\sigma_x + \sigma_y) + 4\tau_{xy}^2 + A^2\sigma_c^2 - 4Ak\sigma_c^2 = 0 \qquad (2.3/7)$$

This is now the mathematical form of Mohr's failure criterion. In the course of substitution, however, some imaginary solutions were incorporated. If, namely,

$$\sigma_x + \sigma_y - A\sigma_c < -2k\sigma_c$$

then the contact point would lie outside the real region of the parabola. Therefore, Equation 2.3/7 applies only if

$$\sigma_x + \sigma_y - A\sigma_c > -2k\sigma_c \qquad (2.3/8)$$

The possibility of a failure configuration exists, however, also in region excluded by Eq. 2.3/8, namely, if the stress circle has the contact point at the vertex of the parabols, i.e.,

$$(k\sigma_c)^2 + (\sigma_x + \sigma_y)\, k\sigma_c + \sigma_y\sigma_x - \tau_{xy}^2 = 0 \qquad (2.3/9)$$

Consequently, the failure criterion has to be expressed separately for the two regions, which are divided by Eq. 2.3/8.

As for the application to failure conditions of beams, use is made of the previous assumotion that $\sigma_y = 0$. A further simplification is possible by relying on experimental findings concerning the ratio of tensile to compressive strength. Although this ratio is not constant, it

would, in view of the complexity of the problem, lead too far to carry this parameter on to the general theory of shear failures. Roš (Ref. 2.3/1), has found that this ratio varies from about one-sixth to one-tenth. Thus an average value of

$$k = \left| \frac{\sigma_T}{\sigma_c} \right| = \frac{1}{8}$$

is chosen hereafter, reducing the failure criterion to

$$\left(\frac{\sigma_x}{\sigma_c}\right)^2 - \frac{\sigma_x}{\sigma_c} + \left(\frac{2\tau_{xy}}{\sigma_c}\right)^2 = 0$$

$$\text{for} \quad \frac{\sigma_x}{\sigma_c} > \frac{1}{4} \qquad (2.3/7b)$$

and

$$\left(\frac{8\tau_{xy}}{\sigma_c}\right)^2 - \left(\frac{8\sigma_x}{\sigma_c}\right) - 1 = 0$$

$$\text{for} \quad \frac{\sigma_x}{\sigma_c} < \frac{1}{4} \qquad (2.3/9b)$$

These findings can geometrically be interpreted in the $\sigma - \tau$ diagram as an affine transformation of the original failure envelope (parabolic part) and the circle of the compressive strength (elliptical part), the ratio of affinity being one-half (Fig. 2.3/4).

2.4 APPLICATION OF FAILURE CRITERION TO BEAMS

Approach by Bresler and Pister. An attempt to apply a failure criterion to determine the shearing strength of reinforced concrete beams has already been made by Bresler and Pister (Ref. 2.4/1, pp. 21 to 31). Instead of only dealing with normal stresses, the authors rightly pointed out the importance of considering the state of stress which causes failure.

Based on the investigations of the ultimate strength of reinforced concrete beams in bending by Hognestad, Hanson, and McHenry (2.4/2), it was assumed that the general normal stress at failure be

$$\sigma_c = \frac{3900 + 0.35\ f'_c}{3200 + f'_c}\ f'_c \qquad (2.4/1)$$

With a further assumption that the steel stress of the longitudinal reinforcing approximately equals the yield stress fy (an assumption of very limited accuracy), the depth of the neutral axis was calculated to be

$$\frac{h_1}{h} = \frac{p\ fy}{o_c} \qquad (2.4/2)$$

The shear force capacity (V) of the concrete compressive zone was then obtained by

$$V = \tau\, bh_1 \qquad (2.4/3)$$

where τ is a function of σ, according to the failure criterion stated by the authors.

This concept implies that for a given concrete cylinder-strength (f'_c) the failure is determined by the shearing force V only, and that σ is constant. This would, in effect, mean that a shear force smaller than indicated by Formula 2.4/3 could never cause failure. Thus one could obtain a moment capacity of any desired magnitude by simply shifting the shearing force V far enough from the support.

A misconception lies in the assumption that for a given f'_c, only τ , but not σ is a variable, or in other terms, only one point of the failure criterion is being considered. In reality, the number of combinations of σ and τ which determine the failure is infinite. For a particular beam, the actual combination causing failure depends on the load configuration.

New Approach. With the aid of the shear and normal stress distribution (established in Section 2.2) and a failure criterion (given in Section 2.3), the

implements are ready for a determination of the manner in which the bending moment and the shear force affect the shear failure.

There is, however, one important question as to where and how a stress configuration has to be critical. One could think of several possibilities, i.e., failure occurs if:

(1) The stress combination at one point is critical

(2) The failure criterion is fulfilled at all the points of the compression zone

(3) The average stresses over the whole compression zone satisfy the failure condition

(4) The average stresses over a certain portion of this zone are critical

From experience, it is known that the first assumption only applies in cases where a sudden failure propagation can develop, such as in a rupture modulus test or in notched bar tests. Due to the small yet present compressive ductility of concrete, such an assumption is unsuitable. So is the second, because the stresses never become critical in the vicinity of the neutral axia. The third and the fourth assumptions both seem reasonable. By considering the shear and the normal

stress diagrams in Fig. 2.2/4, however, it is evident that with Assumption (3) the influence of the normal stresses is somewhat underestimated. In this paper preference is therefore given to Assumption (4) by considering the critical portion to extend from the vertex of the shear distribution curve to the top of the beam.

Thus the average stresses which serve to formulate the failure condition are defined as

$$\sigma_{av}^{*} = \frac{\int_0^{h_1/\sqrt{3}} \sigma \, dy}{h_1/\sqrt{3}} = \frac{4\,C}{3\,bh_1} \qquad (2.4/4)$$

and

$$\tau_{av}^{*} = \frac{\int_0^{h_1/\sqrt{3}} \tau \, dy}{h_1/\sqrt{3}} \sim \frac{V}{bh_1}$$

(See Fig. 2.2/4)

Hence,

$$\tau_{av}^{*} = \frac{3\,V}{4\,C}\,\sigma_{av}^{*} \,. \qquad (2.4/5)$$

By substituting this expression in the equations of the failure criterion (Eqs. 2.3/7b and 2.3/9b) one obtains:

$$\text{for} \quad \frac{\sigma_{av}^{*}}{\sigma_c} > \frac{1}{4}$$

$$\left(\frac{\sigma_{av}^{*}}{\sigma_c}\right)^2 - \frac{\sigma_{av}^{*}}{\sigma_c} + \left(\frac{3\,V}{2\,C}\,\frac{\sigma_{av}^{*}}{\sigma_c}\right)^2 = 0$$

or

$$\boxed{\frac{\sigma_{av}^*}{\sigma_c} = \frac{1}{1 + (\frac{3}{2}\frac{V}{C})^2}} \qquad (2.4/6a)$$

and for

$$\frac{\sigma_{av}^*}{\sigma_c} < \frac{1}{4}$$

$$\left(\frac{6\ \sigma_{av}^*\ V}{\sigma_c\ C}\right)^2 - \left(\frac{8\ \sigma_x}{\sigma_c}\right) - 1 = 0$$

or

$$\boxed{\frac{\sigma_{av}^*}{\sigma_c} = \frac{1 + \sqrt{1 + \frac{1}{4}\ (\frac{3\ V}{C})^2}}{(\frac{3\ V}{C})^2}} \qquad (2.4/6b)$$

These formulas express the influence of the shear force on the problem of shear failure. They show that the average normal stress (σ_{av}^*), at which the beam fails, is by no means a function only of the concrete strength, but depends very significantly on the ratio of the shear force to the horizontal compressive force. The larger this ratio gets, the smaller becomes the normal stress capacity of the concrete compressive zone. One can, in the same way also express the shear stress capacity,

$$\frac{\tau_{av}^*}{\sigma_c} = \frac{\frac{3\ V}{4\ C}}{1 + (\frac{3}{2}\frac{V}{C})^2} \qquad (2.4/7a)$$

and

$$\frac{\tau_{av}^*}{\sigma_c} = \frac{1 + \sqrt{1 + \frac{1}{4}\left(\frac{3\,V}{C}\right)^2}}{4\left(\frac{3\,V}{C}\right)} \qquad (2.4/7b)$$

A direct application of these relations to beam problems is obviously made difficult, since C, in contrast to V, is not given by the loading condition, but depends on the depth of the compressive zone (h_1). If one would like to convert these last formulas to a direct determination of the shear strength of beams, one would have to find accurate expressions for h_1 and C, which would necessarily involve functions of all the parameters known to influence the shear strength. This procedure would be rather inaccurate. One can expect greater accuracy by working with the variation of the normal stresses (Eq. 2.4/6 and 2.4/6b; Fig. 2.4/1) as follows: The shear strength is considered to be a problem of moment capacity, where the presence of the shear force results in a reduction of the normal stress capacity of the concrete compressive zone (according to Eq. 2.4/6 and 2.4/6b) and naturally, in the formation of diagonal cracks.

On the basis of this view, it seems permissible to introduce practical simplifications, i.e., firstly in

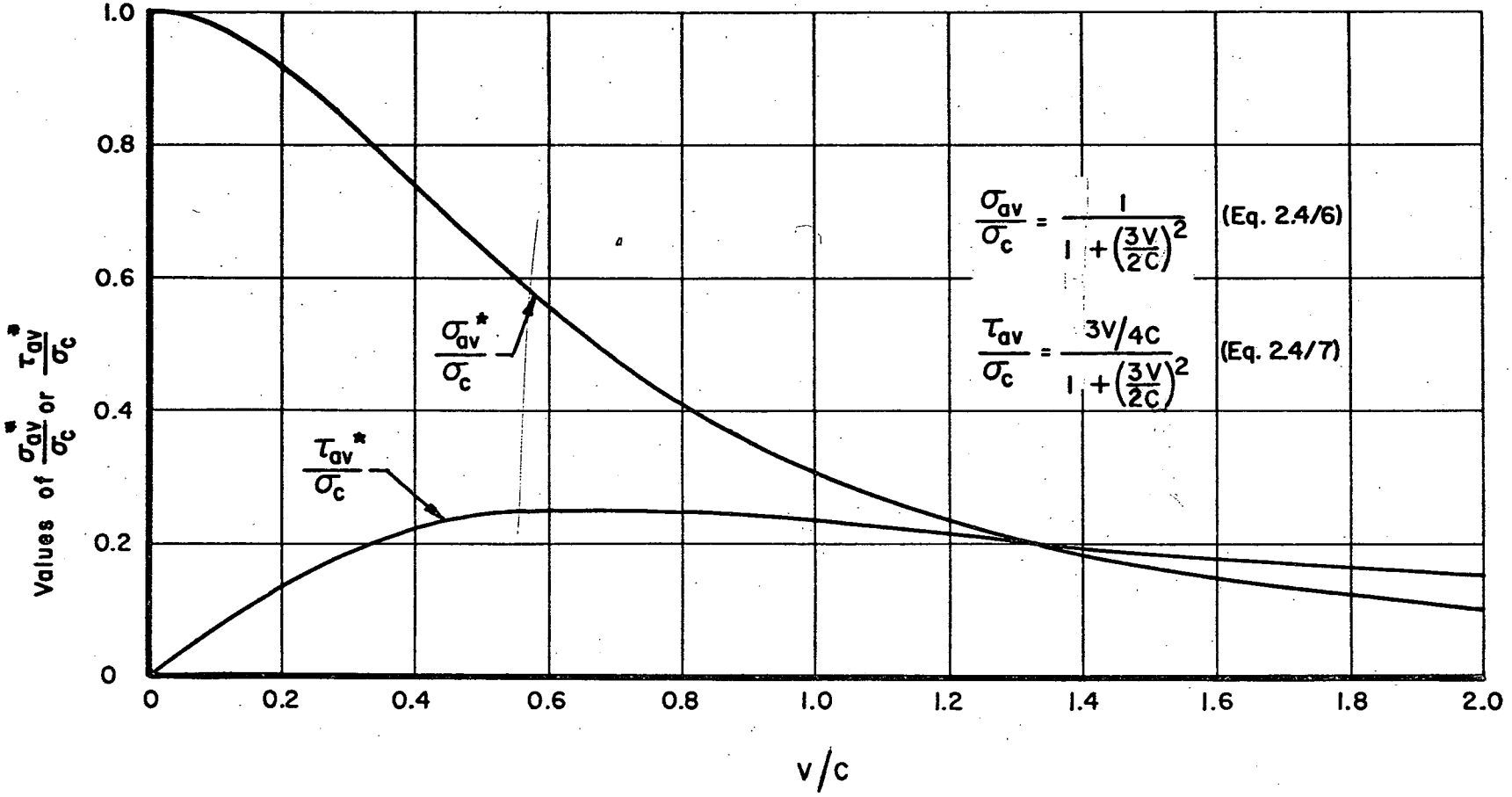
1.0
0.8
0.6
0.4
0.2
0
0
0.2
0.4
0.6
0.8
1.0
1.2
1.4
1.6
1.8
2.0
V/C
Values of $\frac{\sigma_{av}^*}{\sigma_c}$ or $\frac{\tau_{av}^*}{\sigma_c}$
$\frac{\sigma_{av}^*}{\sigma_c}$
$\frac{\tau_{av}^*}{\sigma_c}$
$\frac{\sigma_{av}}{\sigma_c} = \frac{1}{1+\left(\frac{3V}{2C}\right)^2}$ (Eq. 2.4/6)
$\frac{\tau_{av}}{\sigma_c} = \frac{3V/4C}{1+\left(\frac{3V}{2C}\right)^2}$ (Eq. 2.4/7)

Fig. 2.4/1

the region

$$1 < V/C < 2$$

or

$$\frac{\sigma_{av}^*}{\sigma_c} < \frac{1}{4}$$

Equations 2.4/6a and 2.4/7a are practically identical to Eq. 2.4/6b and 2.4/7b, respectively, thus sparing the need of the latter. Secondly, no grave error results by assuming that

$$C = \frac{M}{0.9h}$$

This last assumption is naturally only used to determine the ratio $\frac{\sigma_{av}^*}{\sigma_c}$, but it constitutes by no means an expression for the direct computation of the ultimate shear moment. Thus, the normal stress capacity of the concrete compressive zone at the end of a diagonal crack becomes

$$\frac{\sigma_{av}^*}{\sigma_c} = \frac{1}{1 + 1.8\ (\frac{Vh}{M})^2}$$

or, with the terms used in the next chapter

$$\boxed{\sigma_o = \frac{f_c'}{1 + 1.8\ (\frac{Vh}{M})^2}} \qquad (2.4/8)$$

It will be noted that σ_c is taken to be equal to f_c', a transition which does not hold true for pure bending,

where the equation $\sigma_c = 0.85\ f'_c$ or more elaborate formulas are used. Such a reduction was found to be unnecessary for shear failures because the critical stresses are, in contrast to the ones of flexural failure, confined to one cross-section. This rational approach is in good agreement with experimental findings as will be seen in Chapter 6. The influence of the M/Vh ratio on σ_o (see Fig. 2.4/2) is somewhat overaccentuated, especially for small values of M/Vh, because, contrary to the simplification assumed, the diagonal crack and the longitudinal reinforcement does contribute to the shear transfer. It is, however, conservative to neglect this contribution.

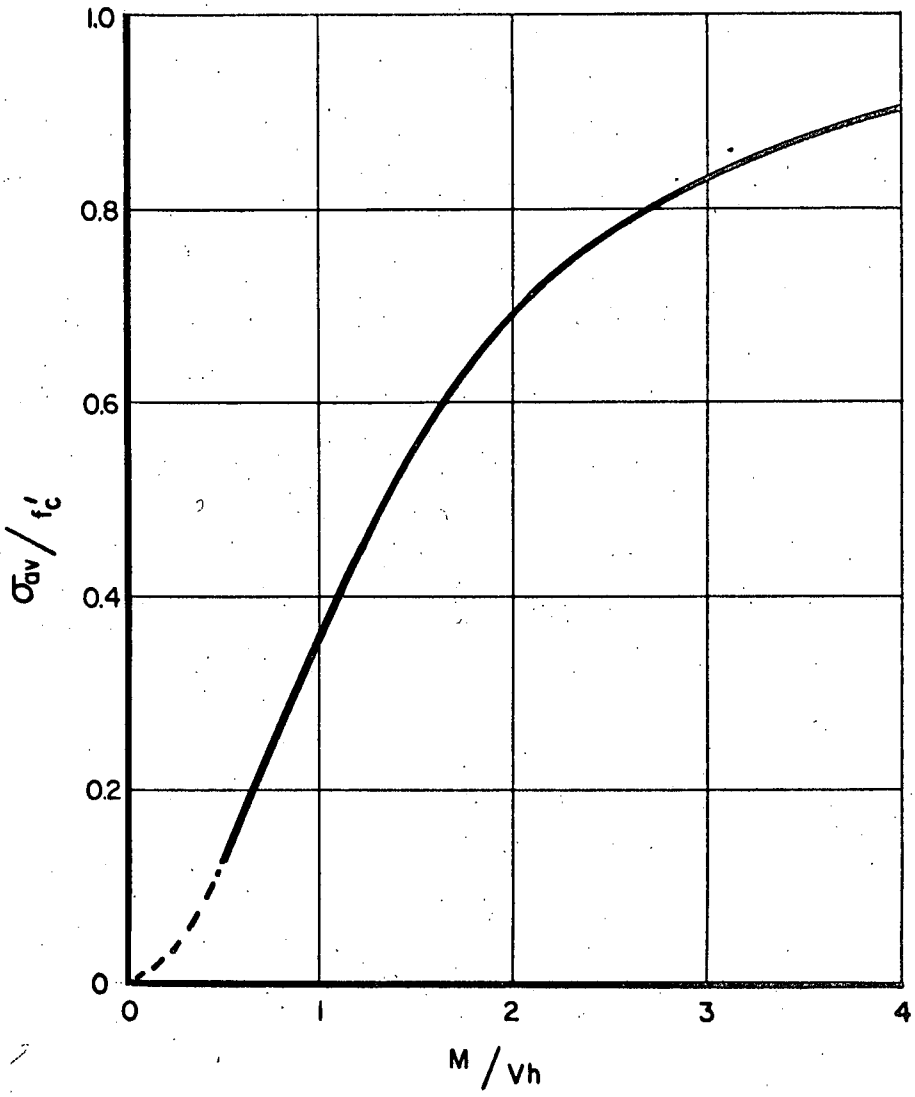

Fig. 2.4/2

$$\frac{\sigma_{av}}{f'_c} = \frac{1}{1 + (1.8)\left(\frac{Vh}{M}\right)^2}$$

3. THEORY OF SHEAR FAILURES FOR CONVENTIONALLY REINFORCED BEAMS WITHOUT WEB AND COMPRESSION REINFORCEMENT

3.1 BASIC CONCEPT

The aim of this chapter is to postulate an idealized deformation mechanism which furnishes the missing compatibility condition. A new approach is first outlined for the simplest case of conventional reinforcement and generalized in the next chapter for prestressing, web and compression reinforcement.

Since Navier-Bernoulli's hypothesis was found to hold approximately, except in the region crossed by a diagonal crack (see Introduction), it follows that the deformations of a beam outside this region result from rotations of vertical cross-sections about the neutral axis. By analogy it is arbitrarily stipulated that the deformation of the diagonally cracked portion stems also from a rotation, i.e. a rotation about the as yet unspecified end of the diagonal crack (see Fig. 3.1/1).

This basic assumption permits the formulation of a compatibility condition by observing the deformations caused

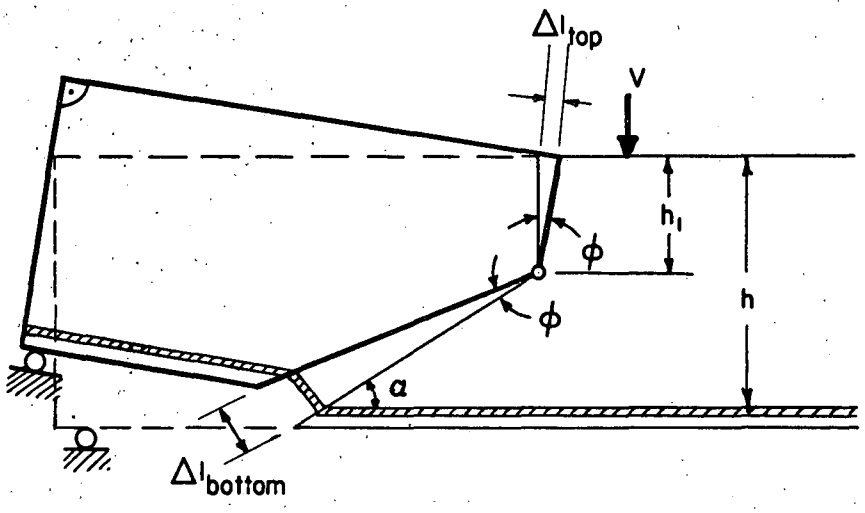

Fig. 3.1/1

Idealized Mechanism of the Relative Displacements Prior to a Shear Failure (Shear Rotation)

by this shear rotation. From Fig. 3.1/1 it can be seen that the shortening of the concrete top zone has to be

$$\Delta l_{top} = \phi \, h_1 \qquad (3.1/1)$$

and the elongation of the bottom zone, attributed to a pull out effect of the reinforcement relative to the concrete becomes

$$\Delta l_{bottom} = \phi (h - h_1) \frac{1}{\sin\alpha} \qquad (3.1/2)$$

(For notations see Fig. 3.1/1)

Hence

$$\boxed{\frac{\Delta l_{top}}{\Delta l_{bottom}} = \frac{h_1}{h - h_1} \sin\alpha} \qquad (3.1/3)$$

This last equation can now be considered as a compatibility condition. Notably, it is stated in terms of finite deformations and not, as usual, in terms of strains. This measure is necessary because the strain singularity associated with shear failure requires a consideration of the deformations in the whole region of the prospective shear failure.

Otherwise the structure of the formula is similar to the one normally used

$$\frac{\epsilon_{top}}{\epsilon_{bottom}} = \frac{h_1}{h - h_1} \qquad (3.1/4)$$

The sin-term enters because the considered cross-section is partially inclined under an angle α .

The next question is now, obviously, to determine the deformations Δl_{top} and Δl_{bottom} . For these considerations only the portion to the left of the crack is observed.

3.2 THE DEFORMATION OF THE CONCRETE TOP FIBER

By using the notation given in Fig. 3.2/1, the contraction of the concrete top fiber can be expressed as

$$\Delta l_{top} = \int_0^{\frac{h-h_1}{\tan\alpha}} \in (x;y = 0)\, dx \qquad (3.2/1)$$

Only one point of the curve $\in (x;y = 0)$ is known beforehand, i.e. the ultimate compressive strain $\in_{cu}$ will certainly occur at the location of crushing, thus

$$\in (x = 0;\ y = 0) = \in_{cu}$$

The remaining portion of the curve has first to be established with the aid of some simplifying assumption with respect to the stress distribution in the deformed portion of the concrete. Since these assumptions will obviously be quite arbitrary, an attempt is made to bound the probable value of Δl_{top} by varying the stipulations concerning the flow of the internal forces. In order to lend the problem to a mathematical treatment, a uniform stress distribution in each vertical cross-section had to be assumed. The variation of flow of internal forces is achieved by choosing different shapes for the lower boundaries of the stress blocks. A plausible choice of such a boundary would be a curve as shown in Fig. 3.2/1, starting tangentially with an angle γ at $x = 0$ $y = h_1$ and proceeding

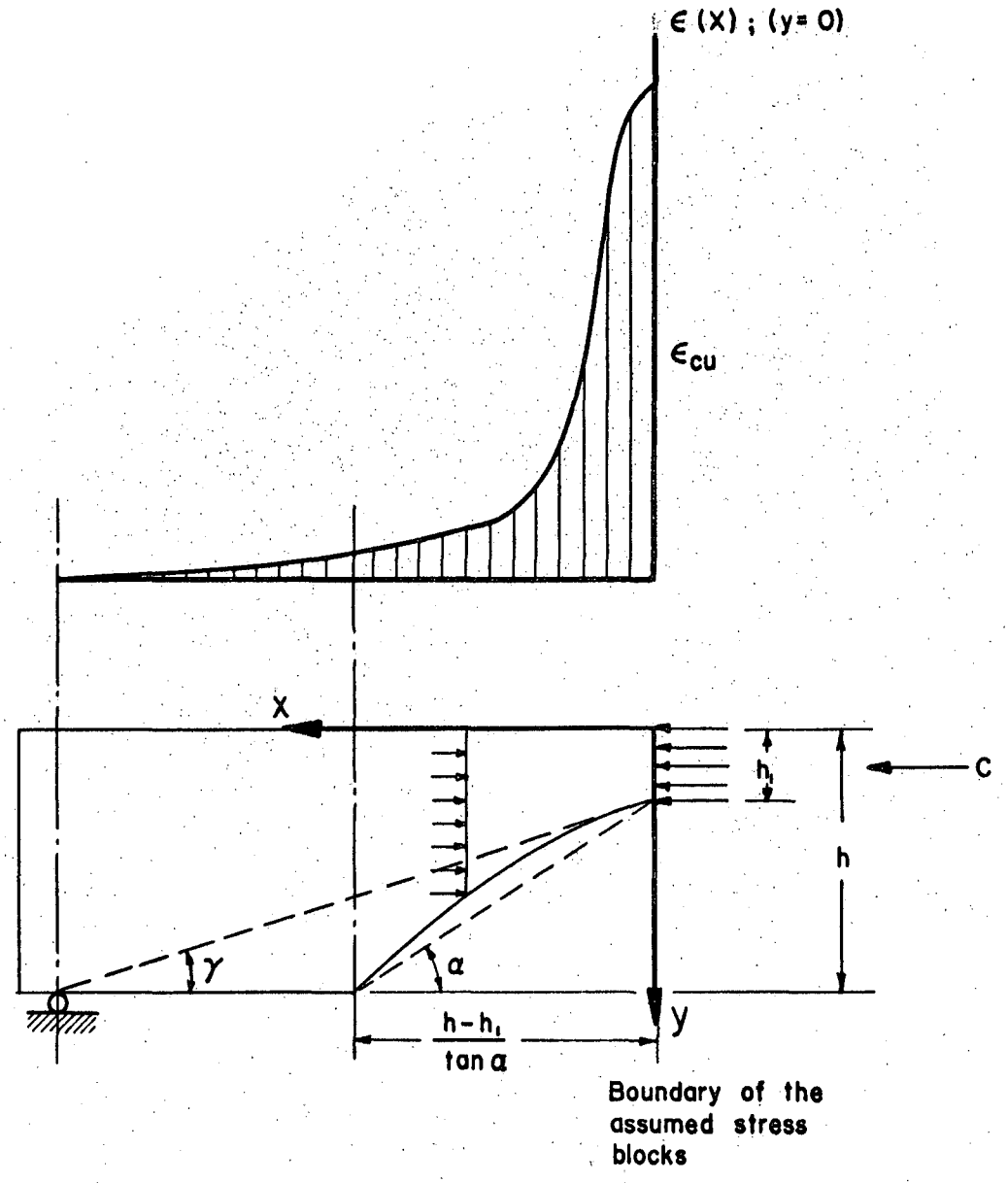

Fig. 3.2/1

Strain Distribution at the Concrete Top Fiber

concavely downwards to the origin of the crack at $x = \frac{h-h_1}{\tan\alpha}$, $y = h_1$. Unfortunately such a curve would lead to an elliptical integral for Δl_{top}, and thus would make a solution in general terms impossible. Therefore, two limiting boundary curves were considered.

(1) A parabola of the second order with a horizontal tangent at $x = 0$; $y = h_1$

(2) A straight line from $x = 0$; $y = h_1$ to the origin of the diagonal crack.

The stress strain relationship, which will serve to convert the assumed stresses into strains is, in agreement with a great number of tests, (Ref. 2.3/1), chosen to be

$$\eta = 2\xi - \xi^2 \qquad (3.2/2)$$

$$\text{or} \quad \xi = 1 - \sqrt{1-\eta}$$

$$\text{where} \quad \eta = \frac{\sigma_x}{\sigma_o}$$

$$\xi = \frac{\epsilon_x}{\epsilon_{cu}}$$

σ_x = stress component in x-direction (variable)

σ_o = maximum stress component in x-direction (usually smaller than the ultimate normal stress according to Formula 2.4/8)

ϵ_x = strain component in x-direction

ϵ_{cu} = ultimate concrete strain

Parabolic Boundary. The equation of a parabolic boundary (Fig. 3.2/2) of the sort outlined before is

$$y = h_1 + \frac{\tan^2\alpha}{h-h_1} x^2 \qquad (3.2/3)$$

On account of the uniform stress distribution assumed, and by considering the equilibrium condition of different stress blocks

$$C = \sigma_o \, bh_1 = \sigma_x \, by$$

one gets

$$\sigma_x = \sigma_o \frac{h_1}{y} = \sigma_o \frac{1}{1 + \frac{\tan^2\alpha}{h_1(h-h_1)} x^2} \qquad (3.2/4)$$

The strain distribution of the concrete top zone (Fig. 3.2/2) can thus be obtained by substituting Equation 3.2/4 in 3.2/2,

$$\epsilon_x = \epsilon_{cu} \left[1 - \sqrt{1 - \frac{1}{1 + \frac{\tan^2\alpha}{h_1(h-h_1)} x^2}} \right] \qquad (3.2/5)$$

hence

$$\Delta l_{top} = \epsilon_{cu} \int_0^{\frac{h_1-h_1}{\tan\alpha}} \left[1 - \sqrt{1 - \frac{1}{1 + \frac{\tan^2\alpha}{h_1(h-h_1)} x^2}} \right] dx$$

the solution of which is

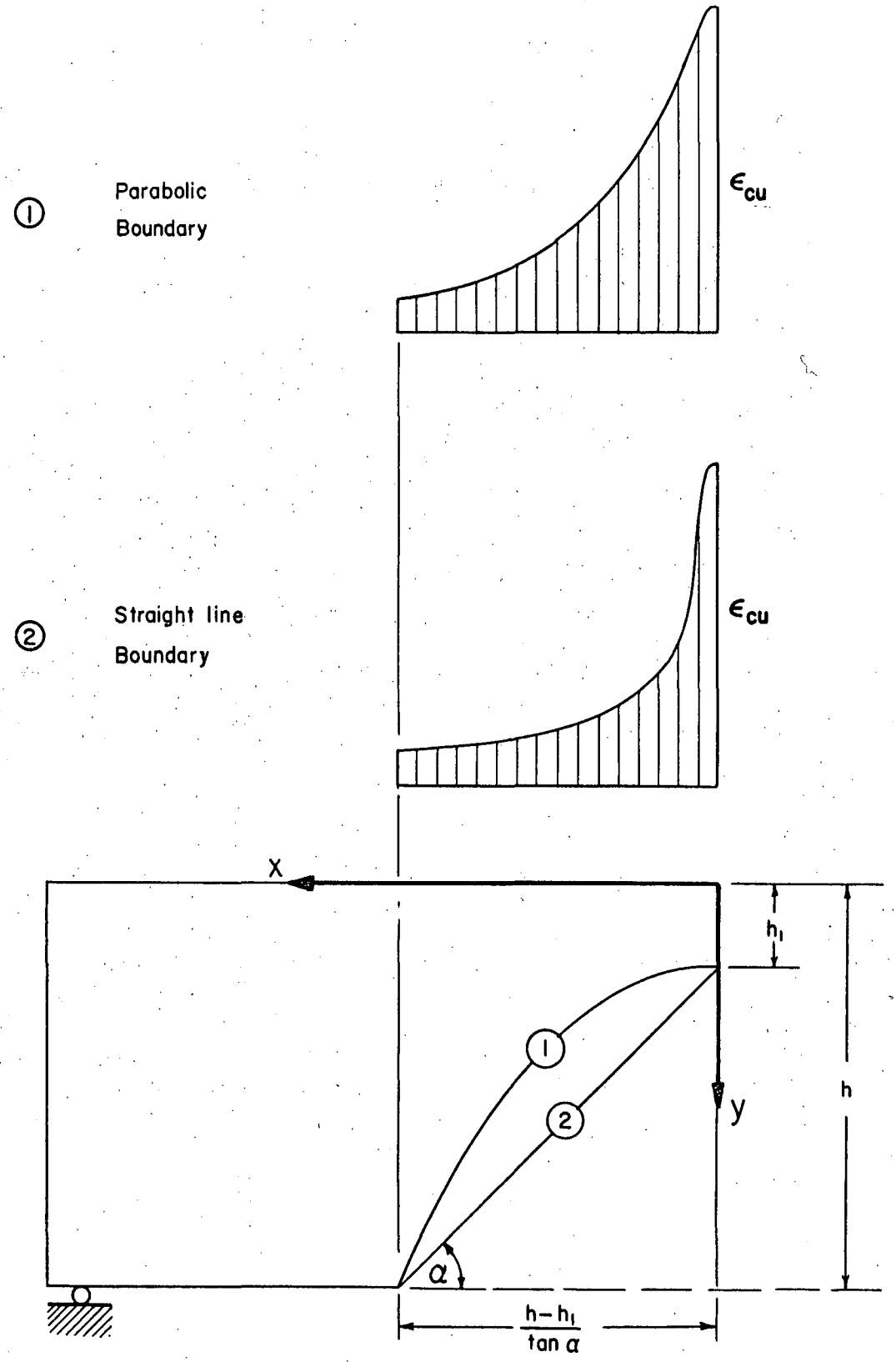

Fig. 3.2/2

Strain Distribution at the Concrete Top Fiber for the Parabolic ① and Straight Line Boundary ② Assumptions

$$\Delta l_{top} = \frac{\epsilon_{cu} \cdot h}{\tan\alpha}\left[1 - \frac{h_1}{h} - \sqrt{1 - \frac{h_1}{h}} + \sqrt{\frac{h_1}{h}\left(1 - \frac{h_1}{h}\right)}\right] \qquad (3.2/6)$$

Straight Line Boundary. The procedure for the straight line assumption follows the same pattern as before with the exception that the origin of the coordinate axis was shifted to the intersection of the straight line with the top fiber (Fig. 3.2/3). Hence

$$y = x \cdot \tan\alpha \qquad (3.2/7)$$

and

$$\Delta l_{top} = \epsilon_{cu} \int_{\frac{h_1}{\tan\alpha}}^{\frac{h}{\tan\alpha}} \left[1 - \sqrt{1 - \frac{h_1}{x \cdot \tan\alpha}}\right] dx \qquad (3.2/8)$$

which after a transformation of the variables becomes

$$\Delta l_{top} = \frac{\epsilon_{cu} \cdot h_1}{\tan\alpha} \int_{\frac{h_1}{h}}^{1} \left[\frac{1}{\xi^2} - \frac{\sqrt{1 - \xi}}{\xi^2}\right] d\xi \qquad (3.2/8a)$$

The solution of this integral is

$$\Delta l_{top} = \frac{\epsilon_{cu} \cdot h}{\tan\alpha}\left[1 - \frac{h_1}{h} - \sqrt{1 - \frac{h_1}{h}} + \frac{h_1}{2h} \ln \frac{1 + \sqrt{1 - \frac{h_1}{h}}}{1 - \sqrt{1 - \frac{h_1}{h}}}\right] \qquad (3.2/9)$$

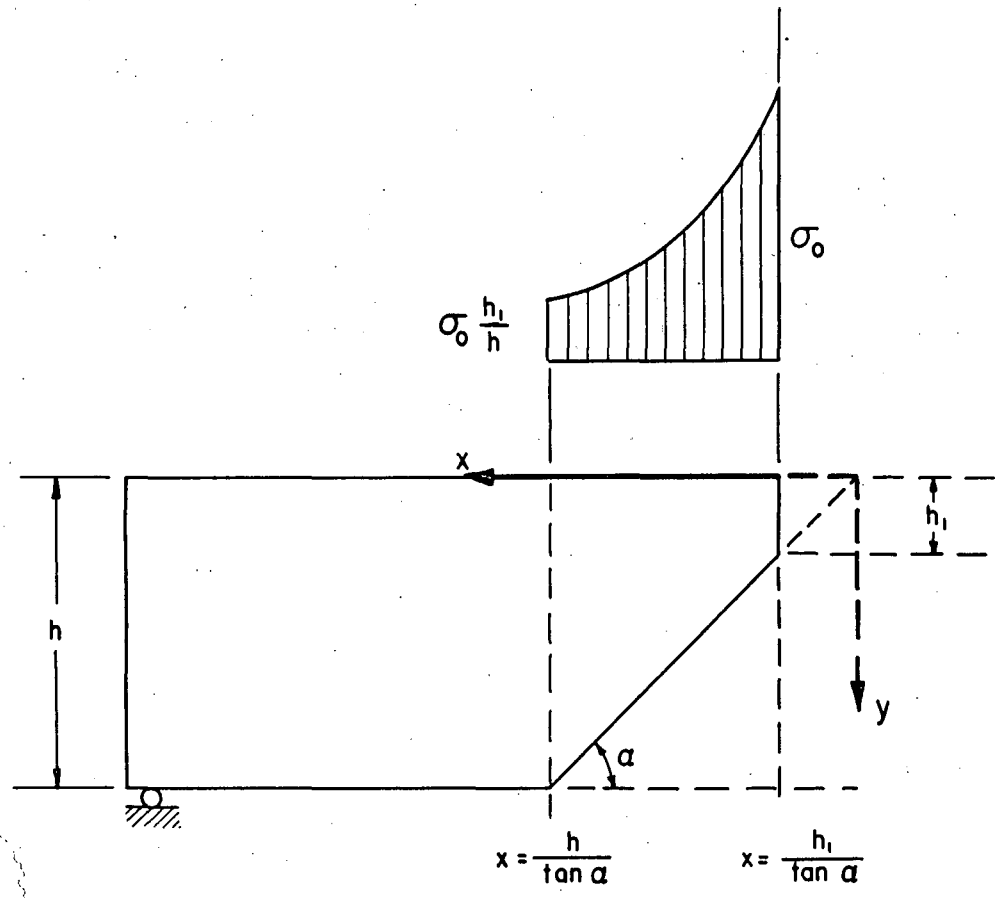

Fig. 3.2/3

Stresses for the Straight Line Assumption

The two functions for Δl_{top} given by Equation 3.2/6 and Eq. 3.2/9 deviate considerably from each other as can be seen in Fig. 3.2/4. It seems plausible, although it cannot be proved, that for any given ratio $\frac{h_1}{h}$ the parabolic assumption overestimates and the straight line assumption underestimates the value of Δl_{top}. It will be seen later, however, that upon combining each of the two curves with the equilibrium conditions, they yield very similar functions for the sought unknown $\frac{h_1}{h}$ or M_{su}. It shall also be mentioned that several other assumptions for the boundary of the stress blocks were considered by choosing parabolas ending not at the bottom of the beam, but somewhere between mid-depth and bottom. Again the difference in Δl_{top} did not greatly affect the outcome of the final result.

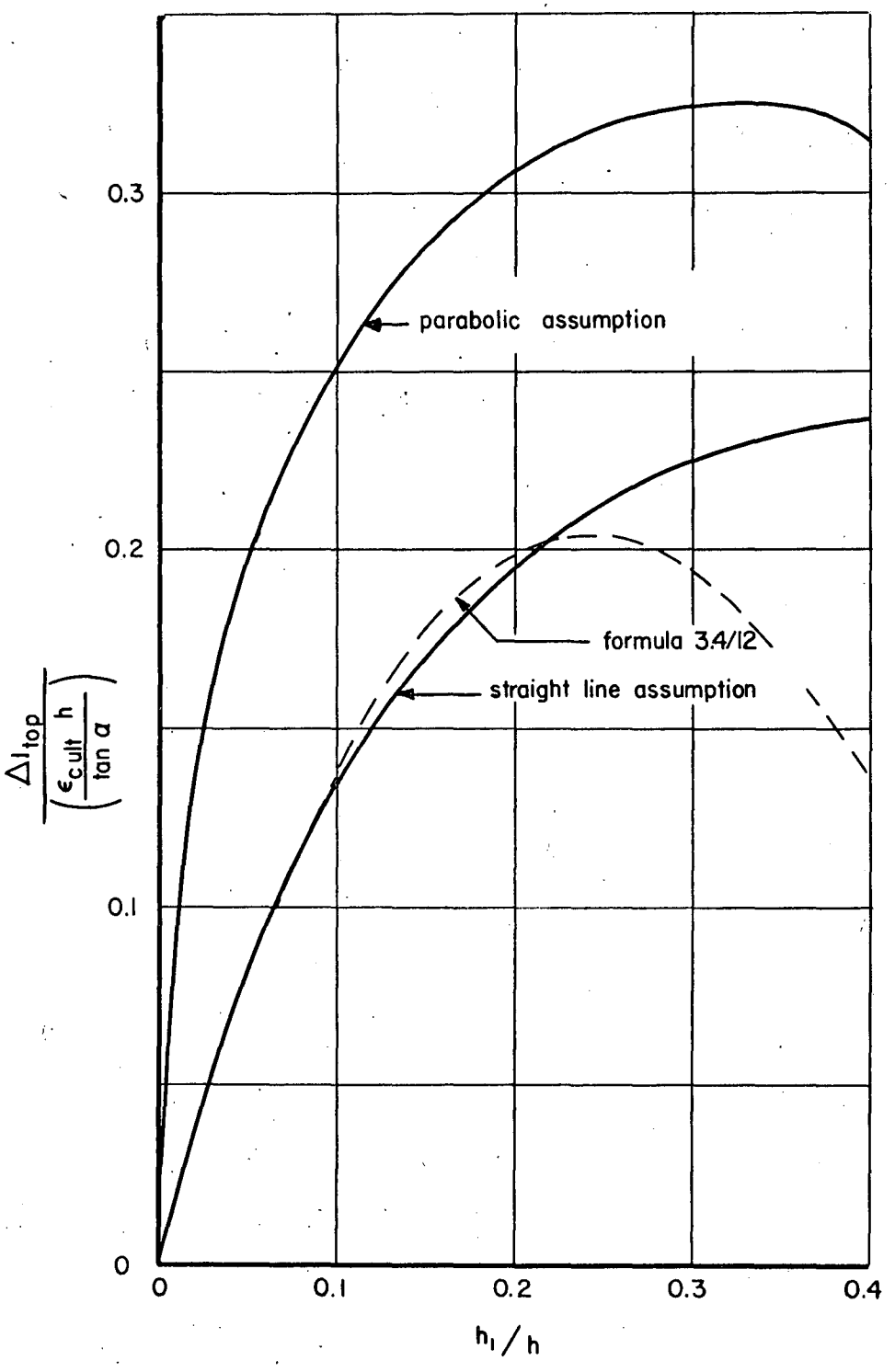

Fig. 3.2/4

Δl_{top} As a Function of h_1/h

3.3 THE DEFORMATION OF THE BOTTOM ZONE

As explained before, the elongation of the bottom zone is attributed to a pull-out effect of the longitudinal reinforcement with respect to the surrounding concrete. Since this pull-out effect is obviously a function of the bond characteristic, it is apparent that the influence of bond will enter the considerations. On the other hand, a new variable is added to the already complicated problem -- a variable which from experience is known to be accompanied by considerable scatter.

Observations of actual pull-out tests suggest that (5.1/2)

$$\Delta l_{bottom} = \lambda \epsilon_{st}^2 \qquad (3.3/1)$$

where λ depends on the bond characteristic. The reciprocal of λ, i.e. $\frac{1}{\lambda}$, will hereafter be called " bond coefficient." As discussed in Chapter 5, conventional pull-out tests do not directly represent the magnitude of Δl_{bottom}, since due to the rotation ϕ the resulting tension force does not act in the direction of the tendons. The coefficient λ will therefore take on a greater value than for axial pull-out.

3.4 SOLUTION

By assuming a rectangular stress block of the magnitude σ_o (see Eq. 2.4/8) over the concrete compressive zone* the ultimate shear moment becomes

$$M_{su} = \sigma_o \, h_1 \, b \, (h - \frac{h_1}{2}) \qquad (3.4/1)$$

This expression contains only one unknown, i.e. h_1. An equation for $\frac{h_1}{h}$ is therefore regarded as the solution of the problem. Similarly to pure bending, this solution is obtained by combining the compatibility and equilibrium conditions.

The Compatibility Condition, derived in Section 3.1 to 3.3 can now be transformed to the two alternative expressions in terms of strains, namely

$$\epsilon_{st} = \sqrt{\frac{\epsilon_{cu} \, h}{\lambda \tan\alpha \sin\alpha} \left[\left(\frac{h}{h_1} - 1\right)\left(1 - \frac{h_1}{h} - \sqrt{1 - \frac{h_1}{h}} + \sqrt{\frac{h_1}{h}\left(1 - \frac{h_1}{h}\right)}\right)\right]} \qquad (3.4/2)$$

* This simplifying assumption, though differing from the one made in Chapter 2, seems permissible, since the shape of the stress block does not greatly affect the ultimate moment.

obtained by substituting Equation 3.2/6 and 3.3/1 in 3.1/3; (parabolic assumption) and

$$\epsilon_{st} = \sqrt{\frac{\epsilon_{cu}\, h}{\lambda \tan\alpha \sin\alpha}\left[\left(\frac{h}{h_1} - 1\right)\left(1-\frac{h_1}{h}-\sqrt{1-\frac{h_1}{h}}\right) + \frac{h_1}{2h}\ln\frac{1+\sqrt{1-\frac{h_1}{h}}}{1-\sqrt{1-\frac{h_1}{h}}}\right]} \qquad (3.4/3)$$

obtained by substituting Equation 3.2/9 and 3.3/1 in 3.1/3 (straight line assumption).

The Equilibrium Condition requires that the compressive force C must be equal and opposite to the tension force T ; i.e. with the assumption and notation used before.

$$\sigma_o\, bh_1 = A_{st}\, E_{st}\, \epsilon_{st} \qquad (3.4/4)$$

$$\text{or} \qquad \frac{\sigma_o}{pE_{st}} = \frac{h}{h_1}\,\epsilon_{st}$$

where A_{st} = Area of longitudinal tension reinforcement.

E_{st} = Modulus of elasticity or secant modulus of steel, depending on whether on not the steel is still in the elastic range.

$\frac{A_{st}}{bh} = p$ = Ratio of reinforcing steel

The Implicit Solution for $\frac{h_1}{h}$ is found, as mentioned before, by combining Equations 3.4/2 or 3.4/3 with Eq. 3.4/4.

$$\frac{\sigma_o}{pE_{st}}\sqrt{\frac{\lambda \tan\alpha \sin\alpha}{\epsilon_{cu} h}} = \frac{h}{h_1}\sqrt{\left(\frac{h}{h_1}-1\right)\left(1-\frac{h_1}{h}-\sqrt{1-\frac{h_1}{h}}+\sqrt{\frac{h_1}{h}\left(1-\frac{h_1}{h}\right)}\right)}$$

(parabolic assumption) (3.4/5)

$$\frac{\sigma_o}{pE_{st}}\sqrt{\frac{\lambda \tan\alpha \sin\alpha}{\epsilon_{cu} h}} = \frac{h}{h}\sqrt{\left(\frac{h}{h_1}-1\right)\left(1-\frac{h_1}{h}-\sqrt{1-\frac{h_1}{h}}+\frac{h_1}{2h}\ln\frac{1+\sqrt{1-\frac{h_1}{h}}}{1-\sqrt{1-\frac{h_1}{h}}}\right)}$$

(straight line assumption) (3.4/6)

These alternative expressions constitute the general solution of the problem treated in this chapter. The righthand side contains only the unknown $\frac{h_1}{h}$; the quantities to the left of the equal sign are given parameters.

The graphical presentation of these solutions (Fig. 3.4/1) permits now the drawing of conclusions as to what boundary assumption is preferable. Since the ultimate shear moment increases with increasing $\frac{h_1}{h}$, it is evident that the straight line assumption yields more conservative results and will therefore be chosen for further applications. The comparatively small difference between the two curves, in spite of the much greater deviation of $\triangle l_{top}$, as seen in Fig. 3.2/4, seems to justify the hope that this theory is not sensitive to inaccuracies in the basic assumptions, especially since the rather uncertain parameters, i.e., α, λ, and ϵ_{cu} occur within the square root.

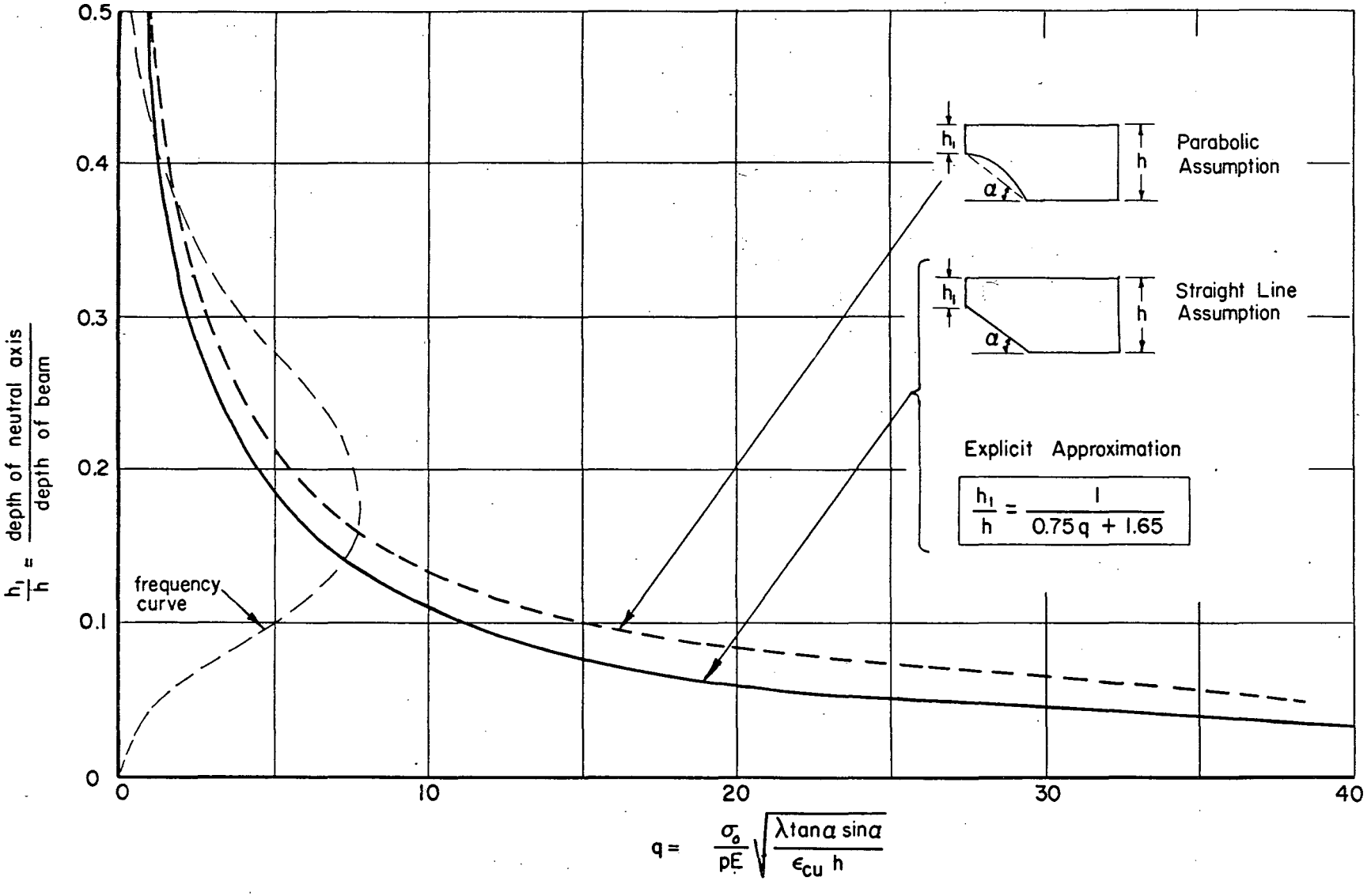

Fig. 3.4/1 Solution for h_1/h as a function of σ_o ; E_{st} ; α ; ϵ_{cu} and h

The Explicit Solution. In order to lend such a solution to practical applications, it should be expressed in an explicit form. It is therefore sought to approximate the original curve by means of the method of least squares, considering also the weight of any portion of curve according to the relative probability of occurrence.

The shape of the curve, given by Equation 3.4/6, suggests an approximation of the following kind

$$\left(\frac{h_1}{h}\right)_{app.} = \frac{1}{k_1\, q + k_2} \qquad (3.4/8)$$

where k_1 and k_2 are the constants to be found by the method of least squares and q stands for

$$q = \frac{\sigma_o}{pE_{st}} \sqrt{\frac{\lambda \tan\alpha \quad \sin\alpha}{\epsilon_{cu} \cdot h}}$$

Unfortunately the method becomes very laborious for this particular case and no explicit expression for k_1 and k_2 can be found, because by choosing, for example, n-reference points, one ends up with two polynomials in k_1 and k_2 of the $(3n + 1)^{th}$ order, the solution of which could only be found by trial and error. Under these circumstances one might as well start out to find k_1 and k_2 directly by trial and error. It was preferred, however, to choose a different approach. If the sought approximation can be expected to coincide closely with the original curve, then one can apply the method of least squares to the reciprocal function

$$\left(\frac{h}{h_1}\right)_{app} = k_1\, q + k_2 \qquad (3.4/8a)$$

and still obtain practically the same k-values.

Consequently it is required that

$$\sum_1^n \left[W_n \left(\left(\frac{h}{h_1}\right)_n - k_1\, q_n - k_2 \right)^2 \right] = \min \qquad (3.4/9)$$

which means: the sum of the squares of the errors over n-reference points of weight W_n be a minimum.

Hence the partial derivatives with respect to k_1 and k_2 have to be zero.

$$\frac{\partial}{\partial k_1} \sum_1^n \left[W_n \left(\left(\frac{h}{h_1}\right)_n - k_1 q_n - k_2 \right)^2 \right] = 0$$

and

$$\frac{\partial}{\partial k_2} \sum_1^n \left[W_n \left(\left(\frac{h}{h_1}\right)_n - k_1 q_n - k_2 \right)^2 \right] = 0 \qquad (3.4/10)$$

or

$$\sum_1^n \left[W_n \left(\left(\frac{h}{h_1}\right)_n - k_1 q_n - k_2 \right) q_n \right] = 0$$

and

$$\sum_1^n \left[W_n \left(\left(\frac{h}{h_1}\right)_n - k_k q_n - k_2 \right) \right] = 0 \qquad (3.4/10a)$$

The two last equations determine the values of the constants k_1 and k_2. The weight of the reference points for the particular curves in question was derived from a

statistical survey of the frequency of test results in specified ranges of $\frac{h_1}{h}$. This frequency curve is shown in Figure 3.4/1. The computations for the k-values is presented in Table 3.4/I. By comparing the first and the last column of this table, it can be seen that the approximation is so accurate as to lie within the thickness of the line for the gratest portion of the curve in Fig. 3.4/1.

Thus the explicit solution for our problem can be written as

$$\frac{h_1}{h} = \frac{1}{0.75\left(\frac{\sigma_o}{pE_{st}}\sqrt{\frac{\lambda \tan\alpha \sin\alpha}{\epsilon_{cu}\, h}}\right) + 1.65} \qquad (3.4/11)$$

where

$$\sigma_o = \frac{f_c'}{1 + 1.8\left(\frac{Vh}{M}\right)^2} \qquad (2.4/8)$$

With these two formulas the ultimate shear moment

$$M_{su} = \sigma_o\, bh_1\, (h - \frac{h_1}{2}) \qquad (3.4/1)$$

can be calculated.

It was thus possible to determine the ultimate shear moment by a rational approach, the applicability of which has, of course, first to be proven by comparison with test results. Anticipating a thorough comparison, it can be seen that the order

h_1/h	q	W	h_1/h	$W \cdot h_1/h$	Wq	q^2	Wq^2	$q \cdot h/h_1$	$Wq \cdot h/h_1$	$\frac{1}{k_1 q + k_2}$
0.05	25.26	1	20	20	25.26	638.07	638.07	502.2	502.2	.0485
.1	10.95	4	10	40	43.8	119.9	479.6	109.5	438.0	.1014
.15	6.51	6	6.67	40.02	39.06	42.38	254.28	43.42	260.52	.1531
.20	4.4	6	5	30	26.4	19.36	116.16	22.0	132.0	.2020
.25	3.2	5	4	20	16	10.24	51.2	12.8	64.0	.2469
.30	2.44	3	3.33	9.99	7.32	5.95	17.85	8.125	24.38	.2874
.35	1.87	2	2.85	5.70	3.74	3.50	7.0	5.33	10.66	.3279
.40	1.49	1	2.5	2.5	1.49	2.22	2.22	3.725	3.73	.3610
.45	1.19	0.5	2.22	1.11	.595	1.42	.71	2.642	1.321	.3937
.50	0.97	0.25	2	0.5	.243	.941	.235	1.94	.485	.4202
	58.28	28.75	58.6	169.82	163.91	843.98	1567.33	714.68	1440.29	

$$1440.29 - 1567.33\, k_1 - 163.91\, k_2 = 0 \qquad k_1 = 0.746 = 0.75$$

$$169.82 - 163.91\, k_1 - 28.75\, k_2 = 0 \qquad k_2 = 1.654 = 1.65$$

TABLE 3.4/I

Derivation of the k-values for the approximation of the expression

$$q = \frac{h}{h_1}\sqrt{\left(\frac{h}{h_1} - 1\right)\left(1 - \frac{h_1}{h} - \sqrt{1 - \frac{h_1}{h}} + \frac{h_1}{2h} \ln \frac{1 + \sqrt{1 - h_1/h}}{1 - \sqrt{1 - h_1/h}}\right.}} \quad \text{by: } \frac{h_1}{h} = \frac{1}{k_1 q + k_2}$$

of the variable is in accordance with experimental evidence in that the formulas indicate an increase of the ultimate moment with

(1) Increasing concrete strength

(2) Increasing ratio of reinforcement

(3) Improvement of bond characteristic (i.e decreasing λ-values)

(4) Increasing deformability of the concrete compressive zone $\left(\frac{\epsilon_{cu}}{\tan\alpha \sin\alpha}\right)$

(5) Increasing ratio of M/Vh (for symmetrical two point loading, with increasing shear span)

For later use it is convenient to trace this solution once again back to the compatibility condition. An exactly identical solution to 3.4/11 could be obtained by taking

$$\Delta l_{top} = \frac{\epsilon_{cu}\, h}{\tan\alpha} \cdot \frac{\left(\frac{1 - k_2 \frac{h_1}{h}}{k_1}\right)^2}{\left(\frac{h}{h_1} - 1\right)} \qquad (3.4/12)$$

(given as a dashed line in Fig. 3.2/4).

This brings the compatibility condition to the simple form

$$\epsilon_{st} = \left(\frac{1 - k_2 \frac{h_1}{h}}{k_1}\right) \sqrt{\frac{\epsilon_{cu}\, h}{\lambda \sin\alpha \tan\alpha}}$$

or by substituting the k-values

$$\epsilon_{st} = \frac{1 - 1.65 \frac{h_1}{h}}{0.75} \sqrt{\frac{\epsilon_{cu}\, h}{\lambda \sin\alpha \tan\alpha}} \qquad (3.4/13)$$

This expression is used later on to derive the formulas for more complicated cases.

4. GENERALIZATION FOR PRESTRESSING WEB AND COMPRESSION REINFORCEMENT

4.1 PRESTRESSING

The approximate knowledge of the failure mechanism, gained by the rational approach, permits a direct determination of additional variables, such as prestressing, web and compression reinforcement. This feature is especially favorable for prestressed members because their shear strength can reliably be related to those of non-prestressed beams, thus sparing the need of experimentally redetermining the influence of all the variables already aggravating the research of conventionally reinforced concrete.

The initial state of stress, produced by the prestressing, forbids a direct application of the compatibility condition stated in the last chapter. Rather than change the compatibility condition itself, one can introduce fictitious forces which compensate the initial state of stress. The following notations will be used for these considerations:

T_i; σ_i; ϵ_i: Initial pretensioning force (stress; strain) before release

T_i'; σ_i'; ϵ_i': Initial post-tensioning force (stress; strain) before creep and shrinkage take place

$\Delta T_{ie}; \Delta\sigma_{ie}; \Delta\epsilon_{ie}$: Losses due to inelastic deformation of concrete (creep and shrinkage) and steel (creep of the tendons)

$\Delta T_{el}; \Delta\sigma_{el}; \Delta\epsilon_{el}$: Losses due to the elastic shortening of the concrete

T_o: Fictitious force which, applied at the centroid of the tendons, would relieve the concrete stresses

$T_{eff}; \sigma_{eff}; \epsilon_{eff}$: Effective prestressing force (stress; strain) after deduction of all the losses

Since the initial state of stress is caused exclusively by the prestressing (the stresses due to dead load are not considered as initial stresses, even though they have to be taken into account for the calculation of the prestressing losses), it must be possible to relieve these stresses by applying a fictitious force (T_o) at the centroid of the prestressing tendons. This force has to be larger than the effective prestressing force, since the elastic losses have to be overcome (but not the inelastic losses which remain as residual strains without causing stresses). Thus the fictitious force is:

for pretensioning,

$$\underline{T_o} = T_i - \Delta T_{ie} = \underline{T_{eff} + \Delta T_{el}} \qquad (4.1/1)$$

or, expressed by the steel strains,

$$\underline{\epsilon_o} = \epsilon_i - \Delta\epsilon_{ie} = \underline{\epsilon_{eff} + \Delta\epsilon_{el}} \qquad (4.1/1a)$$

and for post-tensioning,*

$$\underline{T_o} = T_i' - \Delta T_{ie} + \Delta T_{el} = \underline{T_{eff} + \Delta T_{el}} \qquad (4.1/2)$$

or

$$\underline{\epsilon_o} = \epsilon_i' - \Delta\epsilon_{ie} + \Delta\epsilon_{el} = \underline{\epsilon_{eff} + \Delta\epsilon_{el}} \qquad (4.1/2a)$$

Considering now a free body diagram at a prospective failure cross section (Fig. 4.1/1), one can always split the external moment M into a couple

$$T = C = \frac{M}{\left(h - \frac{h_1}{2}\right)} \qquad (4.1/3)$$

The tensile force acting at the centroid of prestressing can be imagined to consist of two parts

$$T = T_o + T_+ \qquad (4.1/4)$$

---

* For post-tensioning, ΔT_{el} cannot be considered as a real loss; it is better defined by the strain $\Delta\epsilon_{el}$, i.e. the elastic shortening of the concrete at the centroid of tendons due to post-tensioning. Thus,

$$\Delta T_{el} = EA_{st}\Delta\epsilon_{el}$$

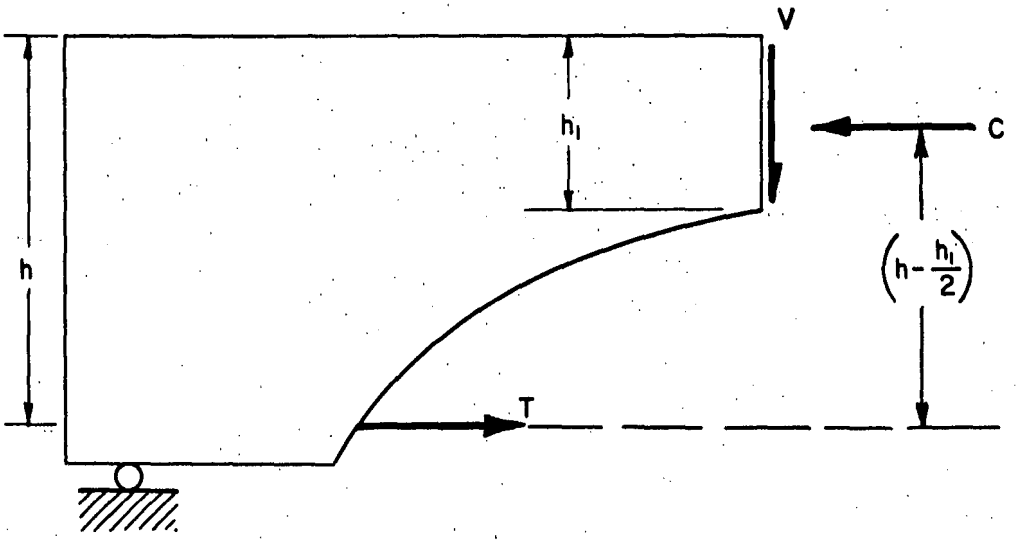

Fig. 4.1/1

Free Body Diagram at a Prospective Failure Cross-Section

$$M = C\left(h-\frac{h_1}{2}\right) = T\left(h-\frac{h_1}{2}\right)$$

i.e., of the force T_o and whatever force T_+ is required to add up to T. From the above discussion, it is seen that T_o acting alone relieves all the initial stresses. From Equation 4.1/4, it follows that

$$\epsilon_{st} = \epsilon_o + \epsilon_+ \qquad (4.1/4a)$$

The compatibility condition, as derived in the last chapter, can therefore be applied to the configuration of the remaining forces, stresses, or strains. Thus, according to Equation 3.4/13,

$$\epsilon_+ = \frac{1 - 1.65 \frac{h_1}{h}}{0.75} \sqrt{\frac{\epsilon_{cu}\, h}{\lambda \sin\alpha \tan\alpha}} \qquad (3.4/13)$$

The equilibrium condition, on the other hand, becomes

$$T = E_{st}\, A_{st}\, (\epsilon_o + \epsilon_+) = C = \sigma_o b h_1 \qquad (4.1/5)$$

which is identical to Equation 3.4/4 except for the replacing of ϵ_{st} by $\epsilon_o + \epsilon_+$.

The solution h_1/h for prestressed concrete can therefore be obtained by combining Equation 3.4/13 and Eq.4.1/5.

$$\frac{h_1}{h} = \frac{1 + 0.75\epsilon_o \sqrt{\frac{\lambda \sin\alpha \tan\alpha}{\epsilon_{cu}\, h}}}{0.75 \frac{\sigma_o}{p E_{st}} \sqrt{\frac{\lambda \sin\alpha \tan\alpha}{\epsilon_{cu}\, h}} + 1.65} \qquad (4.1/6)$$

This solution accounts numerically for the empirically known fact that prestressing increases the shear strength. This becomes clearly evident by transforming Equation 4.1/6 to

$$\left(\frac{h_1}{h}\right)_{\substack{\text{with}\\ \text{prestressing}}} = \left(\frac{h_1}{h}\right)_{\substack{\text{without}\\ \text{prestressing}}} \left(1 + 0.75\epsilon_o \sqrt{\frac{\lambda \sin\alpha \tan\alpha}{\epsilon_{cu}\, h}}\right) \qquad (4.1/6a$$

Since ϵ_o is a direct measure of the degree of prestressing. Equation 4.1/6a suggests that the ratio of depth of the neutral axis increases linearly with the degree of prestressing. Thus also, the ultimate shear moment increases, according to

$$M_{su} = \sigma_o\, b h_1 \left(h - \frac{h_1}{2}\right)$$

Furthermore, it can be presumed that the effect of an error in the somewhat uncertain estimation of the coefficient λ is lessened, since its influence on the two factors on the right hand side of Eq. 4.1/6a is of opposite rate.

There might arise some concern that the percent-wise increase of the ratio h_1/h increases also with λ, i.e. with deterioration bond conditions. The absolute value of h_1/h however, increases with improved bond characteristic. What Eq. 4.1/6a expresses, in effect, is that the percent-wise improvement which can be gained by prestressing becomes greater with poorer bond conditions, a statement which seems conceivable. It is naturally implied that no bond failure develops.

4.2 WEB REINFORCEMENT

The remarks made in the beginning of the last chapter concerning the advantage of a rational approach prevail also for the determination of the influence of the web reinforcement: it is possible to trace the solution back to the case without web reinforcement.

The beneficial influence of stirrups is rooted in the following four points:

(1) The stirrup forces contribute directly to the ultimate shear moment.

(2) A portion of the shear force V is carried by the stirrups, thus increasing the normal stress capacity of the concrete compressive zone.*

(3) The ductility of the concrete compressive zone, i.e. ϵ_{cu}, is increased by the presence of stirrups.

(4) The quality of bond is improved when the longitudinal reinforcement is laced by stirrups.

---

* This is the reason why beams with stirrups show a smaller influence of the shear span than beams without web reinforcement.

For the time being, only the first two points are considered numerically, since first, ϵ_{cu} does not affect the ultimate shear moment significantly, and second, only qualitative information concerning the improvement of the bond due to stirrups is available at present.

Actual measurements of the stirrup forces by means of strain gages (Ref. 1.2/1 and 4.2/1) permit the conclusion that the stirrups crossed by the diagonal failure crack reach or surpass the yield point of the steel, thus sparing the need for a consideration of the shear rotation ϕ .*

In order to avoid the carrying on of insignificant details, it is furthermore assumed that the diagonal crack subtends an angle of 45° and extends over the whole depth of the beam, yielding the following formulas (see Fig. 4.2/1).

$$V_{stirrup} = rbh\, f_y' \qquad (4.2/1)$$

$$(V_{stirrup} \leq V)$$

and

$$M_{stirrup} = \frac{rbh^2}{2} f_y' \qquad (4.2/2)$$

---

* Such a consideration showed that only if h_1/h is larger than 0.3 is it theoretically possible that the stirrups in the immediate proximity of the concrete crushing zone may be stressed below the yield point.

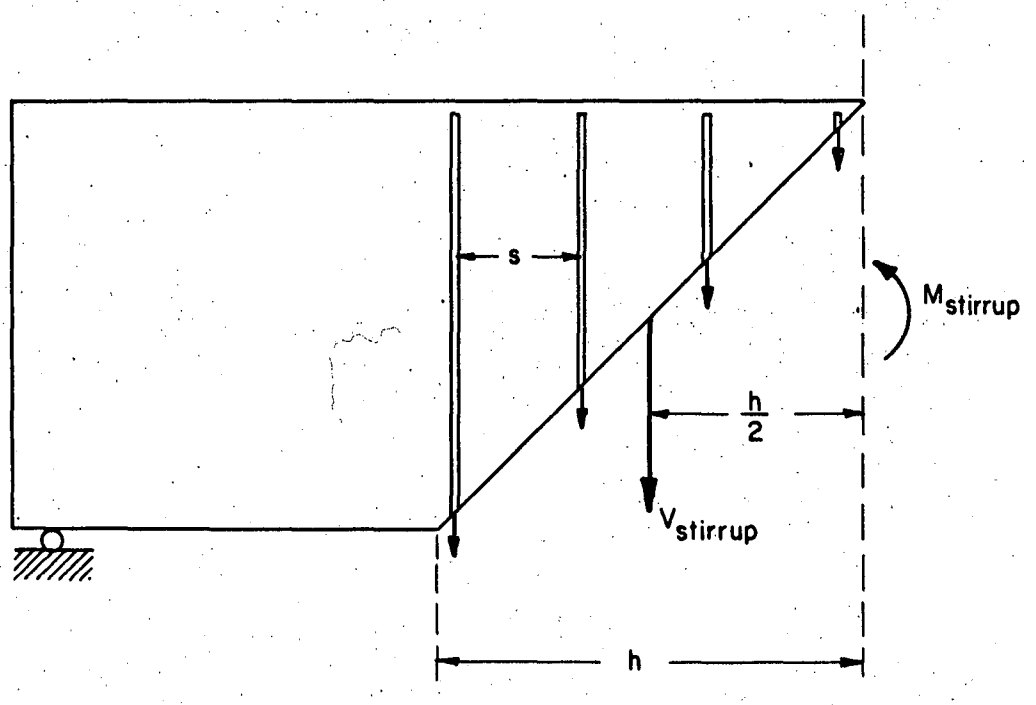

Fig. 4.2/1

Simplified Assumption for the Computation of the Stirrup Moment ($M_{stirrup}$)

where

$$r = \frac{A_w}{bs} = \text{ratio of stirrup reinforcement}$$

A_w = area of two legs of one stirrup

s = spacing of the stirrups

f_y' = yield strength of the stirrups

As for Equation 4.2/11, it has naturally to be observed that V_{st} cannot exceed the total shear force V.

On account of the contribution of the stirrups to the shear transfer, Equation 2.4/8 has to be modified to

$$\sigma_o = \frac{f_c'}{1.8\left(\frac{(V-V_{st})h}{M}\right)^2 + 1} \qquad (4.2/3)$$

Since only the ratio of M/V, but not the forces themselves, are determined beforehand by the loading conditions, it would be necessary to solve Eq. 4.2/3 in connection with Eq. 3.4/1 and 3.4/11 by iteration. For the practice, such a procedure would certainly be too involved. It can safely be omitted, since this results only in a slight underestimation of the ultimate shear strength. The reason for introducing Equation 4.2/3 is mainly for the purpose of checking tests results where M_{su}/V_u is known.

4.3 COMPRESSION REINFORCEMENT

In order to avoid unnecessary repetition of similar derivations, the influence of the compression reinforcement is given directly for prestressed concrete, keeping in mind that for non-prestressed members ϵ_o is zero and ϵ_+ has to be replaced by ϵ_{st}.

The compatibility condition suffers no change by the introduction of compression reinforcing, thus

$$\epsilon_+ = \frac{1 - 1.65 \frac{h_1}{h}}{0.75} \sqrt{\frac{\epsilon_{cu}\, h}{\lambda \tan\alpha \sin\alpha}} \qquad (3.4/13)$$

As for the equilibrium condition, the contribution of the compression reinforcement to the total force C has to be taken into account, using the following notations:

A'_{st} = area of compression reinforcement

f_y'; (ϵ_y') = yield stress (strain) of the compression reinforcement

and for later use,

$p' = \frac{A'_{st}}{bh}$ = ratio of compression reinforcement

f'; (ϵ') = steel stress (strain) of compression reinforcement at failure

Since the concrete strains of the prospective failure zone are considerably larger than the yield strain of steel ($\epsilon_{cu} \sim 0.0036$, as compared to $\epsilon_y' \sim 0.0015$), one could be inclined to presume that the compressive reinforcement always reaches its yield strength. Experimental evidence contradicts, however, such a presumption. If, for example, $p = p'$, then the tensile reinforcement would have to exceed the yield strength (equilibrium), which is incompatible with test results.

Thus it has to be concluded that the steel strains do not follow the concentration of the concrete strains. For reasons of simplicity, the strain of the compression reinforcement at failure is arbitrarily assumed as

$$\epsilon' \cong 0.5\ \epsilon_y' \qquad (4.3/1)$$

and

$$f' \cong 0.5\ f_y' \quad . \qquad (4.3/2)$$

Thus the equilibrium condition becomes

$$\sigma_o b h_1 + 0.5\ A'_{st}\ f_y' = E(\epsilon_o + \epsilon_+)\ A_{st} \qquad (4.3/3)$$

Consequently the solution for h_1/h is obtained by substituting Equation 4.3/3 in Eq. 3.4/13;

$$\frac{h_1}{h} = \frac{\epsilon_o + \frac{1}{0.75}\sqrt{\frac{\epsilon_{cu}\, h}{\lambda \sin\alpha \tan\alpha}} - \frac{\epsilon_y' p'}{2 p}}{\frac{\sigma_o}{pE} + \frac{1.65}{0.75}\sqrt{\frac{\epsilon_{cu}\, h}{\lambda \sin\alpha \tan\alpha}}} \qquad (4.3/4)$$

This is now the most general solution for the ratio h_1/h .

The compression reinforcement has, naturally, also to be taken into account for the formulation of the ultimate shear moment, which, by including the contribution of vertical stirrups, becomes

$$M_{su} = bh^2 \left[\underbrace{\left(\sigma_o \frac{h_1}{h}\right.}_{\text{contribution of the beam}} + \underbrace{\left.\frac{p' f_y'}{2}\right)}_{\text{cont. of compressive reinforcement}} \left(1 - \frac{h_1}{2h}\right) + \underbrace{\frac{r f_y'}{2}}_{\text{contribution of stirrups}} \right] \qquad (4.3/5)$$

For the interpretation of test results of beams with unnaturally high percentage of compression reinforcement, it is stipulated that the compression force carried by the reinforcement cannot exceed the force carried by the concrete compression zone, i.e.

$$0.5\ bh\ f_y' \leq \sigma_o\ bh_1 \qquad (4.3/6)$$

This condition will scarcely ever be critical for the practice.

5 DERIVATION OF PARAMETERS

5.1 THE BOND COEFFICIENT $1/\lambda$

The derivation of the bond coefficient $1/\lambda$, defined by the equation

$$\Delta l_{bottom} = \lambda \epsilon_{st}^2 \qquad (3.3/1)$$

constitutes one of the major difficulties of the theory because it is hardly accessible to direct tests. Axial pull-out tests are not representative in magnitude, since due to the shear rotation ϕ , the pull-out force in the beam does not act in the direction of the tensile reinforcement, but under some angle, depending on the actual rotation and on the local split-away of concrete. A duplication of these complex conditions, by means of pull-out tests with lateral forces, seems hopeless because an application of the latter -- complicated and undetermined in itself -- would make reliable measurements practically impossible. An attempt is therefore made to compose the derivation of λ in part from findings of various investigators.

Most of these findings are given by the authors in the form of diagrams, and scarcely any explicit formulations, even for linear pull-out tests, can be found, probably because

of the large scatter always associated with such tests. For the application to the theory presented herein, this scatter is not alarming, because the final solution (Eq. 4.3/4) is relatively insensitive to normal errors in the estimation of λ. As will be seen, the range of variation of λ (from about 1000 to 100,000 inches) far exceeds the possible errors of a particular λ -value, thus justifying a consideration of the bond characteristic.

The general characteristic of pull-out tests can, for example, be observed in the thorough bond investigations reported by Clark (5.1/1), which covered pull-out tests on standard specimens as well as on beams. For the latter, the longitudinal reinforcement was exposed at a certain distance from the supports (see Fig. 5.1/1) in order to permit measurements of the relative displacement of steel and concrete by means of dial gages. The results of these beam tests coincided closely with those of the standard pull-out tests with the same anchorage length. The magnitude of the relative displacement ($\Delta 1$) as obtained from these tests is, however, not representative for the purpose of our theory because the obliquity of the pull-out force due to the shear rotation ϕ is, compared to the one in a normal beam, significantly decreased by the exposure of the bar over a considerable

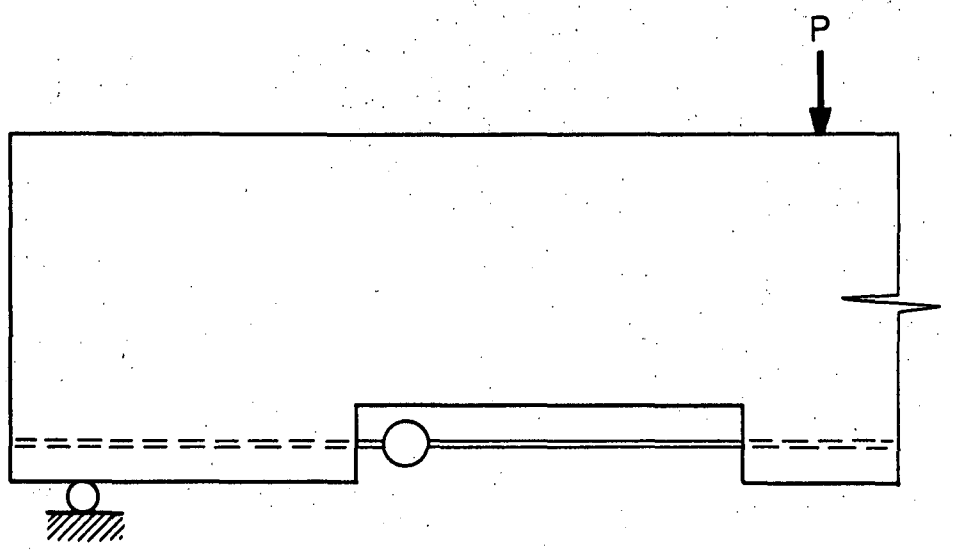

Fig. 5.1/1

Test Set-Up Used by Clark

length. Nevertheless, these tests may certainly serve to indicate the general trend of the relation between $\triangle 1$ and the pull-out force (P).

Figure 5.1/2 shows one of the diagrams from Clark's tests which is also representative for the pull-out data of many other authors.

The factors which will have to be considered for an empirical formulation of the λ -values are in accordance with experience,*

(1) The concrete strength

(2) The diameter of the reinforcing bars

(3) The prestressing

(4) The roughness of the reinforcing bars

The influence of the concrete strength was directly derived from beam tests. In Series B of the shear investigation of Moody, Viest, Elstner, and Hognestad (1.4/10), 16 beams were tested, the only variable of which was the concrete strength. Their ultimate shear moment vs. concrete strength is plotted in Fig. 5.1/3. The corresponding λ -values (Fig. 5.1/4) were calculated backwards with the aid of the

---

* The anchorage length was found to be of negligible influence as long as no slip at the non-loaded end of the bar occurs.

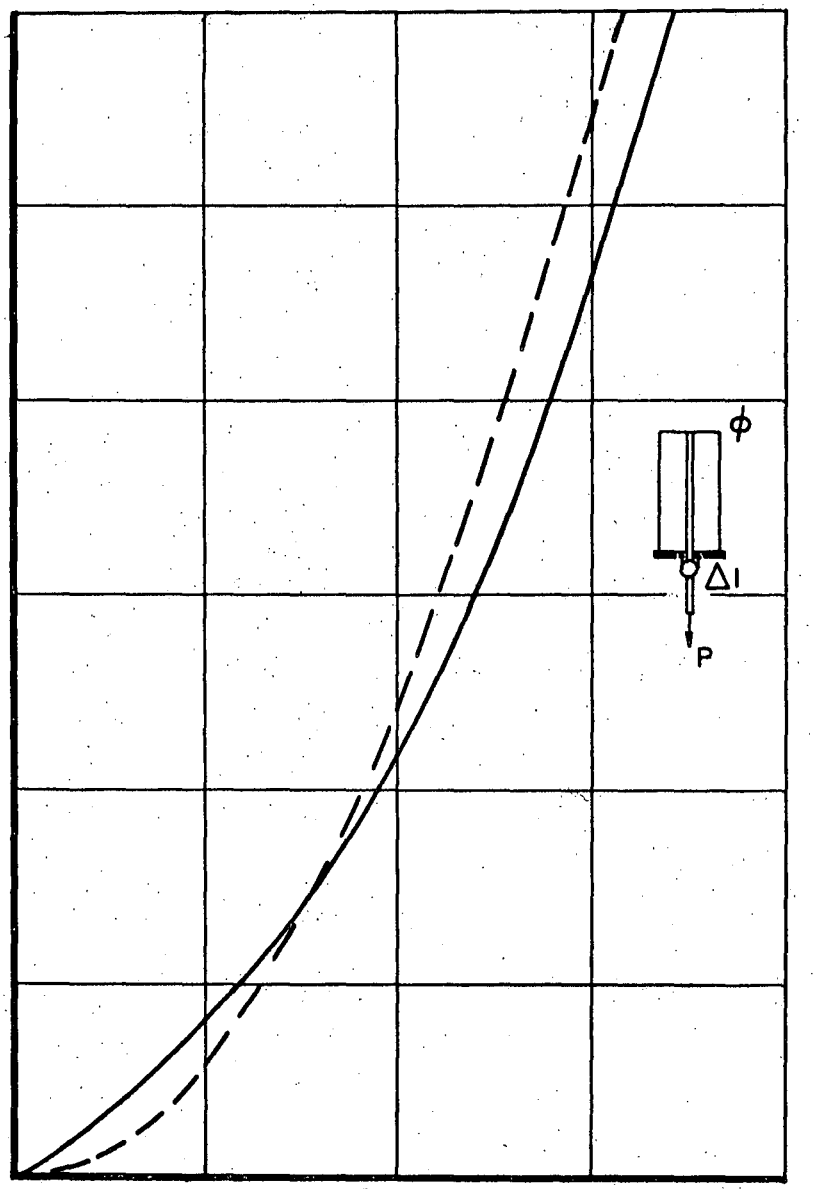

Fig. 5.1/2

Pull-Out Characteristic

——— From tests

— — Assumption $\Delta l = \lambda \epsilon^2$

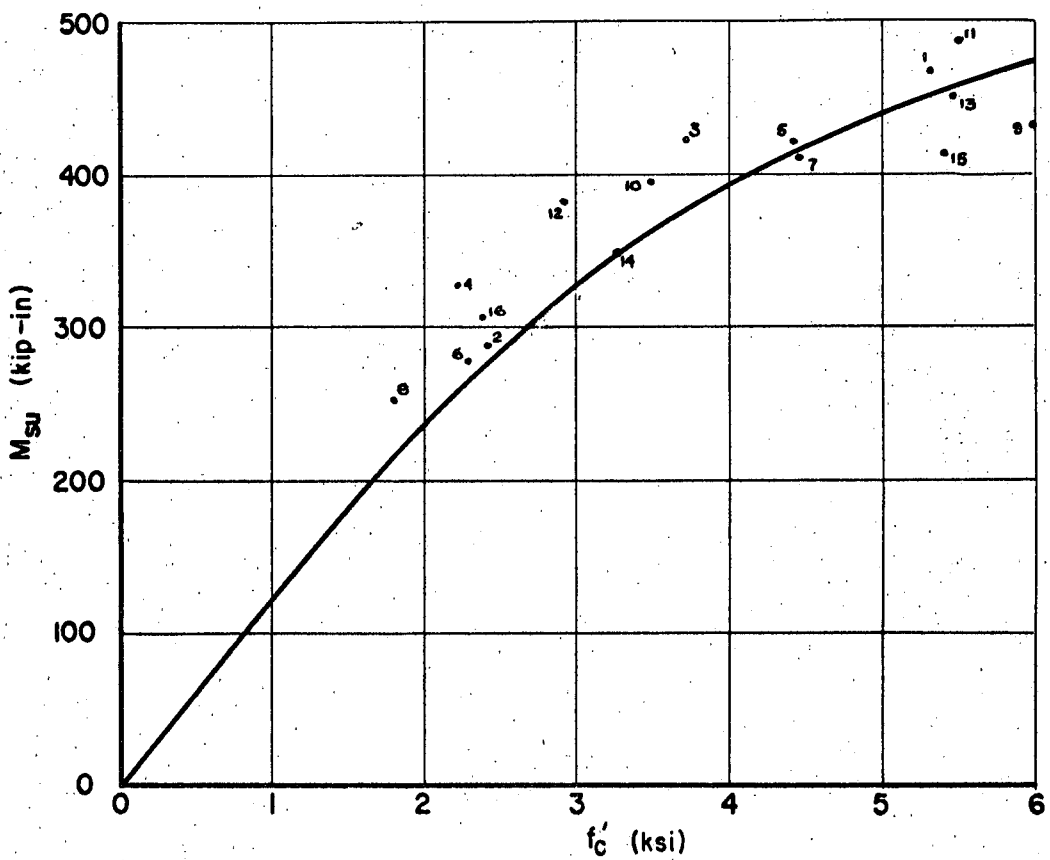

Fig. 5.1/3 M_{su} as a function of f_c' from the series B of the tests by Moody, Viest, Elstner and Hognestad

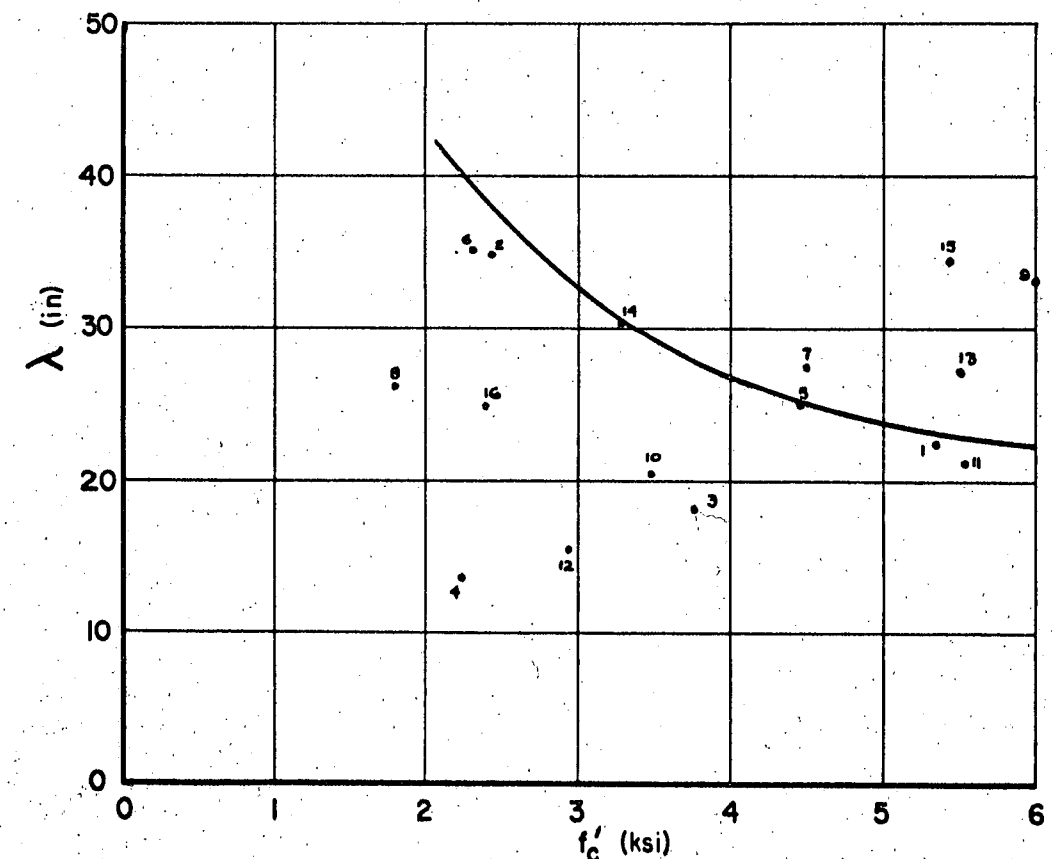

Fig. 5.1/4 Bond coefficient λ as a function of f_c' (derived from the tests above)

theory outlined in this paper, taking $\epsilon_{cu} = 0.0036$ and $\alpha = 45°$. The large scatter of the λ-diagram is a logical consequence of the favorable feature that the ultimate shear moment has a relatively small response to variations in λ. In order to determine the influence of the concrete strength on λ, it is therefore necessary to select an idealized conservative curve in the moment-strength diagram (Fig. 5.1/3) and trace this curve forth into the λ-diagram (Fig. 5.1/4). This permits an estimation of the sought relationship with

$$\lambda = \lambda_5 (0.5 + \frac{2500 \text{ psi}}{f_c'}) \qquad (5.1/1)$$

where λ_5 is the coefficient at the arbitrary chosen reference strength of $f_c' = 5000$ psi. Obviously λ_5 still depends on the other influencing factors mentioned before.

Equation 5.1/1 is in qualitative agreement with findings of other authors, notably with those of Clark (5.1/1).

The influence of the bar-diameter d, was, for example, studied by Djabry (5.1/2) by means of pull-out tests with plain round bars, the results of which are summarized in Figure 5.1/5. Three sets of λ-values were derived from this data, such that the assumption

$$\Delta 1 = \lambda \epsilon_{st}^2$$

coincided with the experimental values at $\Delta 1$ equal 0.01, 0.02 and 0.03 cm respectively. Plotting these λ-values as a function of the bar diameter d (Figure 5.1/6) suggests

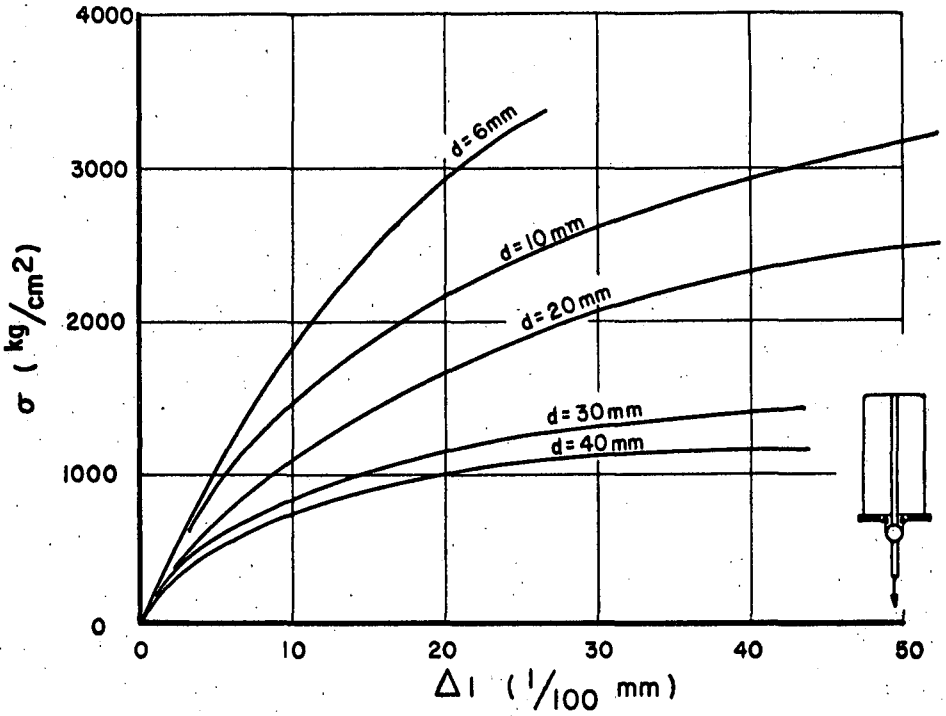

Fig. 5.1/5 Tests by Djabry. Pull-Out Displacement vs. Steel Stress. (Plain Round Bars)

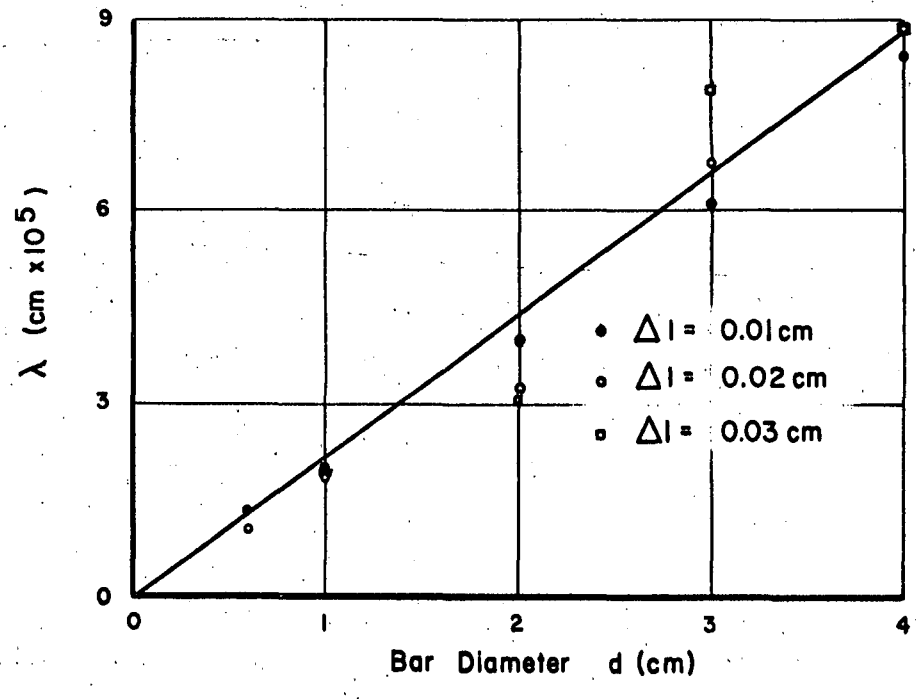

Fig. 5.1/6 Coefficient λ vs. Bar Diameter Derived from Djabry's Tests.

a straight line assumption

$$\lambda = k \cdot \varkappa \left(0.5 + \frac{2500 \text{ psi}}{f_c'}\right) \cdot d \qquad (5.1/2)$$

where $\varkappa$ is a coefficient which may still be dependent on the prestressing and the bar roughness and k is a factor for the transition from straight pull-out tests to the actual pull-out effect in beams.

If a cross-section contains bars of different diameters, the question arises, what value of d should be used in Equation 5.1/2. It is believed that a plausible assumption should be based on the arithmetic mean value of the bar cross-areas

$$A_{equ} = \frac{\sum_{1}^{n} A_n}{n}$$

where n is the number of bars of one cross-section. Thus

$$d_{equ} = 2\sqrt{\frac{A_{equ}}{\pi}}$$

or

$$d_{equ} = \sqrt{\frac{\sum_{1}^{n} d_n^2}{n}} \qquad (5.1/3)$$

The influence of prestressing was studied in the course of an investigation at Lehigh University (Ref. 5.1/3) which had as its primary object the anchorage characteristic of prestressing strands. A great number of pull-out specimens

of various lengths were cast around 7/16 inch pretensioned strands. The prestressing was only released at the free end whereas the pull-out end remained under tension, thus simulating the prestressing condition occurring at a crack. It was shown in this investigation that the distribution of the bond stresses and, consequently, the pull-out characteristic is not appreciably altered by varying the prestressing. Thus λ can be considered as being independent of the degree of prestressing.

The Influence of the Roughness. The term roughness, as interpreted in this paper, does not only refer to the surface of the bar, it includes also other means of improving the bond characteristic, i.e. notches, ridges (deformed bars) and distortion of bars or wires (strands).

Since no comprehensive treatment of this subject including strands could be found, a series of pull-out tests was performed at the Fritz Laboratory, the results of which are given in the appendix.

The tentative values for the coefficient of roughness obtained from these tests are given in Table 5.1/I.

	Not Rusted	Rusted
Plain Round Bars	18500	13500
Deformed Bars	9500	6500
Strands	6500	4500

TABLE 5.1/I

Coefficients of Roughness (χ) for Standard Pull-out Tests

With the aid of these χ -values, it is now possible to compare numerically the difference between axial pull-out and pull-out in beams. One could obtain, for example, the same idealized curve of the λ -values as given in Figure 5.1/4 by choosing the transition factor k to be three. In other words, due to the obliquity of the pull-out force in beams, the displacement $\Delta 1$ is approximately three times larger than for axial pull-out.

Consequently the coefficient λ can be calculated as

$$\lambda = 3(0.5 + \frac{2500 \text{ psi}}{f_c'}) \chi d \qquad (5.1/4)$$

In spite of the somewhat vague basis of these derivations, this empirical formula for λ substituted in the solution for the ultimate shear moment showed satisfactory agreement with test results (see Chapter 6).

5.2/1 THE INCLINATION α OF DIAGONAL CRACKS

Since it was found that under given load conditions diagonal cracks more or less follow the stress trajectories, the angle α could always be determined accordingly. In experimental investigations there occur, however, always cases where the crack pattern differs considerably from the stress-trajectories without significantly affecting the ultimate shear moment. By comparing the outlined theory with a great number of test results, it was furthermore found that the best agreement was achieved by assuming an angle α of $45°$. Thus it seems permissible to idealize the real conditions by assuming always

$$\boxed{\alpha = 45°}$$

more so, since this assumption yields theoretically conservative results.

5.3 THE ULTIMATE CONCRETE STRAIN ϵ_{cu}

The uncertainty about the magnitude of the ultimate concrete strain, reflected in many investigations, is to a great degree caused by its sensitivity to the speed of loading and by the difficult techniques of measurement. It seems conceivable that the loading speed cannot be a determining factor for the ultimate strength, a contention which is substantiated by considering the small influence of ϵ_{cu} on the final solution of the theory presented herein. Thus an average value of

$$\boxed{\epsilon_{cu} = 0.0036}$$

is assumed for later computations and recommendations.

Some qualitative reflections on the influence of the state of strain on ϵ_{cu} may, however, serve to explain an experimentally observed phenomenon. If, namely, a simply supported beam is unsymmetrically loaded with one concentrated load, it can always be observed that the opening of the diagonal cracks in the short shear span is larger than in the longer shear span, although the maximum moment is the same. This can only be attributed to the different state of strain due to the different magnitude of the shear force on either side of the applied load. One can thus conclude

that the deformation and consequently ϵ_{cu} , is greater the larger the magnitude of the shear force becomes.

6 COMPARISON OF THE THEORY WITH TEST RESULTS

The theory of shear failures stated herein is compared in this chapter with the results of 278 beam tests which could be found in the more recent literature. According to the general validity of the theory, a broad field of variables could be considered in this comparison, including:

Cross-Section

Shear Span

Prestressing

Web Reinforcement

Compression Reinforcement

End Restraint

The following tables give the properties of the test beams and the major steps of computation required for the theoretical solution, the latter involving always:

(1) $\sigma_o \longrightarrow$ Eq. 2.4/8

(2) $\lambda \longrightarrow$ Eq. 5.1/4 and Table 5.1/I

(3) $h_1/h \longrightarrow$ Eq. 4.3/4

(4) $M_{su} \longrightarrow$ Eq. 4.3/5

For T-beams it has naturally to be observed that the depth of the neutral axis should not be taken larger than the depth of the flange.

For the computation of the ultimate strength of restrained beams the contributions of the compression reinforcement and the shear transfer (V_{st}) of the stirrups were neglected. This conservative measure seems justifiable on account of rapid changes of the free body forces within the relatively short shear span: firstly, the change from negative moments over the support to the positive moment at the end of the shear span makes a full development of the steel compression force according to the concrete compression strains unlikely; and secondly, the stirrups close to the concrete crushing zone probably do not reach their yield strength. Thus a reduction of the shear force carried by the concrete should not be considered. This presumption has on the other hand little effect on the moment contribution of the stirrups.

The ratios $M_{calculated}/M_{test}$ are given in the last column of the tables including those results where large deviations could be assigned to definitely known reasons, for example, very short shear spans (theory underestimates the shear strength) or erratic results within a test series. The frequency curves of the ratio M_{calc}/M_{test} are given for all the tests in Fig. 6/1 and 6/2. It should be noted that the theory resulted from rationally founded assumptions which had

at times been chosen conservatively. The peaks of the frequency curves lie therefore in general on the conservative side.

As for the prestressed beams (with the frequency peak at 0.8) no empirical modification was sought for the time being, since only one test series with a limited number of variables was available. As mentioned in the introduction, it is planned to study the particular conditions of prestressed concrete in the light of this theory by a series of tests which might eventually suggest an empirical or theoretical modification.

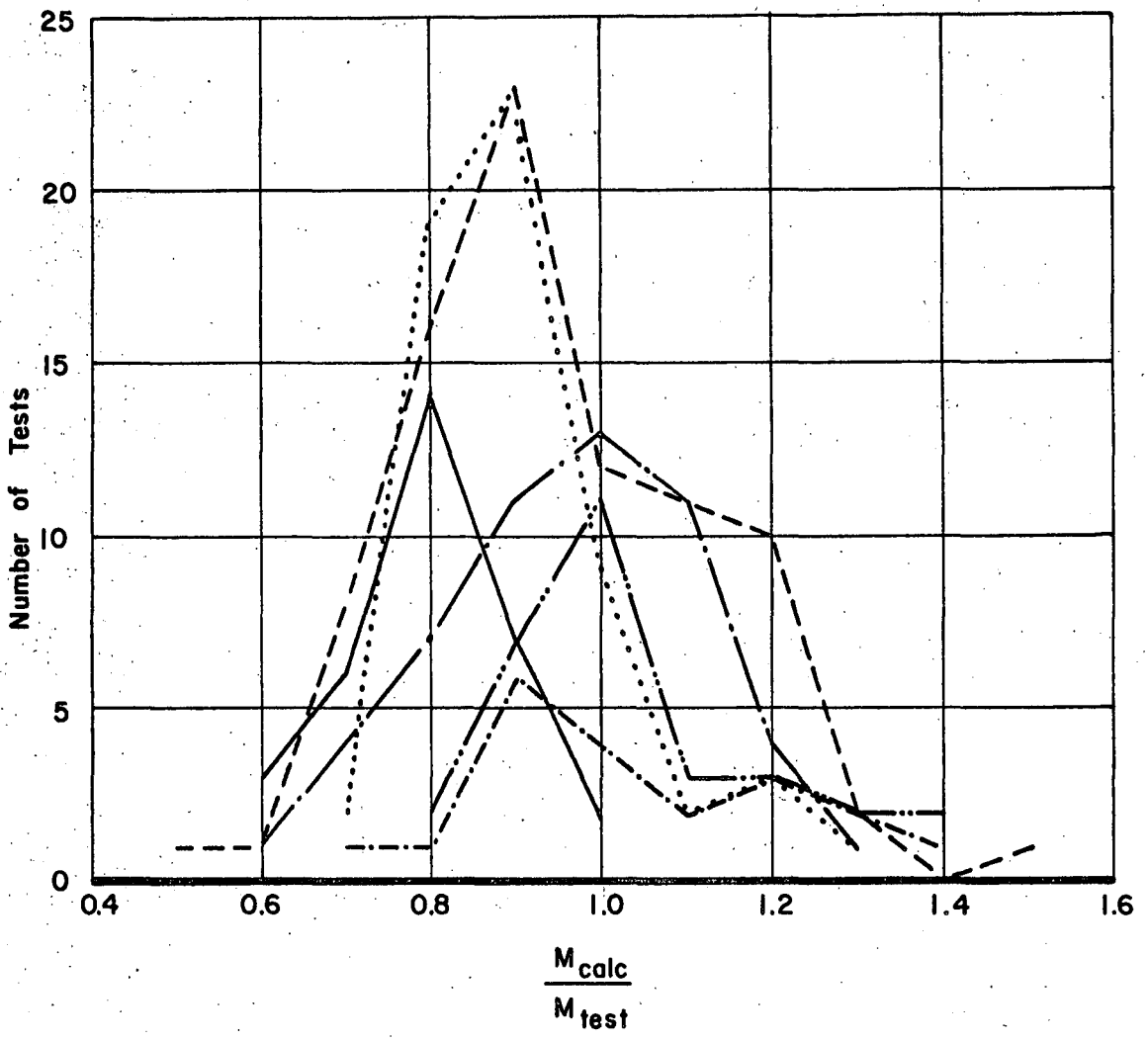

		N	m	σ
—·—	Simply supported; no web or comp. reinf.	52	0.96	0.15
—··—	Simply supported; with comp. reinf.	30	1.04	0.15
·····	Simply supported; with web reinf.	59	0.90	0.12
—·—·—	T Section	20	1.04	0.18
———	Prestressed	32	0.80	0.10
– – –	Restrained	85	0.94	0.17
	TOTAL	278	0.94	0.16

Note: N = number of tests
m = mean value of M_{calc}/M_{test}
σ = standard deviation

Fig. 6/1

Frequency Curve of the Ratio $\frac{M_{calc}}{M_{test}}$

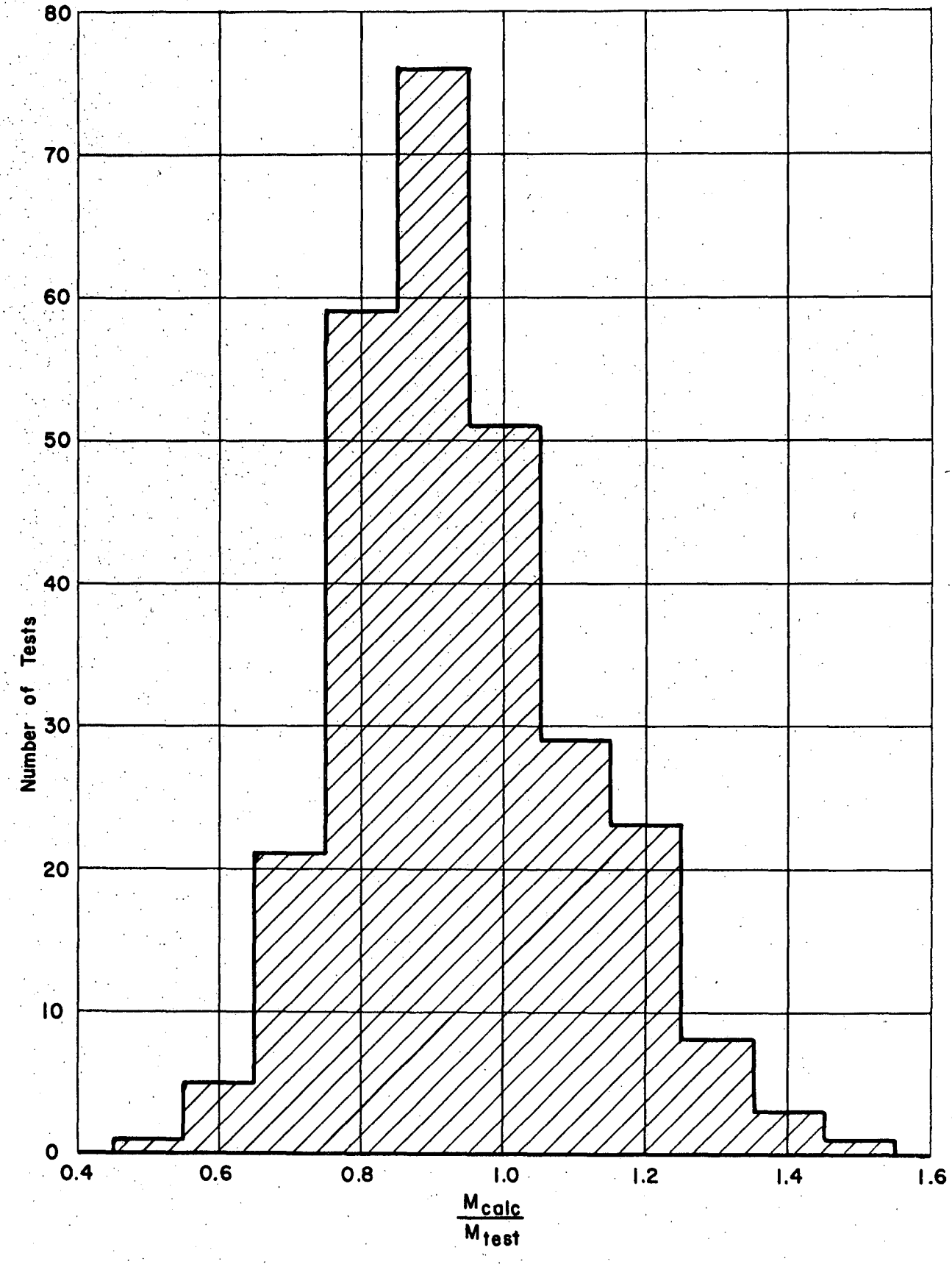

Fig. 6/2 Composite Frequency Curve of the Ratio $\frac{M_{calc}}{M_{test}}$

(Number of tests = 278)

Beam	$\frac{M}{Vh}$	f'_c	p	σ_o	λ	$h_{1/h}$	M_{calc}	M_{test}	$\frac{M_{calc}}{M_{test}}$
		psi	%	ksi	in.		k-in	k-in	
1	3.41	5320	1.90	4.607	23763	0.176	495.0	468	1.06
2	"	2420	"	2.095	37560	0.253	309.6	288	1.08
3	"	3735	"	3.234	28649	0.210	407.2	423	0.96
4	"	2230	"	1.931	39717	0.261	293.2	327.6	0.89
5	3.41	4450	1.90	3.853	26014	0.193	450.0	421.2	1.07
6	"	2290	"	1.982	38997	0.258	298.3	279	1.07
7	"	4480	"	3.897	25922	0.193	451.5	414	1.09
8	"	1770	"	1.533	46855	0.283	249.2	252	0.99
9	3.41	5970	1.90	5.169	22509	0.165	524.4	432	1.21
10	"	3470	"	3.005	29901	0.217	389.6	396	0.98
11	"	5530	"	4.788	23326	0.172	504.7	486	1.04
12	"	2925	"	2.533	33190	0.234	350.6	381.6	0.92
13	3.41	5480	1.90	4.745	23427	0.173	502.5	450	1.12
14	"	3265	"	2.827	31010	0.224	375.5	349.2	1.08
15	"	5420	"	4.693	23551	0.174	499.6	414	1.21
16	"	2370	"	2.052	38094	0.255	305.5	306	1.00

Reference: 1.4/10
Reinforcement: 2 No. 7 Deformed bars
Dimensions: 6" x 12" Beams. a = 36", h = 10.56, L = 108"
Total length = 120"

TABLE 6/1 - Tests By Moody (Series B), 1953. Simple Span Rectangular Beams Without Web Reinforcement

Beam	h	$\frac{M}{Vh}$	f'c	p	Reinf Bars	σ_o	λ	$h_{1/h}$	M_{calc}	M_{test}	$\frac{M_{calc}}{M_{test}}$
	in.		psi	%	No.-Size	ksi	in.		k-in	k-in	
A1	10.30	3.06	4400	2.17	1-11	3.689	42173	0.183	455.9	425	1.07
2	10.50	3.00	4500	2.15	2-8	3.749	29555	0.205	531.1	472	1.13
3	10.55	2.99	4500	2.22	2-7; 1-6	3.744	24679	0.222	575.4	535	1.08
4	10.63	2.96	4570	2.37	4-6	3.793	21988	0.238	629.1	504	1.25
B1	10.50	3.00	3065	1.62	1-8; 2-4	2.554	26045	0.227	397.0	398	1.00
2	10.55	2.99	3125	1.63	2-7	2.600	31850	0.212	383.5	425	0.90
3	10.63	2.96	2785	1.60	2-6; 1-5	2.312	27824	0.236	380.7	394	0.97
4	10.69	2.95	2430	1.66	4-5	2.013	26754	0.265	351.4	394	0.89
C1	10.55	2.99	920	0.81	1-7	0.766	78826	0.222	117.6	142	0.83
2	10.70	2.94	880	0.83	2-5	0.728	58466	0.255	129.7	173	0.75
3	10.75	2.93	1000	0.80	3-4	0.827	42000	0.256	149.1	180	0.83
4	10.80	2.92	980	0.82	2-4; 2-3	0.808	37759	0.271	154.5	178	0.87

Reference: 1.4/10
Reinforcement: Deformed Bars
Dimensions: 7" x 12" Beams. a = 31.5", h = Variable, 10.30 — 10.80. L = 63".
Total Length = 75".

TABLE 6/2 - Tests by Moody (Series A), 1953.
Simple-Span Rectangular Beams Without Web Reinforcement

Beam	a	h	$\frac{M}{Vh}$	f'c	p	Reinf Bars	σ_o	λ	$h_{1/h}$	M_{calc}	M_{test}	$\frac{M_{calc}}{M_{test}}$
	in	in.		psi	%	No.Size	ksi	in.		k-in	k-in	
S-2	48	10.58	4.54	3900	2.08	3-No.6	3.587	23962	0.221	473.4	458.4	1.03
S-3	"	10.44	4.60	4690	2.52	2-No.8	4.322	28925	0.208	526.3	573.6	0.92
S-4	"	10.37	4.63	4470	3.21	2-No.9	4.124	33457	0.238	557.5	600.0	0.93
S-5	48	10.31	4.66	4330	4.11	2-No.10	3.998	38311	0.269	592.7	537.6	1.10
S-11	"	10.51	4.57	2140	1.90	2-No.7	1.969	40871	0.255	290.7	364.8	0.80
S-13	"	10.31	4.66	3800	4.11	2-No.10	3.508	41175	0.283	542.9	537.6	1.01
S-1	51	10.65	4.79	3940	1.46	3-No.5	3.653	19854	0.184	415.3	428.4	0.97
S-9	48	10.72	4.48	2140	0.93	3-No.4	1.964	23355	0.196	239.4	276.0	0.87
S-10	"	10.58	4.54	2280	1.39	2-No.6	2.096	33527	0.216	271.4	369.6	0.73

Reference: 1.4/2
Reinforcement: Deformed Bars
Dimensions: 6" x 12" Beams. h = 10.31 to 10.72. L = 108". Total Length = 120".

TABLE 6/3 - Tests by Laupa, 1953.
Simple-Span Rectangular Beams Without Web Reinforcement

Beam	$\frac{M}{Vh}$	f'c	p	Reinf. Bars	σ_o	λ	$h_{1/h}$	M_{calc}	M_{test}	$\frac{M_{calc}}{M_{test}}$
		psi	%	No. Size	ksi	in.		k-in	k-in	
T2 Ma	3.40	4320	1.38	2-No.6	3.739	22653	0.166	381.2	332.3	1.15
T2 Mb	"	4020	1.38	2-No.6	3.479	23560	0.172	366.9	351.7	1.04
T2 Mc	"	4470	1.90	2-No.7	3.868	25953	0.193	452.8	450.2	1.01

Reference: 6.1/1
Reinforcement: Deformed Bars
Dimensions: 6" x 12" Beams, a = 36", h = 10.58", L = 108",
Total length = 120".

TABLE 6/4 - Tests by Gaston, 1952. Simple-Span Rectangular Beams Without Web Reinforcement

Beam	a	$\frac{M}{Vh}$	f'c	p	σ_o	λ	$h_{1/h}$	M_{calc}	M_{test}	$\frac{M_{calc}}{M_{test}}$
	in		psi	%	ksi	in		k-in	k-in	
AO-1	36	2.34	3120	0.98	2.349	31882	0.183	737.0	720.0	1.02
2	"	"	3770	"	2.839	28497	0.166	817.2	873.0	0.94
3	"	"	3435	"	2.586	30081	0.174	777.2	963.0	0.81
BO-1	30	1.95	3420	0.98	2.322	30160	0.188	746.8	816.0	0.92
2	"	"	3468	"	2.355	29912	0.187	752.7	636.0	1.18
3	"	"	3410	"	2.315	30212	0.188	745.2	864.0	0.86
CO-1	24	1.56	3580	0.98	2.060	29358	0.206	717.8	940.8	0.76
2	"	"	3405	"	1.959	30238	0.210	696.7	958.8	0.73
3	"	"	3420	"	1.967	30160	0.210	698.4	901.2	0.77
DO-1	18	1.17	3750	0.98	1.621	28583	0.241	649.6	896.4	0.72
2	"	"	3800	"	1.644	28369	0.240	655.3	1052.1	0.62
3	"	"	3765	"	1.628	28518	0.240	651.2	903.6	0.72

Reference: 4.2/1
Reinforcement: 2 No. 7 Deformed bars.
Dimensions: 8" x 18" Beams. a = Variable, 18" to 36". h = 15.37". L = 72".

TABLE 6/5 - Tests by Clark, 1951.
Simple-Span Rectangular Beams Without Web Reinforcement

Beam	$\frac{M}{Vh}$	f'c	p	p'	σ_o	λ	$h_{1/h}$	M_{calc}	M_{test}	$\frac{M_{calc}}{M_{test}}$
		psi	%	%	ksi	in.		k-in	k-in	
24a	1.52	2580	2.72	1.36	1.453	46397	0.322	2004.8	2128	0.94
b	"	2990	"	"	1.685	42199	0.314	2173.2	2176	1.00
25a	"	3530	3.46	1.73	1.988	42964	0.321	2662.2	1920	1.39
b	"	2500	"	"	1.408	53340	0.338	2220.1	2080	1.07
26a	1.52	3140	4.25	2.13	1.768	51174	0.340	2764.7	3024	0.91
b	"	2990	"	"	1.685	52749	0.342	2698.9	2848	0.95
27a	"	3100	2.72	1.36	1.746	41263	0.312	2216.2	2496	0.89
b	"	3320	"	"	1.871	39575	0.307	2302.0	2560	0.90
28a	1.52	3380	3.46	1.73	1.904	44082	0.324	2601.4	2176	1.20
b	"	3250	"	"	1.831	45135	0.326	2546.7	2448	1.04
29a	"	3150	4.25	2.13	1.774	51073	0.340	2769.9	2800	0.99
b	"	3620	"	"	2.039	47005	0.333	2976.3	3136	0.95

Compression Reinforcement: fy $\cong$ 45 ksi
Reinforcement: Deformed bars
Reference: 1.4/10
Dimensions: 7" x 24" Beams. a = 32", h = 21", L = 96",
Total length = 120".

TABLE 6/6 - Tests by Moody (Series III), 1953. Simple Span Rectangular Beams Without Web Reinforcement, With Compression Reinforcement

Beam	b	$\frac{M}{Vh}$	f'c	p	p'	Reinf. Bars	σ_o	λ	$h_{1/h}$	M_{calc}	M_{test}	$\frac{M_{calc}}{M_{test}}$
	in		psi	%	%	No. Size	ksi	in.		k-in	k-in	
T-2b	4.00	4.29	3580	1.40	1.40	2-1/2"	3.260	16776	0.104	125.5	150.0	0.84
c	"	"	"	"	"	"	"	"	"	"	"	"
T-3a	4.00	4.29	3470	3.14	3.14	2-3/4"	3.160	25629	0.130	150.3	157.5	0.95
b	"	"	"	"	"	"	"	"	"	"	105.0	1.43
c	"	"	"	"	"	"	"	"	"	"	127.5	1.18
T-5a	4.00	4.29	3460	2.18	2.18	2-5/8"	3.151	21395	0.120	139.6	142.5	0.98
b	"	"	"	"	"	"	"	"	"	"	151.5	0.92
c	"	"	"	"	"	"	"	"	"	"	154.5	0.90
T-6b	4.00	4.29	3130	1.40	1.40	2-1/2"	2.851	18182	0.108	114.3	114.0	1.00
c	"	"	"	"	"	"	"	"	"	"	123.0	0.93
T-11b	6.25	"	4190	"	"	2-5/8"	3.816	19191	0.084	188.1	180.0	1.05
T-12a	5.75	4.29	4880	2.18	2.18	2-3/4"	4.445	21258	0.096	228.9	237.0	0.97
b	"	"	"	"	"	"	"	"	"	"	225.0	1.02
c	"	"	"	"	"	"	"	"	"	"	214.5	1.07

Dimensions: 4 to 6.25 x 8 Beams. h = 7", L = 60", total length 65".
Compression Reinforcement: fy $\cong$ 48 ksi.
Reference: 6.1/2

TABLE 6/7 - Tests at M. I. T., 1951. Simple Span Rectangular Beams Without Web Reinforcement, With Compression Reinforcement

Beam	$\frac{M}{Vh}$	f'c	p	p'	σ_o	λ	$h_{1/h}$	M_{calc}	M_{test}	$\frac{M_{calc}}{M_{test}}$
		psi	%	%	ksi	in.		k-in	k-in	
1N1	1.75	3550	3.98	0.50	2.239	38069	0.373	1424.1	1120	1.27
1N2	"	3620	"	"	2.284	37637	0.371	1444.3	1408	1.03
2N1	"	4340	"	"	2.738	34016	0.355	1644.3	1256	1.31
2N2	"	4640	"	"	2.927	32839	0.348	1723.6	1448	1.19

Reference: 1.4/8
Compression Reinforcement: fy $\cong$ 48 ksi
Reinforcement: Deformed bars
Dimensions: 5.5" x 21" Beams, h = 18.25", a = 32", L = 96", total length = 120".

TABLE 6/8 - Tests By Moretto, 1945. Simple-Span Rectangular Beams Without Web Reinforcement, With Compression Reinforcement

Beam	a	$\frac{M}{Vh}$	f'_c	p	r	σ_o	λ	$h_{1/h}$	M_{bend}	M_{stir}	M_{calc}	M_{test}	$\frac{M_{calc}}{M_{test}}$
	in.		psi	%	%	ksi	in.		k-in.	k-in.	k-in.	k-in.	
		h = 15.37"		b = 8"		L = 72"		fy = 46.5 ksi					
A1-1	36	4.24	3575	3.10	0.38	3.25	42647	0.279	1475	172	1647	1800	0.92
2	36	4.48	3430	3.10	.38	3.14	43698	.282	1440	172	1613	1692	.95
3	36	4.27	3395	3.10	.38	3.08	43966	.284	1423	172	1595	1800	.89
4	36	3.95	3590	3.10	.38	3.21	42544	.280	1468	172	1640	1980	.83
B1-1	30	2.99	3388	3.10	.37	2.82	44020	.298	1352	167	1519	1880	.81
2	30	3.14	3680	3.10	.37	3.11	41938	.286	1445	167	1613	1730	.93
3	30	2.96	3435	3.10	.37	2.84	43661	.297	1362	167	1529	1920	.80
4	30	3.06	3380	3.10	.37	2.83	44082	.297	1355	167	1523	1808	.84
5	30	3.26	3570	3.10	.37	3.05	42683	.288	1422	167	1590	1628	.98
B2-1	30	5.37	3370	3.10	.73	3.17	44160	.280	1443	331	1774	2030	.87
2	30	4.82	3820	3.10	.73	3.54	41052	.268	1559	331	1890	2173	.87
3	30	4.56	3615	3.10	.73	3.32	42372	.275	1495	331	1826	2258	.81
B6-1	30	2.62	6110	3.10	.37	4.84	32329	.240	1935	167	2103	2558	.82
C1-1	24	2.30	3720	2.07	.34	2.77	41678	.244	1123	154	1278	1498	.85
2	24	2.19	3820	2.07	.34	2.77	41052	.245	1129	154	1283	1678	.77
3	24	2.45	3475	2.07	.34	2.67	43362	.246	1093	154	1247	1326	.94
4	24	2.27	4210	2.07	.34	3.11	38896	.232	1210	154	1364	1542	.88
C2-1	24	4.16	3430	2.07	.69	3.10	43698	.223	1170	313	1483	1564	.95
2	24	3.92	3625	2.07	.69	3.24	42304	.220	1204	313	1517	1624	.93
3	24	3.54	3400	2.07	.69	3.06	43181	.227	1165	313	1478	1746	85
4	24	4.20	3910	2.07	.69	3.54	40517	.211	1266	313	1579	1554	1.02
C3-1	24	2.60	2040	2.07	.34	1.61	61359	.296	769	154	923	1206	.77
2	24	2.82	2000	2.07	.34	1.62	62239	.293	771	154	925	1080	.86
3	24	2.97	2020	2.07	.34	1.67	61789	.289	786	154	940	1014	.93

Tension reinforcement: Deformed bars Reference: 4.2/1 (Continued on next page)
Web reinforcement: Deformed bars, 3/8-in; Vertical stirrups, fy = 48 ksi

TABLE 6/9 - TESTS BY CLARK, 1951
Simple-Span Rectangular Beams With Web Reinforcement

Beam	a	$\frac{M}{Vh}$	f'_c	p	r	σ_o	λ	$h_{1/h}$	M_{bend}	M_{stir}	M_{calc}	M_{test}	$\frac{M_{calc}}{M_{test}}$
	in.		psi	%	%	ksi	in.		k-in.	k-in.	k-in.	k-in.	
C4-1	24	2.19	3550	3.10	0.34	2.58	42823	0.313	1290	154	1444	1668	0.87
C6-2	24	1.98	6560	3.10	.34	4.49	31332	.253	1880	154	2035	2286	.89
3	24	1.96	6480	3.10	.34	4.41	31499	.255	1862	154	2016	2346	.86
4	24	1.97	6900	3.10	.34	4.71	30663	.248	1959	154	2114	2312	.91
		h = 15.37"		b = 8"		L = 72"		fy = 48.63 ksi					
D1-1	18	1.95	3800	1.63	.46	2.58	36571	.229	991	208	1200	1218	.99
2	18	1.77	3790	1.63	.46	2.40	36626	.239	959	208	1167	1443	.81
3	18	2.21	3560	1.63	.46	2.60	37972	.225	984	208	1192	1038	1.15
D2-1	18	2.62	3480	1.63	.61	2.75	38482	.216	1006	276	1283	1173	1.09
2	18	2.41	3755	1.63	.61	2.86	36821	.214	.036	276	1313	1263	1.04
3	18	2.25	3595	1.63	.61	2.65	37756	.223	994	276	1270	1353	.94
4	18	2.24	3550	1.63	.61	2.61	38035	.224	986	276	1262	1355	.93
D3-1	18	3.02	4090	2.44	.92	3.41	35098	.250	1413	417	1830	1598	1.15
D4-1	18		3350	1.63	1.22	3.35	39362	.188	1082	539	1622	1263	1.28
		h = 12.37"		b = 6"		L = 96"		fy = 46.5 ksi					
D1-6	24	3.33	4010	3.42	.46	3.44	39950	.273	747	101	848	942	.90
7	24	3.27	4060	3.42	.46	3.47	39676	.272	751	101	852	966	.88
8	24	3.19	4030	3.42	.46	3.42	39840	.274	745	101	846	1002	.84
		h = 12.37"		b = 6"		L = 115"		fy = 46.5 ksi					
E1-2	25	4.22	4375	3.42	.73	3.97	38101	.255	813	160	974	1246	.78
		h = 12.37"		b = 6"		L = 120"		fy = 46.5 ksi					
D2-6	30	5.69	4280	3.42	.61	4.05	38551	.252	819	134	954	1135	.84
7	30	6.29	4120	3.42	.61	3.94	39358	.254	803	134	938	1060	.89
8	30	5.69	3790	3.42	.61	3.59	41237	.265	757	134	892	1135	.79
D4-1	30	4.50	3970	3.42	.49	3.64	40172	.264	768	108	876	1135	.77
2	30	4.79	3720	3.42	.49	3.44	41678	.270	739	108	847	1060	.80
3	30	4.58	3200	3.42	.49	2.94	45561	.287	665	108	773	1113	.70
D5-1	30	4.05	4020	3.42	.37	3.62	39895	.266	767	81	848	985	.86
2	30	3.86	4210	3.42	.37	3.75	38896	.262	786	81	867	1060	.82
3	30	3.86	3930	3.42	.37	3.50	40401	.270	752	81	833	1060	.79

* Mst = V x $\frac{h}{2}$, (Vst V)

TABLE 6/9 (Continued)

Beam	h	$f'c=\sigma_o^*$	p	r	λ	$h_{1/h}$	M_{bend}	M_{st}*	M_{calc}	M_{test}	$\frac{M_{calc}}{M_{test}}$
	in.	psi	%	%	in.		k-in	k-in	k-in	k-in	
T1Lb	10.72	2520	0.62	0.28	20889	0.126	205.0	36.1	241.1	242.4	0.99
T2La	10.65	2120	0.97	0.42	29387	0.176	232.0	43.0	275.0	290.4	0.95
T4Lb	10.44	2810	2.52	0.92	38912	0.248	399.1	83.2	482.3	573.6	0.84
T5L	10.37	2500	3.22	0.92	47376	0.287	396.0	93.2	489.2	646.8	0.76
T11L	9.23	2900	7.22	1.83	43019	0.383	459.1	104.0	563.1	811.2	0.69
T1Ha	10.58	5880	1.38	1.05	19428	0.124	460.7	61.9	522.6	421.2	1.24
T2H	10.44	5400	2.52	1.05	26963	0.183	587.0	93.8	680.8	646.8	1.05
T3H	9.52	5920	4.20	1.83	22596	0.247	695.6	107.2	802.8	812.4	0.99
T5H	9.23	5900	7.22	1.83	29176	0.307	782.9	132.8	915.7	1035.6	0.88

* $V_{st} > V$ therefore: $M_{st} = V \cdot \frac{h}{2}$, $\sigma_o = f'c$, $\frac{M}{(V-V_{st})h} = \infty$

Reference: 6.1/1
Tension Reinforcement: Deformed bars
Web Reinforcement: Vertical deformed stirrups, fy ≅ 45 ksi
Dimensions: 6" x 12" beams. a = 36", h = 9.23" — 10.72".
Total Length = 120" L = 108"

TABLE 6/10 - Tests by Gaston, 1952.
Simple-Span Rectangular Beams With Web Reinforcement

Beam	a	$\frac{M}{Vh}$	f'c	p	σ_o	λ	$h_{1/h}$	M_{calc}	M_{test}	$\frac{M_{calc}}{M_{test}}$
	in		psi	%	ksi	in.		k-in	k-in	
6	10.0	2.00	3935	0.34	2.714	11923	0.066	55.96	81.50	0.69
12	12.5	2.45	3650	0.61	2.808	16590	0.091	79.34	75.75	1.05
11	17.0	3.32	4150	"	3.568	15435	0.076	85.09	66.47	1.28
2	"	3.36	4043	0.34	3.485	11744	0.052	57.80	55.08	1.05
3	20.0	4.00	3945	0.34	3.546	11902	0.052	58.27	64.40	0.90
10	"	"	4150	0.62	3.730	15435	0.075	87.61	66.20	1.32
4	"	4.02	3850	0.35	3.462	12070	0.053	58.15	62.40	0.93
13	"	"	4165	0.63	3.746	15400	0.076	88.44	76.40	1.16
5	21.0	4.18	3950	0.34	3.581	11897	0.051	58.06	66.99	0.87
18	22.5	4.39	3900	0.61	3.565	15974	0.076	84.59	70.88	1.19
1	"	4.44	3925	0.34	3.598	11939	0.051	58.00	63.79	0.91
22	"	4.50	4150	"	3.811	11576	0.049	59.44	65.92	0.90
7	22.5	4.50	4690	0.63	3.388	16485	0.080	84.05	68.51	1.23
17	27.5	5.35	4290	0.61	4.036	15162	0.070	88.12	85.53	1.03
8	"	5.49	3810	0.63	3.594	16186	0.076	85.71	83.05	1.03
19	"	"	4440	0.97	4.189	18603	0.092	119.73	86.63	1.38
9	32.5	6.49	4600	0.63	4.410	14609	0.067	92.27	103.35	0.89
20	"	6.54	3955	0.97	3.796	19810	0.097	114.30	109.53	1.04
14	37.0	7.46	3920	0.62	3.798	15932	0.073	86.70	105.45	0.82
23	"	7.75	4090	1.02	3.971	19444	0.098	120.14	116.55	1.03

Reference: 6.1/3
Reinforcement: Deformed Bars
Dimensions: b' = 3". b = 13". h = 5". a = 10" — 37". t = 1 1/4".
Total length = 42" — 92".

TABLE 6/11 - Tests by Alusi, 1956.
Simple-Span T-Beams Without Web Reinforcement

Beam	a	h	$\frac{M}{Vh}$	f'_c	p	σ_o	λ	ϵ_o	h_1/h	M_{calc}	M_{test}	$\frac{M_{calc}}{M_{test}}$
	in.	in.		psi	%	ksi	in.	10^{-3}		k-in.	k-in.	
S-1	36	9.16	3.93	3620	0.320	3.24	9144	0.35	0.08	135	224	0.60
S-2	36	9.28	3.88	3660	.316	3.26	9086	1.75	.12	192	312	.62
S-3	36	9.38	3.84	4290	.312	3.82	8316	0.84	.08	168	252	.67
S-4	36	8.00	4.50	3085	.916	2.83	10063	4.06	.45	383	387	.99
S-5	36	8.30	4.34	6260	.883	5.71	6907	2.62	.25	527	558	.94
S-6	36	8.20	4.39	7990	.893	7.30	6243	3.85	.22	580	593	.98
S-7	36	8.44	4.27	3550	.868	3.23	9249	3.66	.38	426	504	.84
S-8	36	8.20	4.34	6120	.758	5.59	6977	0.18	.11	244	315	.77
S-9	36	8.20	4.34	4760	.774	4.35	7874	1.99	.21	333	412	.81
S-10	36	8.20	4.34	5790	.774	5.29	7156	2.52	.20	391	475	.82
S-11	36	8.80	4.09	2580	.333	2.32	11282	1.26	.14	142	192	.74
S-12	36	8.20	4.34	4760	.774	4.35	7874	1.06	.17	278	376	.74
S-13	36	8.20	4.34	4840	.774	4.42	7807	4.90	.33	492	539	.91
S-14	36	8.20	4.34	4660	.715	4.26	7960	4.60	.30	447	502	.89
S-15	36	8.35	4.31	2896	.351	2.63	10484	3.08	.19	194	264	.74
S-16	36	8.06	4.47	3530	.364	3.23	9279	3.13	.17	199	268	.74

Reference: 1.4/11
Reinforcement: Rusted Wires
Dimensions: 6" x 12" Beams. a = Variable 24—54. h = Variable 8.00—9.38

TABLE 6/12 - Tests By Zwoyer, 1953
Simple-Span Prestressed Concrete Rectangular Beams Without Web Reinforcement

Beam	a	h	$\frac{M}{Vh}$	f'_c	p	σ_o	λ	ϵ_o	$h_{1/h}$	M_{calc}	M_{test}	$\frac{M_{calc}}{M_{test}}$
	in.	in.		psi	%	ksi	in.			k-in.	k-in.	
S-18	36	8.31	4.31	4150	0.470	3.78	8466	2.06	0.15	229	247	0.93
S-19	36	8.38	4.30	3850	.350	3.50	8827	2.10	.13	181	249	.73
S-20	36	8.45	4.26	5350	.347	4.86	7429	2.14	.10	203	260	.78
S-22	54	8.12	6.65	5630	.958	5.41	7401	2.07	.21	417	463	.90
S-23	54	8.02	6.74	4360	.776	4.19	8415	4.36	.31	434	502	.86
S-24	54	8.41	6.42	2900	.924	2.77	10678	4.07	.46	422	507	.83
S-25	54	8.44	6.40	3900	.491	2.77	10678	4.00	.28	293	373	.79
S-26	54	8.95	6.04	3130	.405	2.98	10182	2.06	.16	219	293	.75
S-27	54	8.45	6.39	3350	.307	3.20	9771	2.14	.12	161	216	.75
S-28	36	8.80	4.09	3470	.277	3.13	9373	2.06	.11	.60	252	.63
S-29	24	8.53	2.81	3320	.608	2.70	9824	4.10	.35	344	435	.79
S-30	24	8.50	2.82	3350	.488	2.73	9771	4.13	.29	300	383	.78
S-31	24	8.42	2.85	2440	.554	1.99	11953	4.13	.41	277	358	.77
S-32	24	8.35	2.87	3350	.435	2.75	9771	4.10	.26	267	347	.77
S-33	36	8.60	4.19	3400	.603	3.08	9685	3.80	.30	354	434	.81
S-34	36	8.64	4.17	5800	.600	5.25	7299	4.00	.21	442	477	.93

TABLE 6/12 (Continued)

Beam	$\frac{M}{Vh}$	f'_c	p	r	fy Stir.	σ_o	λ	$h_{1/h}$	M_{bend}	M_{st*}	M_{calc}	M_{test}	$\frac{M_{calc}}{M_{test}}$
		psi	%	%	ksi	ksi	10^2"		k-in.	k-in.	k-in.	k-in.	
		Series I. 7" x 15" Beams.					a = 32".		h = 12"				
I-10a	1.33	3070	4.76	0.52	47	1.52	415	0.432	521	124	645	869	0.74
b	1.33	2810	4.76	.52	47	1.39	438	.440	482	124	607	736	.82
11a	1.33	3560	4.76	.95	44	1.76	379	.419	591	210	802	1013	.79
b	1.33	3180	4.76	.95	44	1.58	406	.429	537	210	748	928	.81
I-12a	1.33	4000	4.76	1.47	41	1.98	355	.408	651	305	957	1013	.94
b	1.33	3220	4.76	1.47	41	1.60	403	.428	543	305	848	848	1.00
I-s	1.33	3470	4.76	1.72	47	1.72	385	.422	578	412	991	1173	.84
t	1.33	3700	4.76	2.14	47	1.83	371	.416	610	480	1090	1280	.85
I-u	1.33	3740	2.86	.52	53	1.85	286	.362	555	141	696	853	.82
v	1.33	3580	2.86	.70	53	1.77	293	.366	536	189	726	906	.80
w	1.33	4210	2.86	.95	45	2.09	267	.349	607	219	826	960	.86
x	1.33	3830	2.86	1.47	47	1.90	282	.359	565	352	918	1157	.79
I-y	1.33	4790	4.76	.52	53	2.38	322	.390	754	141	895	1173	.76
z	1.33	4850	.476	.70	53	2.41	320	.389	761	189	951	1184	.80
α	1.33	5070	4.76	.95	45	2.51	313	.384	789	219	1008	1386	.73
β	1.33	5130	4.76	1.47	47	2.54	311	.383	796	352	1149	1488	.77

*$M_{st} \leq V \times \frac{h}{2}$ Ref: 1.4/10 Longitudinal Reinforcement: Deformed Bars

Length: 15' 4" Span: 8' Web Reinforcement: Stirrups (deformed)

TABLE 6/13 - Tests By Elstner, 1954

Restrained Rectangular Beams With Web Reinforcement

Beam	$\frac{M}{Vh}$	f'_c	p	r	$f_{y\,Stir.}$	σ_o	λ	h_1/h	M_{bend}	M_{st}^*	M_{calc}	M_{test}	$\frac{M_{calc}}{M_{test}}$
		psi	%	%	ksi	ksi	10^{2}"		k-in.	k-in.	k-in.	k-in.	
Series II. 7" x 24" Beams. a = 32". h = 21"													
II-21a	0.76	3580	2.72	0.52	47	0.87	378	0.470	969	379	1348	1653	0.82
b	.76	3640	2.72	.52	47	.88	374	.468	982	379	1362	1509	.90
22a	.76	3000	2.72	.95	44	.73	421	.482	826	652	1478	1600	.92
b	.76	2710	2.72	.95	44	.66	449	.489	754	652	1406	1546	.91
II-23a	.76	3230	2.72	1.47	41	.78	402	.477	883	934	1818	1600	1.14
b	.76	3160	2.72	1.47	41	.77	407	.479	866	934	1801	1866	.96
II-e	.76	3420	2.72	1.72	43	.83	388	.473	930	1153	2085	2080	1.00
f	.76	3330	2.72	2.14	43	.81	395	.475	908	1189	2097	1813	1.16
Series IV. 7" x 15" Beams. a = 48". h = 12"													
IV-m	2.00	2860	4.76	0.52	53	1.97	434	.396	631	141	773	1001	.77
n	2.00	3710	4.76	.95	45	2.55	370	.370	779	219	998	1357	.74
o	2.00	3420	4.76	1.47	47	2.35	3888	.378	730	352	1083	1494	.72

TABLE 6/13 (Continued)

Beam	$\frac{M}{Vh}$	f'_c	p	σ_o	λ	$h_{1/h}$	M_{calc}	P_{calc}	P_{test}	$\frac{M_{calc}}{M_{test}}$
		psi	%	ksi	10^2"		k-in.	kips	kips	
Series I. a = 32". 7" x 15" Beams. h = 12"										
I-g	1.33	4430	0.95	2.20	149	0.222	437	82	90	0.91
h	1.33	3540	1.47	1.75	211	.293	443	83	89	0.93
i	1.33	3320	2.10	1.65	263	.340	469	88	99	0.89
I-1a	1.33	2510	2.86	1.24	366	.401	403	75	77	0.98
b	1.33	2800	2.86	1.39	341	.391	441	82	87	0.95
2a	1.33	2370	3.76	1.17	435	.433	402	75	75	1.01
b	1.33	2730	3.76	1.35	396	.421	454	85	95	0.90
c	1.33	3790	3.76	1.88	324	.390	596	111	94	1.19
3a	1.33	2290	4.76	1.13	502	.456	404	75	89	0.85
b	1.33	2970	4.76	1.47	423	.436	506	95	101	0.94
I-j	1.33	4850	1.47	2.41	177	.259	547	102	105	0.98
k	1.33	3860	2.10	1.91	241	.324	525	98	109	0.90
I-4a	1.33	4320	2.86	2.14	264	.347	620	116	100	1.16
b	1.33	4040	2.86	2.00	274	.354	589	110	89	1.24
5a	1.33	4060	3.76	2.01	312	.383	629	118	120	0.98
b	1.33	4040	3.76	2.00	313	.384	627	117	110	1.07
6a	1.33	4550	4.76	2.26	331	.396	723	135	115	1.18
b	1.33	3570	4.76	1.77	379	.420	592	111	120	0.93
I-1	1.33	5100	1.47	2.53	173	.254	565	106	107	0.99
m	1.33	4390	2.10	2.18	224	.310	576	108	105	1.03
I-7a	1.33	4790	2.86	2.38	250	.336	669	125	115	1.09
b	1.33	5000	2.86	2.48	245	.331	691	129	100	1.28
8a	1.33	4790	3.76	2.38	286	.366	717	134	145	0.93
b	1.33	4690	3.76	2.33	289	.368	705	132	110	1.20
9a	1.33	5270	4.76	2.61	307	.381	813	152	130	1.17
b	1.33	4650	4.76	2.31	327	.394	736	138	130	1.06
I-n	1.33	5240	1.47	2.60	.70	.250	575	107	118	0.91
o	1.33	5050	2.10	2.50	208	.294	635	119	128	0.93
p	1.33	5970	2.86	2.96	225	.310	783	146	133	1.10
q	1.33	4880	3.76	2.42	283	.364	727	136	130	1.05
r	1.33	5930	4.76	2.94	291	.368	891	167	140	1.19
Series II. a = 32". 7" x 24" Beams. h = 21"										
II-a	0.76	3820	0.54	0.93	161	.301	734	137	130	1.06
b	.76	3720	0.84	.90	205	.353	814	152	145	1.05
c	.76	4040	1.20	.98	234	.383	941	176	168	1.05
d	.76	3440	1.63	.83	300	.429	872	163	210	0.78

Tension Reinforcement: Deformed Bars
Span = 8 ft.
Total Length = 15' 4"
Reference: 1.4/10

Continued on next page

TABLE 6/14 - Tests By Moody, 1954
Restrained Rectangular Beams Without Web Reinforcement

Beam	$\frac{M}{Vh}$	f'_c	p	σ_o	λ	h_1/h	M_{calc}	P_{calc}	P_{test}	$\frac{M_{calc}}{M_{test}}$
		psi	%	ksi	10^2"		k-in.	kips	kips	
II-17a	0.76	2650	2.15	0.64	404	0.474	720	135	188	0.72
b	.76	3000	2.15	.72	373	.465	895	151	170	.89
18a	.76	2170	2.72	.52	521	.403	614	115	220	.52
b	.76	2700	2.72	.65	450	.490	751	140	180	.78
19a	.76	3030	3.46	.73	471	.499	854	160	241	.66
b	.76	3240	3.46	.79	452	.495	908	170	219	.78
20a	.76	2890	4.25	.70	538	.514	831	155	235	.66
b	.76	2960	4.25	.72	530	.513	850	159	249	.64
Series IV. a = 48". 7" x 15" Beams. h = 12"										
IV-g	2.00	3390	0.95	2.33	173	.203	430	62	63	1.00
h	2.00	3750	1.47	2.58	204	.239	547	79	70	1.14
i	2.00	3490	2.10	2.40	255	.286	593	86	68	1.27
j	2.00	3600	2.86	2.48	292	.317	668	97	83	1.17
k	2.00	3630	3.76	2.50	332	.348	724	105	88	1.20
l	2.00	3920	4.76	2.70	359	.365	813	118	81	1.46
SERIES VI. a = 32". 7" x 15" Beams. h = 12"										
VI-a	1.78	4090	0.95	2.60	155	.196	463	72	77	0.94
b	1.78	4160	1.47	2.65	192	.239	562	87	129	.68
c	1.78	3580	2.10	2.28	251	.295	577	90	110	.82
d	1.78	3900	2.86	2.48	279	.321	674	105	118	.89
e	1.78	4120	3.76	2.62	309	.346	756	118	128	.92
VI-f	1.78	5570	2.10	3.54	199	.246	772	120	140	0.86
g	1.78	5530	2.86	3.52	233	.282	859	134	130	1.03
h	1.78	5300	3.76	3.37	272	.318	909	142	155	0.92
i	1.78	5020	4.76	3.83	289	.329	1064	166	146	1.14

TABLE 6/14 (Continued)

7 SUMMARY AND CONCLUSIONS

(1) The prediction of the ultimate strength of prestressed and conventionally reinforced concrete beams under the combined action of moment and shear was approached by stating a hypothesis concerning the failure mechanism in the region of diagonal cracks.

(2) The failure mechanism is considered to consist of a "shear-rotation" ϕ about the neutral axis of the broken failure cross-section. The depth of the neutral axis at failure could then be obtained by observing

   (a) the deformations caused by the shear rotation;

   (b) the critical stresses resulting from these deformations; and

   (c) The equilibrium conditions of the internal forces.

(3) The failure is ultimately attributed to the destruction of the concrete compressive zone. The strength of this zone, depending on the prevailing state of stress, was derived according to Mohr's failure criterion for plain concrete.

(4) The deformation of the tension zone was attributed to a pull-out effect of the longitudinal reinforcement relative to the surrounding concrete. This measure

permitted a numerical consideration of the influence of the bond characteristic on the shear strength.

(5) The information concerning the ultimate strength of a beam is expressed in terms of moment capacity (ultimate shear moment), while considering, however, the influence of the magnitude of the shear force ($\frac{M}{Vh}$ ratio).

(6) The comparison with 278 test results confirmed the satisfactory validity of the theory for:

   (a) Simply supported beams with and without web or compression reinforcement

   (b) Prestressed beams

   (c) Restrained beams

   (d) Beams of various cross-sections

(7) According to the theory and in agreement with experimental findings, the ultimate shear moment increases with

   (a) concrete strength;

   (b) ratio of tension reinforcement;

   (c) ratio of web reinforcement;

   (d) ratio of compression reinforcement;

   (e) prestressing;

   (f) bond coefficient $1/\lambda$; and

   (g) ratio M/Vh (for symmetrical loading: shear span).

The rate of moment increase with these parameters is shown in an example in Fig. 7/1.

(8) The mode of failure of a given beam depends on the load configuration. It is therefore impossible to provide against shear failure for the beam as such without due regard to the particular load conditions.

(9) With the theory outlined in this paper it is easily possible to specify an adequate factor of safety (s) against shear failures in the form

$$\left| \frac{M_{su/calc}}{M_{design}} \right|_{min} \geq S$$

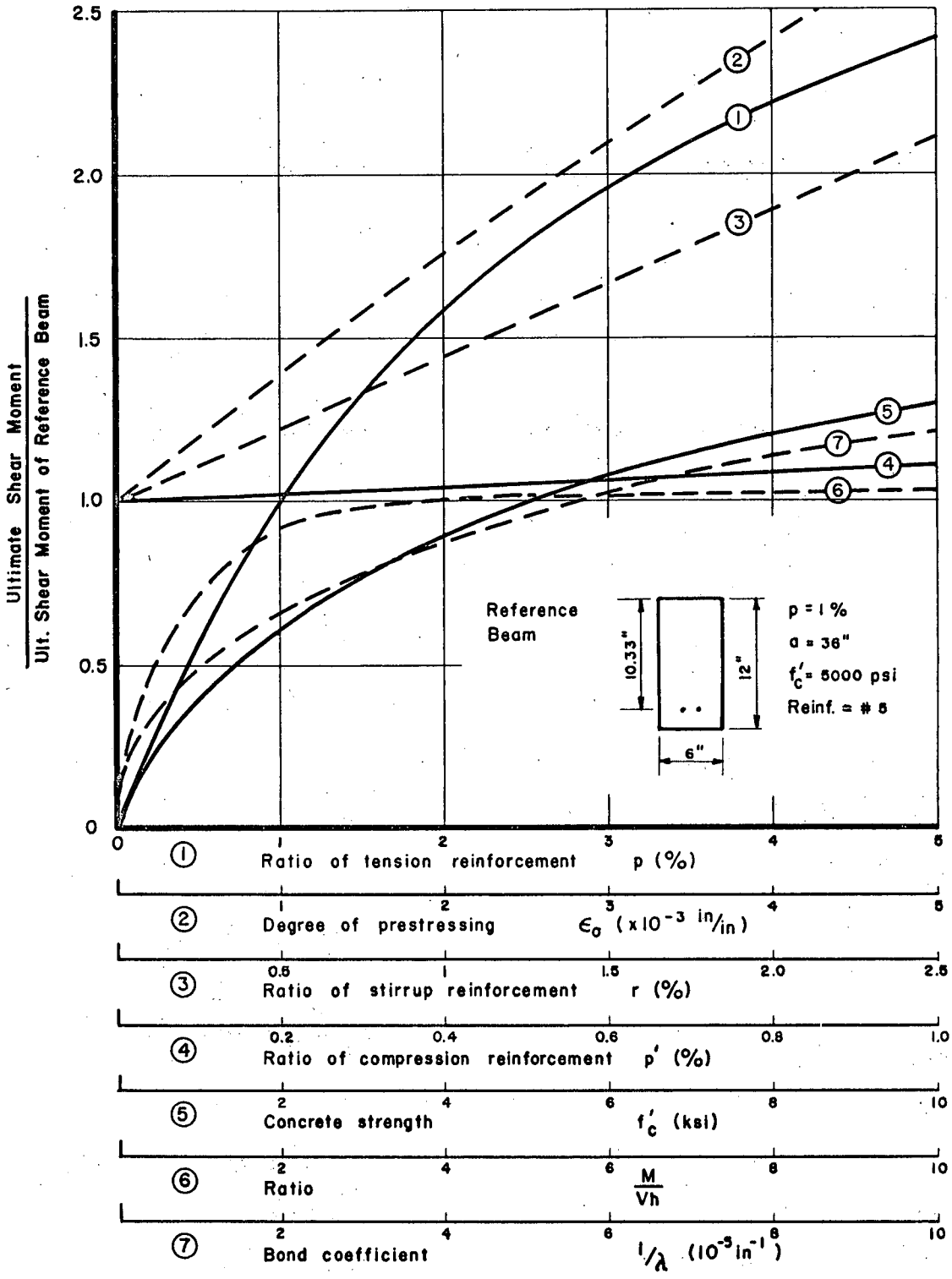

Fig. 7.1
Rate of Influence of Various Parameters

BIBLIOGRAPHY

1.3/1 Walther, R. "Beanspruchung der Schubarmierund von Eisenbetonbalken." Schweizerische Bauzeitung. Nr. 2, 14 Jan. 1957, p. 13.

1.4/1 Hognestad, E. What Do We Know About Diagonal Tension and Web Reinforcement in Concrete? University of Illinois Bulletin, Vol. 49, No. 50. March, 1952.

1.4/2 Laupa, A.; Siess, C. P.; Newmark, N. M. Strength in Shear of Reinforced Concrete Beams. University of Illinois Bulletin, Vol. 52, No. 55. March, 1955.

1.4/3 Mörsch, E. Der Eisenbetonbau, (6 Edition). Stuttgart: Konrad Wittwer. 1923

1.4/4 Ritter, W. "Die Bauweise Hennebique." Schweizerische Bauzeitung, Vol. 33, No. 7. Zürich: February, 1899.

1.4/5 Dischinger, F. "Massivebau." Taschenbuch für Bauingenieure. herausgegeben von F. Schleicher. Berlin: Springer Verlag, 1949.

1.4/6 Rausch, E. Drillung (Torsion), Schub und Scheren im Stahlbetonbau. Düsseldorf: Deutscher Ingenieur Verlag GmbH, 1953.

1.4/7 Richart, F. E. An Investigation of Web Stresses in Reinforced Concrete Beams. Bulletin No. 166, Engineering Experiment Station. University of Illinois: 1927.

1.4/8 Moretto, O. "An Investigation of the Strength of Welded Stirrups in Reinforced Concrete Beams." A.C.I. Journal, Proc. 42:141-162. November, 1945.

1.4/10 Moody, K. G.; Viest, I. M.; Elstner, R. C.; Hognestad, E. "Shear Strength of Reinforced Concrete Beams." A.C.I. Journal. Vol. 26, No. 4 (Dec., 1954), No. 5 (Jan., 1955), No. 6 (Feb., 1955), and No. 6 (March, 1955).

1.4/11 Zwoyer, E. M. Shear Strength of Simply-Supported Pre-Stressed Concrete Beams. Ph.D. Thesis. University of Illinois: June, 1953.

2.1/1 Mohr, O. "Die Schubfestigkeit des Betons." Armierter Beton, 1911.

2.3/1 Roš, M. Die materialtechnischen Grundlagen und Probleme des Eisenbetons im Hinblick auf die zukünftige Gestaltung der Stahlbeton Bauweise. EMPA Bericht Nr. 162. Zürich: 1950.

2.4/1 Bresler, B.; Pister K. Strength of Concrete Under Combined Stresses. University of California Institute of Research. Series 100, Issue 1. November, 1956.

2.4/2 Hognestad, E.; Hanson, N.; McHenry D. "Concrete Stress Distribution in Ultimate Strength Design." A.C.I. Journal, Vol. 27, No. 4. December, 1955.

4.2/1 Clark, A. P. "Diagonal Tension in Reinforced Concrete Beams." A.C.I. Journal, Vol. 48. October, 1951.

5.1/1 Clark, A. P. "Bond of Concrete Reinforcing Bars." A.C.I. Proceedings, 46:161-184. 1950.

5.1/2 Djabry, W. Contribution à l'étude de l'adhérence des fers d'armature au béton. EMPA Bericht Nr. 184. Zürich: October, 1952.

5.1/3 Dinsmore, G. A.; Deutsch, P. L. Anchorage Characteristics of Strand in Pretensioned Prestressed Concrete. Lehigh University, Fritz Laboratory Report 223.16. July, 1957.

6.1/1 Gaston, J. R.; Siess, C. P.; Newmark, N. M. An Investigation of the Load-Deformation Characteristics of Reinforced Concrete Beams Up to the Point of Failure. University of Illinois Civil Engineering Studies, Structural Research Series No. 40. December, 1952.

6.1/2 Galletly, G. D.; Hosking, N. G.; Ofjord, A. Behavior of Structural Elements Under Impulsive Loads III. Mass. Institute of Technology Dept. of Civil and Sanitary Engineering. July, 1951.

6.1/3 Al-Alusi, A. F. "Diagonal Tension Strength of Reinforced Concrete T-Beams with Varying Shear Span." A.C.I. Journal, Vol. 28, No. 11. May, 1957.

NOTATIONS

A	Parameter given by Eq. 2.3/6
A_{st}	Area of longitudinal tension reinforcement
A_{st}'	Area of longitudinal compression reinforcement
A_w	Area of two legs of one stirrup
a	Shear span (for symmetrical loading)
b	Width of beam
C	Longitudinal compressive force
C'	Inclined compressive force
d	Bar diameter
E, E_{st}	Modulus of Elasticity of longitudinal tension reinforcement
e	Eccentricity of prestressing force
F	Effective prestressing force
f'	Steel stress of compression reinforcement at failure
f_c'	Compressive strength of 6 x 12 in. concrete cylinders
f_s	Stress in the tension reinforcement at failure
f_y'	Yield strength of steel
h	Effective depth of the beam
h_1	Depth of the neutral axis at shear failure
I	Moment of inertia of the uncracked section
jh	Lever arm of the internal forces

k	Transition factor (see Eq. 5.1/2)
k_1	(a) Coeff. of stress block as used in Ref. 1.4/10
k_2	(b) Coeff. of the function defined by Eq. 3.4/8
L	Length of beam
M	Bending moment
M_{stir}	Moment contribution of the stirrups
M_{su}	Ultimate shear moment
n	Ratio of moduli of elasticity
P	Concentrated load
p	$p = \frac{A_{st}}{bh}$ = ratio of tension reinforcement
p'	$p' = \frac{A_{st}'}{bh}$ = ratio of compression reinforcement
Q	Static moment of the cross-section with respect to the neutral axis
q	Parameter given by Eq. 3.4/8
R	Reaction
r	$r = \frac{A_w}{bs}$ = ratio of stirrup reinforcement
s	Spacing of the stirrups
T	Tension force
T_{eff}	Effective prestressing force
T_i	Initial pretensioning force before release
T_i'	Initial post-tensioning force before creep and shrinkage take place
T_o	Fictitious tension force
V	Shear force

V_c	Shear force carried by the concrete compressive zone
V_{st}	Shear force carried by the stirrups
V_u	Ultimate shear force
W_n	Weight of a reference point "n" of the curve given by Eq. 3.4/6
α	Angle defined in Fig. 3.2/1
γ	Angle defined in Fig. 3.2/1
Δl_{bot}	Deformation of the bottom zone (see Fig. 3.1/1)
Δl_{top}	Deformation of the top zone (see Fig. 3.1/1)
ΔT_{el}	Loss of prestress due to elastic shortening of concrete
ΔT_{ie}	Loss of prestress due to inelastic deformations of concrete and steel
$\Delta \epsilon_{el}$	Elastic change of strain due to prestressing
$\Delta \epsilon_{ie}$	Inelastic change of strain due to prestressing and sustained load
$\Delta \sigma_{el}$	Elastic change of stress due to prestressing
$\Delta \sigma_{ie}$	Inelastic change of stress due to prestressing and sustained load
ϵ	Strain
ϵ'	Steel strain of compression reinforcement at failure
ϵ_t	Steel strain in excess of prestressing strain at failure
ϵ_{cb}	Concrete bottom strains
ϵ_{ct}	Concrete top strains
ϵ_{cu}	Ultimate concrete strain

Fig. 1.3/2

ϵ_{eff}	Effective steel strain in prestressing tendons
ϵ_i	Initial pretensioning strain before release
ϵ_i'	Initial post-tensioning strain before creep and shrinkage take place
ϵ_{st}	Steel strain
ϵ_x	Strain in x direction (3.2/1)
ϵ_y'	Yield strain of compression or web reinforcement
η	$\eta = \frac{\sigma_x}{\sigma_o}$
κ	Coefficient of roughness
$1/\lambda$	Bond coefficient
ξ	$\xi = \frac{\epsilon_x}{\epsilon_{cu}}$
σ	Normal stress
σ'	Concrete stress defined in Fig. 2.2/3
σ_{av}	Average stress in the concrete compressive zone
σ_{av}^*	Average stress of a portion of the concrete compression zone (Eq. 2.4/4)
σ_c	Compressive strength of concrete
σ_o	Concrete normal stress at failure (Eq. 2.4/8)
σ_o'	Concrete stress defined in Fig. 2.2/3
σ_{st}	Steel stress
σ_t	Tensile strength of concrete
σ_x, σ_y	Stress components (Fig. 2.3/3)

σ_1, σ_2, σ_3	Principle stresses
τ	Shear stress
τ_{av}	Average shear stress of the concrete compressive zone
τ_{av}^*	Average shear stress of a portion of the concrete compressive zone (Eq. 2.4/4)
τ_s	Shear stress (Fig. 2.3/2)
τ_{xy}, τ_{yx}	Shear stresses (Fig. 2.3/1 and 2.3/3)
ϕ	Shear rotation

APPENDIX

Pull-out Tests to Derive the Coefficient of Roughness $\varkappa$.

Pull-out specimens:

Cylinders 6"x 12" vertically cast

Concrete strength $f_c' = 4660$ psi

Steel (two specimens of each)

1/2" plain bar

7/8" plain bar

1/2" deformed bar

7/8" deformed bar

1/2" strand

7/16" strand

The average pull-out displacements $\Delta 1$ as a function of the steel strain are plotted in the following figures, together with the theoretically assumed curves:

$$\Delta 1 = \varkappa \left(0.5 + \frac{2500 \text{ psi}}{f_c'}\right) d\epsilon^2$$

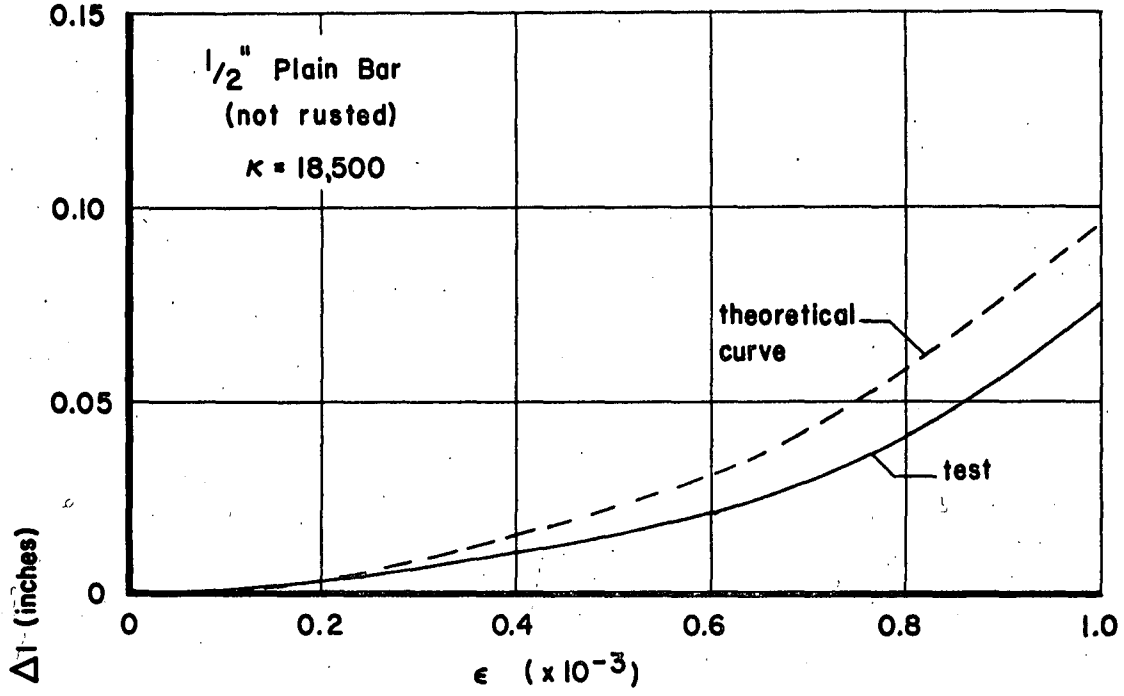

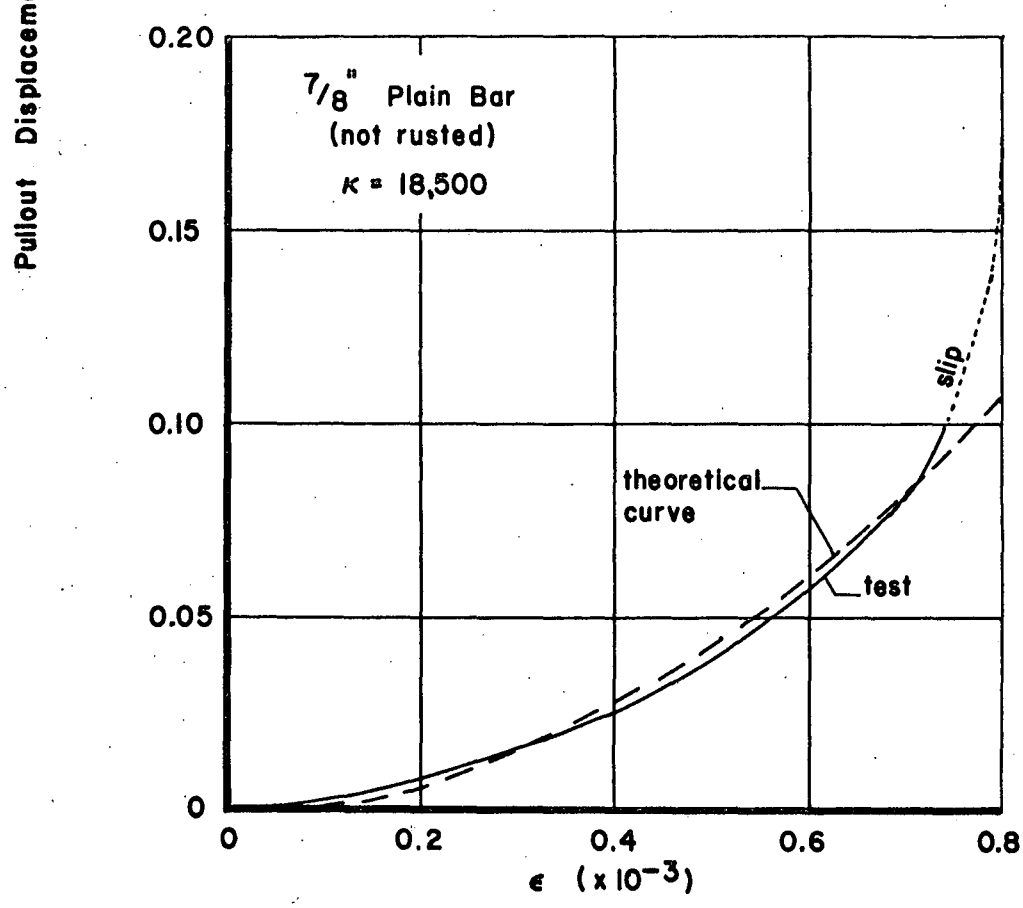

Pullout Displacement Δ1 (inches)

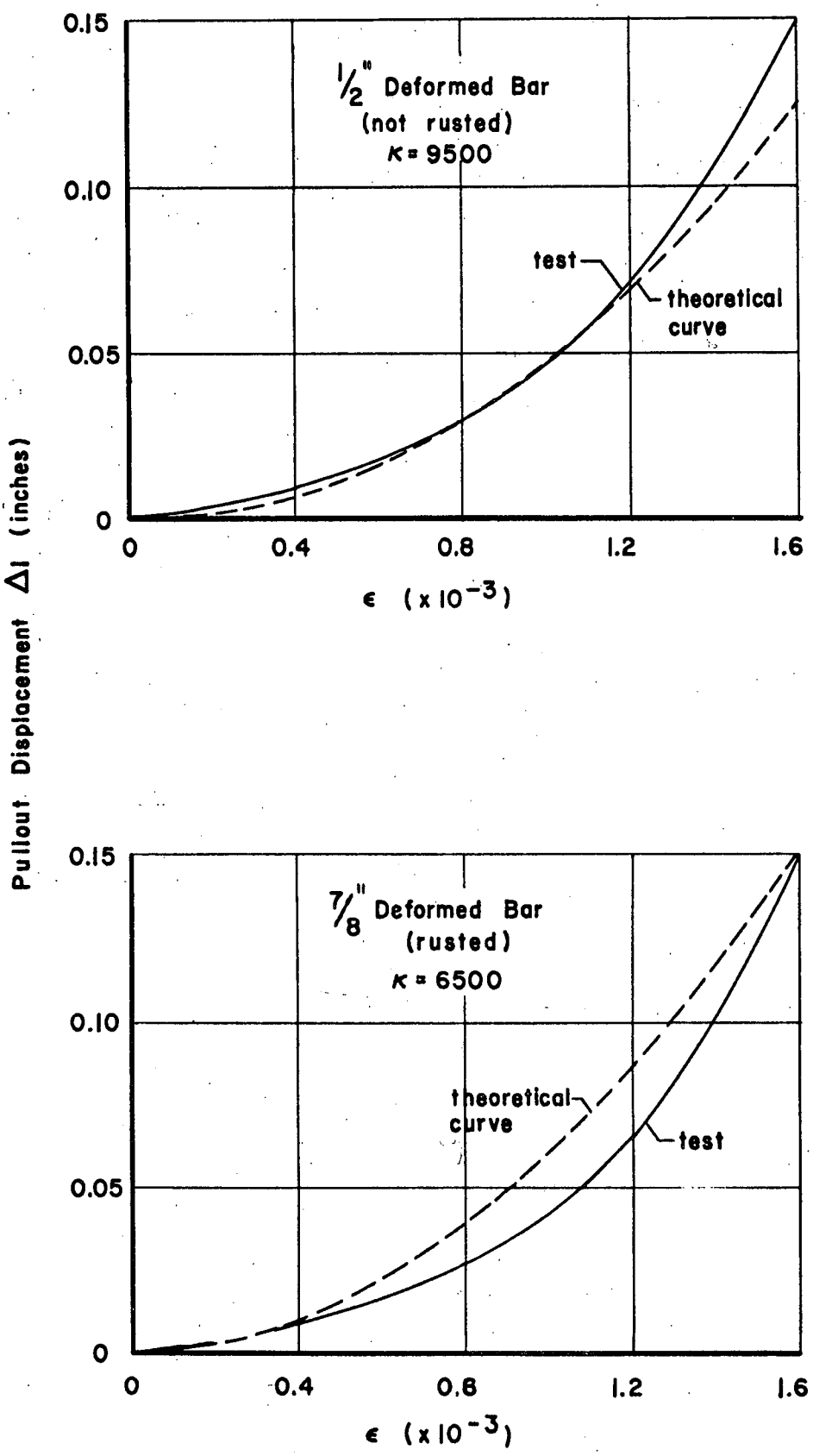
0.15
0.10
0.05
0
1/2" Deformed Bar
(not rusted)
κ = 9500
test
theoretical curve
0
0.4
0.8
1.2
1.6
ε (x 10⁻³)
Pullout Displacement Δl (inches)
0.15
0.10
0.05
0
7/8" Deformed Bar
(rusted)
κ = 6500
theoretical curve
test
0
0.4
0.8
1.2
1.6
ε (x 10⁻³)

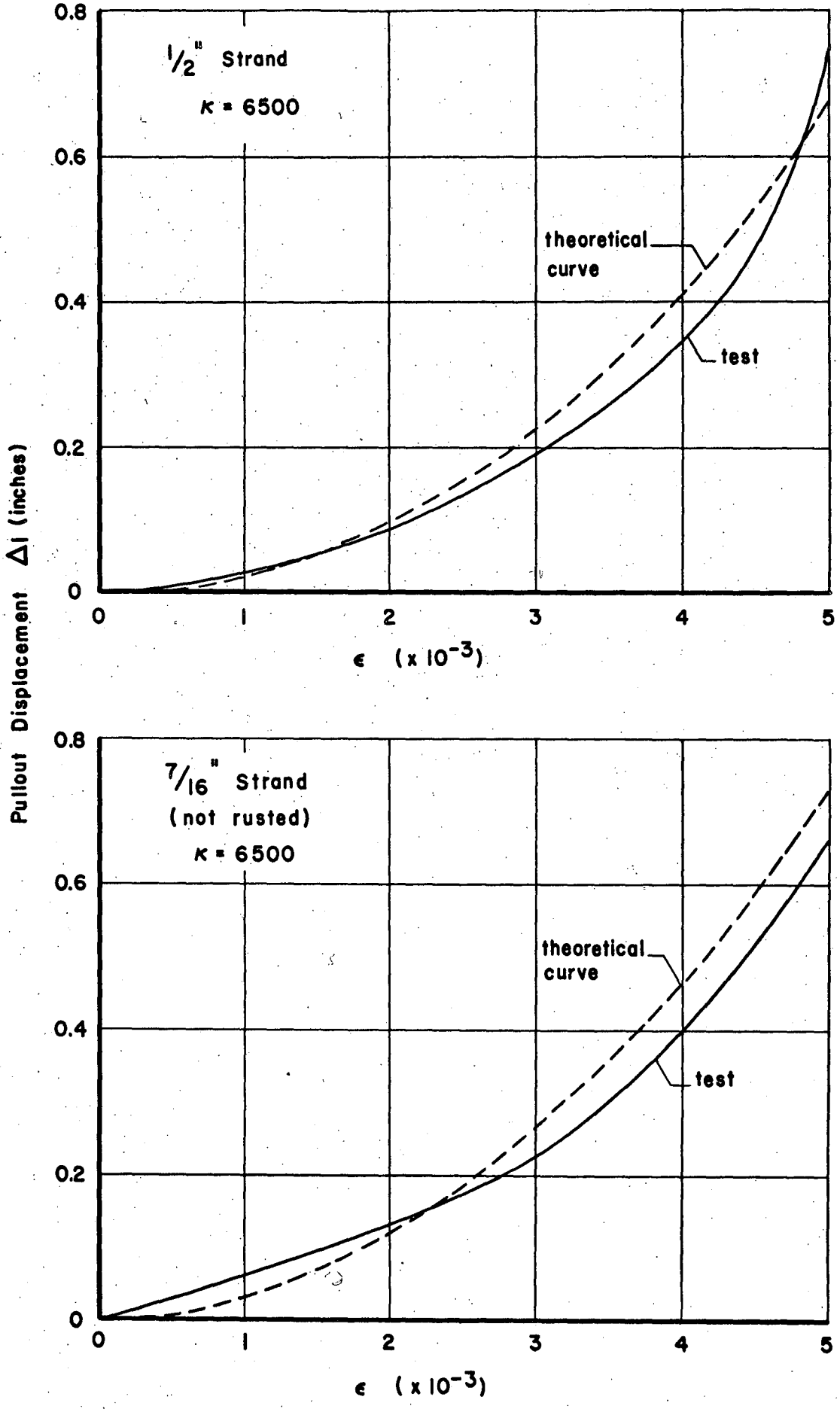
1/2" Strand
κ = 6500
theoretical curve
test
7/16" Strand
(not rusted)
κ = 6500
theoretical curve
test
Pullout Displacement Δl (inches)
0.8
0.6
0.4
0.2
0
0
1
2
3
4
5
ε (x 10⁻³)